

Practical Implementation and Applications of DFT Methods

David J. Singh
Oak Ridge National Laboratory



*Theory Winter School,
Tallahassee, Florida*

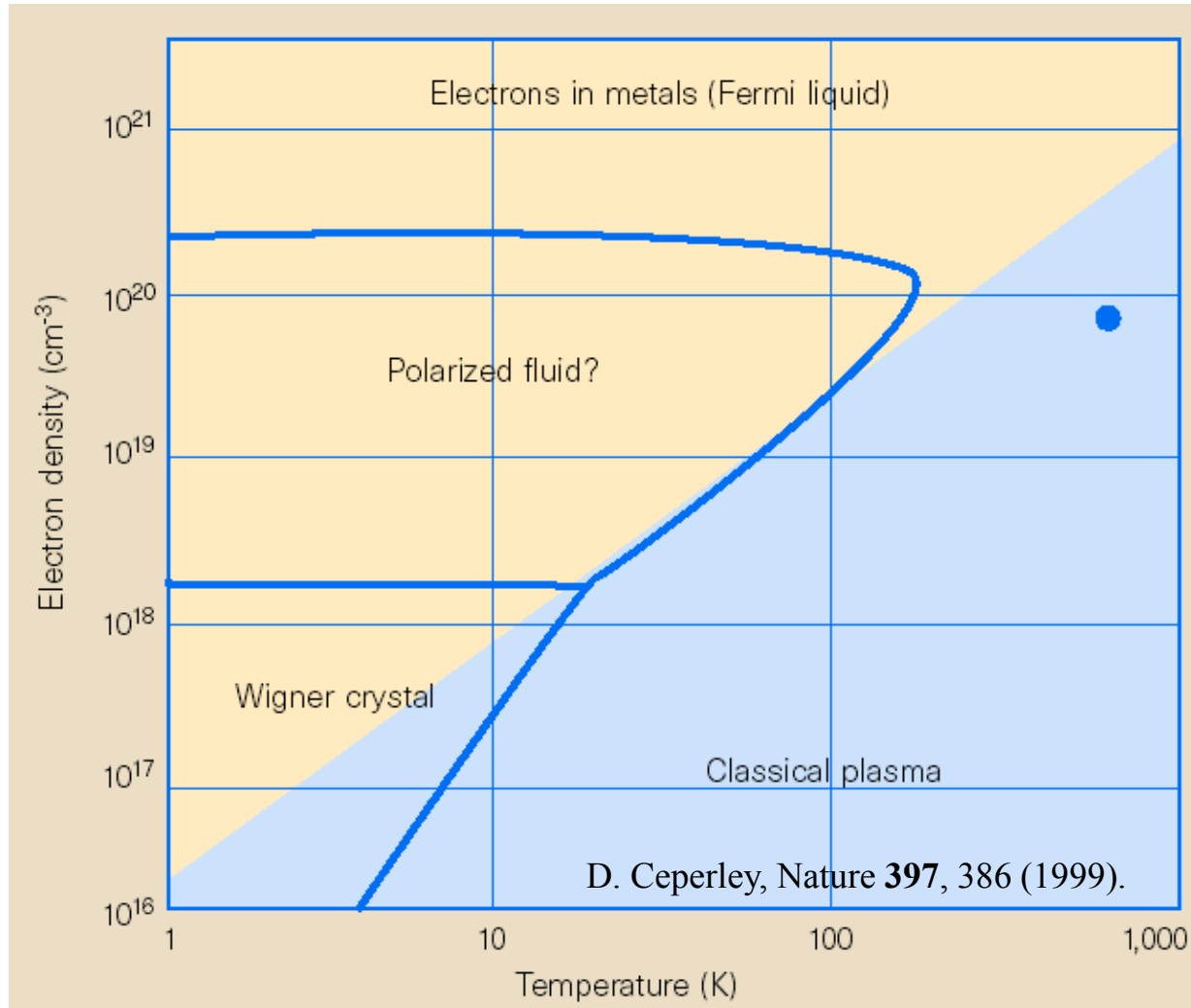
January 10, 2012

Blueberry Muffins

The blueberries change the taste, but the muffin is still basically a muffin.

The taste does not depend much on the distribution of berries.

The Electron Gas



bcc Fe: $n_{av} = 2.2 \times 10^{24}$ e/cm^3 (total); $n_{av} = 6.8 \times 10^{23}$ e/cm^3 (valence)

Nothing Interesting Happens in the Uniform Electron Gas at Densities of Solids

The Electron Gas Now With Nuclei

1 H Hydrogen 1.007 94																	Group 18 2 He Helium 4.002 602
Group 1 3 Li Lithium 6.941	Group 2 4 Be Beryllium 9.012 182																
11 Na Sodium 22.989 770	12 Mg Magnesium 24.3050	Group 3	Group 4	Group 5	Group 6	Group 7	Group 8	Group 9	Group 10	Group 11	Group 12	Group 13 5 B Boron 10.811	Group 14 6 C Carbon 12.0107	Group 15 7 N Nitrogen 14.006 74	Group 16 8 O Oxygen 15.9994	Group 17 9 F Fluorine 18.998 4032	10 Ne Neon 20.1797
19 K Potassium 39.0983	20 Ca Calcium 40.078	21 Sc Scandium 44.955 910	22 Ti Titanium 47.867	23 V Vanadium 50.9415	24 Cr Chromium 51.9961	25 Mn Manganese 54.938 049	26 Fe Iron 55.845	27 Co Cobalt 58.933 200	28 Ni Nickel 58.6934	29 Cu Copper 63.546	30 Zn Zinc 65.39	31 Ga Gallium 69.723	32 Ge Germanium 72.61	33 As Arsenic 74.921 60	34 Se Selenium 78.96	35 Br Bromine 79.904	36 Kr Krypton 83.80
37 Rb Rubidium 85.4678	38 Sr Strontium 87.62	39 Y Yttrium 88.905 85	40 Zr Zirconium 91.224	41 Nb Niobium 92.906 38	42 Mo Molybdenum 95.94	43 Tc Technetium (98)	44 Ru Ruthenium 101.07	45 Rh Rhodium 102.905 50	46 Pd Palladium 106.42	47 Ag Silver 107.8682	48 Cd Cadmium 112.411	49 In Indium 114.818	50 Sn Tin 118.710	51 Sb Antimony 121.760	52 Te Tellurium 127.60	53 I Iodine 126.904 47	54 Xe Xenon 131.29
55 Cs Cesium 132.905 45	56 Ba Barium 137.327	57 La Lanthanum 138.9055	72 Hf Hafnium 178.49	73 Ta Tantalum 180.9479	74 W Tungsten 183.84	75 Re Rhenium 186.207	76 Os Osmium 190.23	77 Ir Iridium 192.217	78 Pt Platinum 195.078	79 Au Gold 196.966 55	80 Hg Mercury 200.59	81 Tl Thallium 204.3833	82 Pb Lead 207.2	83 Bi Bismuth 208.980 38	84 Po Polonium (209)	85 At Astatine (210)	86 Rn Radon (222)
87 Fr Francium (223)	88 Ra Radium (226)	89 Ac Actinium (227)	104 Rf Rutherfordium (261)	105 Db Dubnium (262)	106 Sg Seaborgium (263)	107 Bh Bohrium (264)	108 Hs Hassium (265) [†]	109 Mt Meitnerium (268) [†]	110 Uun* Ununium (269) [†]	111 Uuu* Ununium (272) [†]	112 Uub* Ununium (277) [†]		114 Uuq* Ununquadium (285) [†]				

Key:

6 — Atomic number
 C — Symbol
 Carbon — Name
 12.0107 — Average atomic mass

- Metals**
- Alkali metals
 - Alkaline-earth metals
 - Transition metals
 - Other metals
- Nonmetals**
- Hydrogen
 - Semiconductors
 - Halogens
 - Noble gases
 - Other nonmetals

A team at Lawrence Berkeley National reported the discovery of elements 116 and 119 in June 1999. The same team retracted the discovery in July 2001. The discovery of element 114 has been reported but not confirmed.

[†] Estimated from currently available IUPAC data.
 * The systematic names and symbols for elements greater than 109 will be used until the approval of final names by IUPAC.

58 Ce Cerium 140.116	59 Pr Praseodymium 140.907 65	60 Nd Neodymium 144.24	61 Pm Promethium (145)	62 Sm Samarium 150.36	63 Eu Europium 151.964	64 Gd Gadolinium 157.25	65 Tb Terbium 158.925 34	66 Dy Dysprosium 162.50	67 Ho Holmium 164.930 32	68 Er Erbium 167.26	69 Tm Thulium 168.934 21	70 Yb Ytterbium 173.04	71 Lu Lutetium 174.967
90 Th Thorium 232.0381	91 Pa Protactinium 231.035 88	92 U Uranium 238.0289	93 Np Neptunium (237)	94 Pu Plutonium (244)	95 Am Americium (243)	96 Cm Curium (247)	97 Bk Berkelium (247)	98 Cf Californium (251)	99 Es Einsteinium (252)	100 Fm Fermium (257)	101 Md Mendelevium (258)	102 No Nobelium (259)	103 Lr Lawrencium (262)

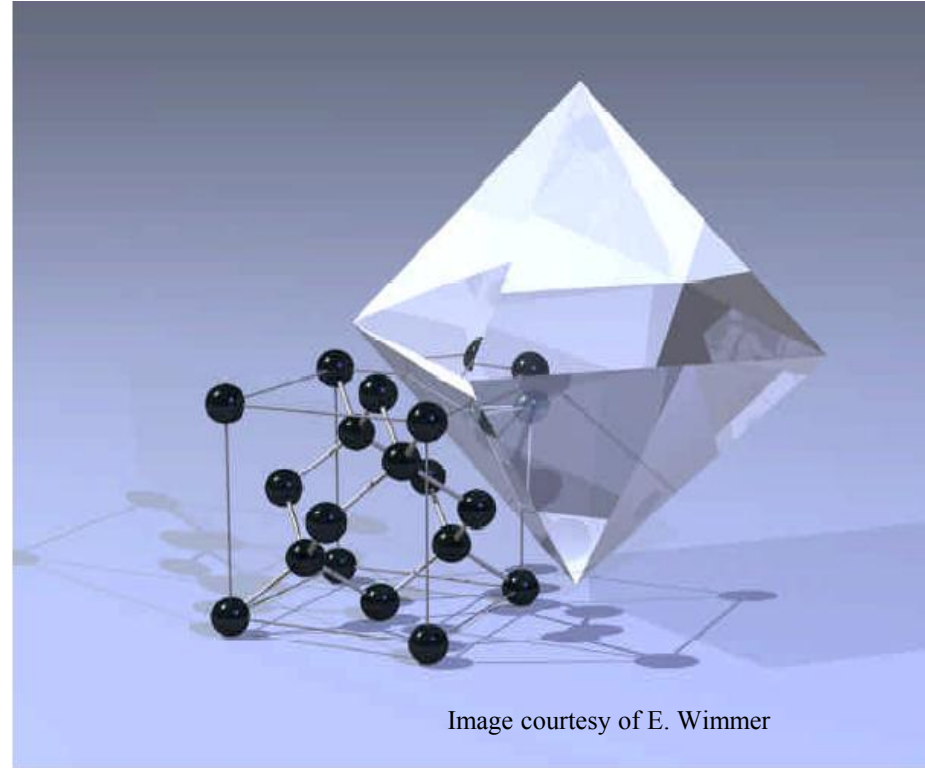
The atomic masses listed in this table reflect the precision of current measurements. (Values listed in parentheses are those of the element's most stable or most common isotope.) In calculations throughout the text, however, atomic masses have been rounded to two places to the right of the decimal.

He: liquid at 0 K

W: melts at 3695 K

First Principles Modeling

- Connect properties with atomic level structure.
- Sort out physical models.
- Ask “what if” questions.
- Microscopic mechanisms and **understanding**.
- Screen ideas for new/modified materials.
- Analyze failures.



Pre-History



Westminster Abbey, London

“The underlying physical laws necessary for the mathematical theory of a large part of physics and the whole of chemistry are thus completely known, and the difficulty is only that the exact application of these laws leads to equations that are much too complicated to be soluble. It therefore becomes desirable that approximate practical methods of applying quantum mechanics should be developed, which can lead to an explanation of the main features of complex atomic systems without too much computation.”

P.A.M. Dirac, *Proc. Roy. Soc. (Lond)* **123**, 714 (1929).

$H\psi = E\psi$: Many Body Problem, with correlated many-body wavefunctions → Too hard.

Wigner and Seitz (1955)



*“If one had a great calculating machine, one might apply it to the problem of solving the Schrodinger equation for each metal and obtain thereby the interesting physical quantities, such as cohesive energy, the lattice constant, and similar parameters. Presumably, the results would agree with experimentally determined quantities and nothing vastly new would be gained from the calculation. **It would be preferable, instead, to have a vivid picture of the behavior of the wave functions, a simple description of the essence of the factors which determine cohesion, and an understanding of the origins ...**”*

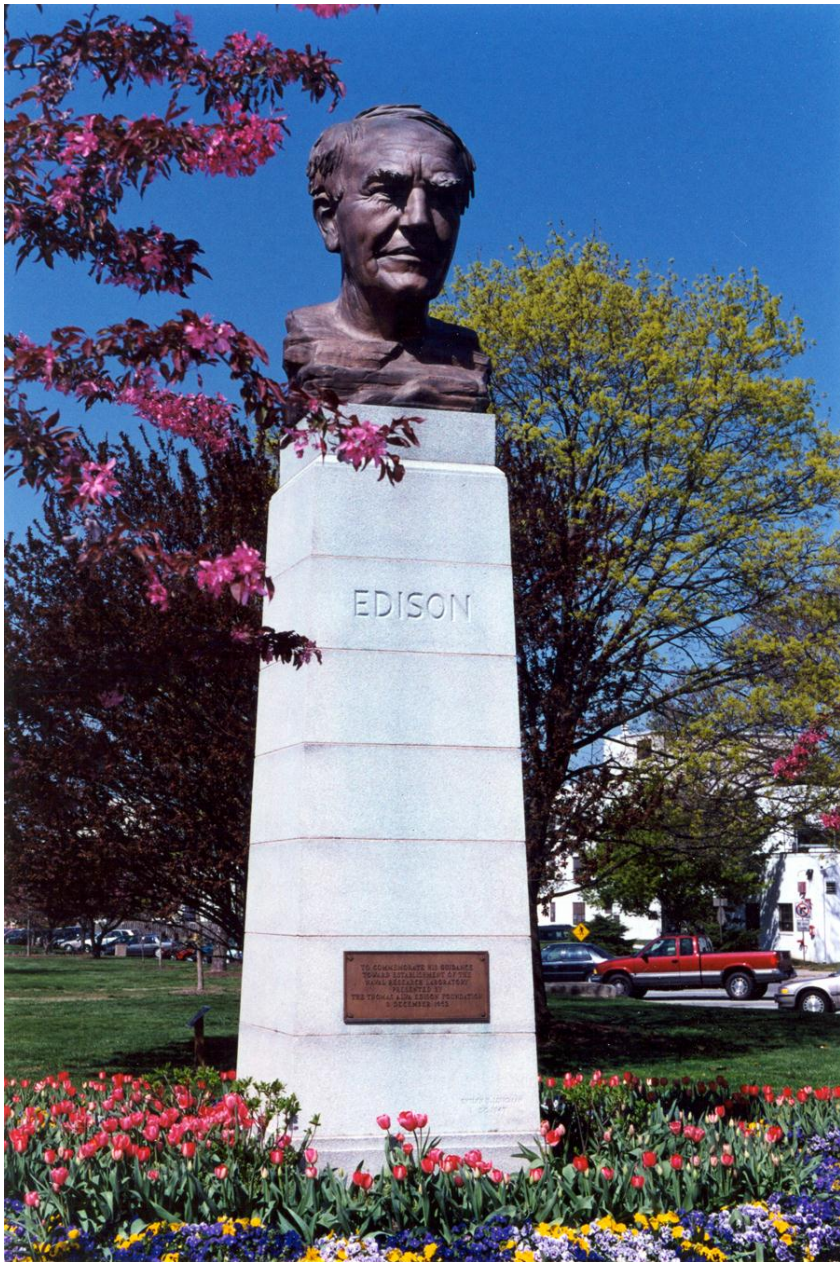
E.P. Wigner and F. Seitz, Solid State Physics, Vol. 1 (1955).

WARNING



If you do not ask questions, I will.

(corollary) If you do not contradict me, I will.



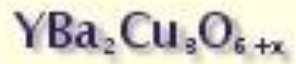
“Hell, there are no rules here - we’re trying to accomplish something.”

Thomas Edison

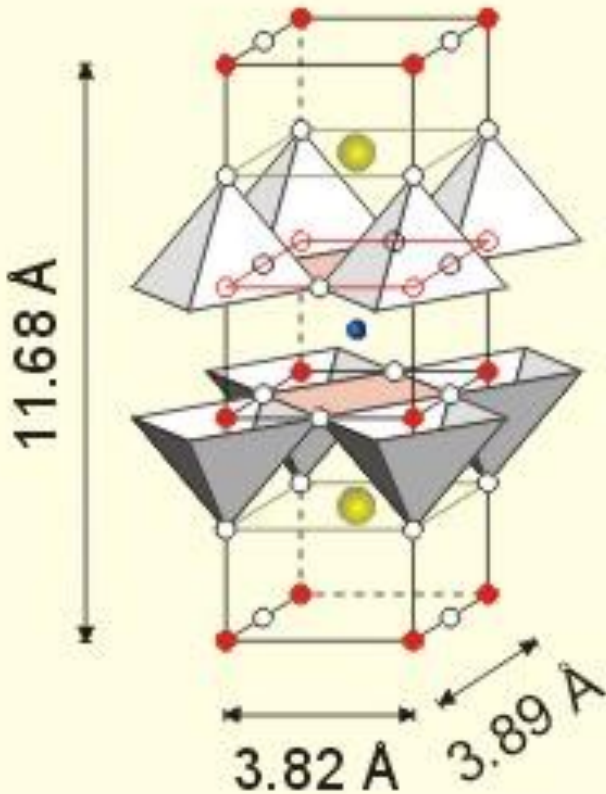
TODAY'S PLAN

- General Remarks about DFT and Applications.
- Magnetism and Superconductivity (Iron-Based Superconductors).
- Very Short Introduction to the LAPW Method and the ELK code for the Hand's-On.

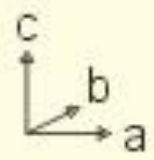
Property Prediction and Surprises



- Y
- Ba
- Cu
- O

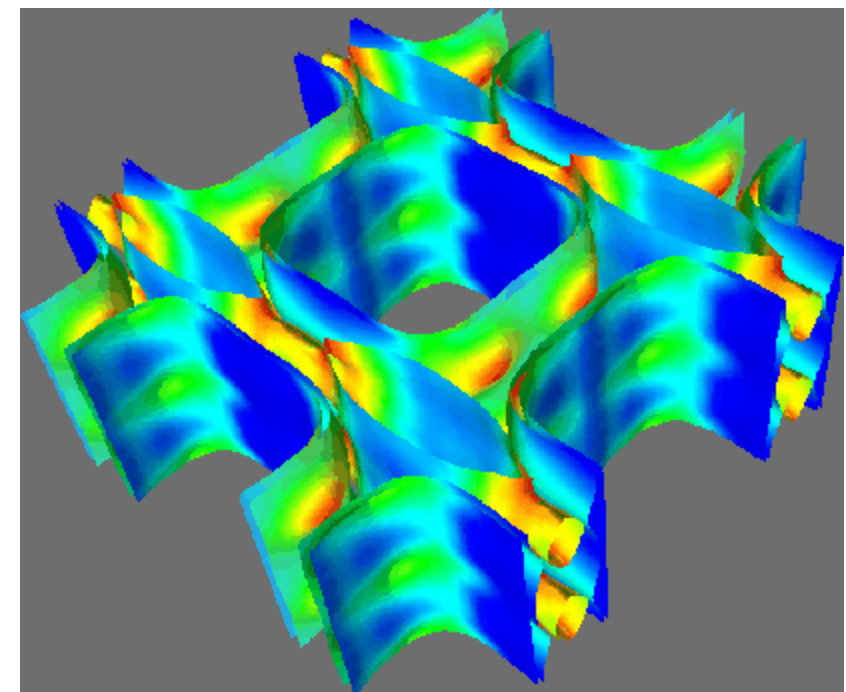


- Cu(1), O(4)
- Ba, O(1)
- Cu(2), O(2), O(3)
- Y
- Cu(2), O(2), O(3)
- Ba, O(1)
- Cu(1), O(4)

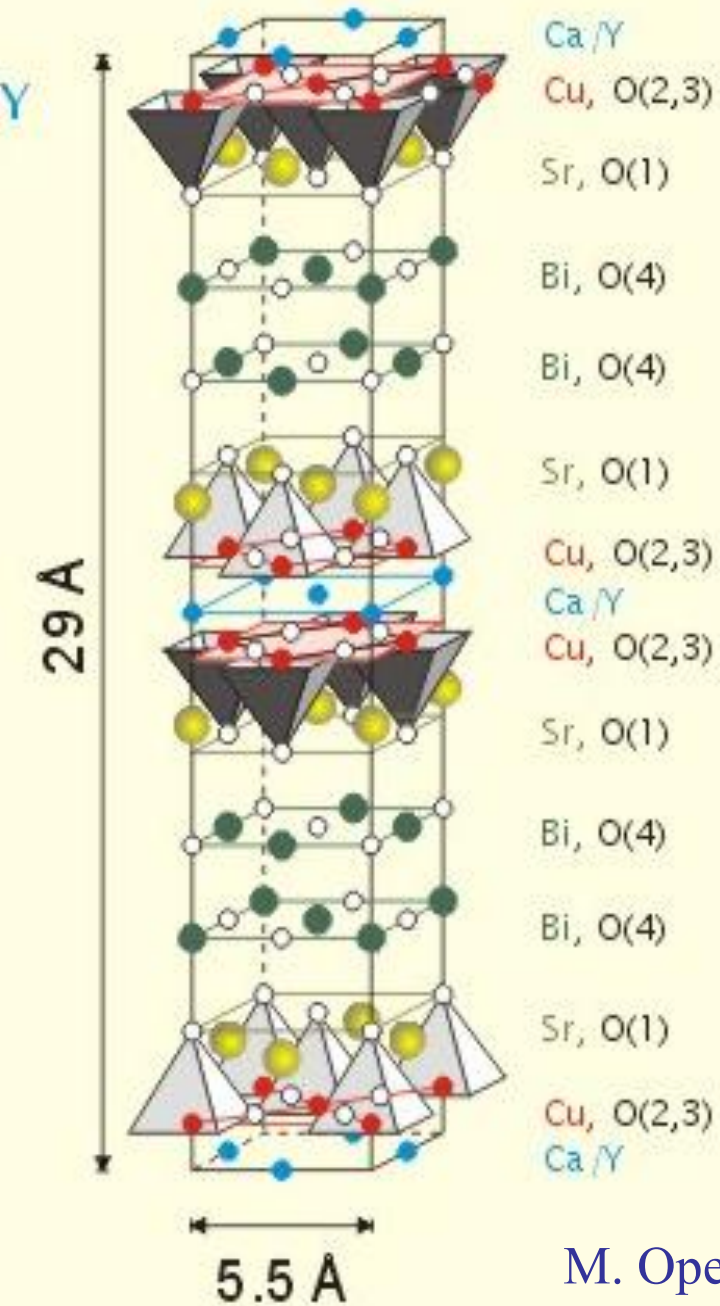


M. Opel

High- T_c Electronic Structures are 2D



Pickett, Cohen, Krakauer, Singh



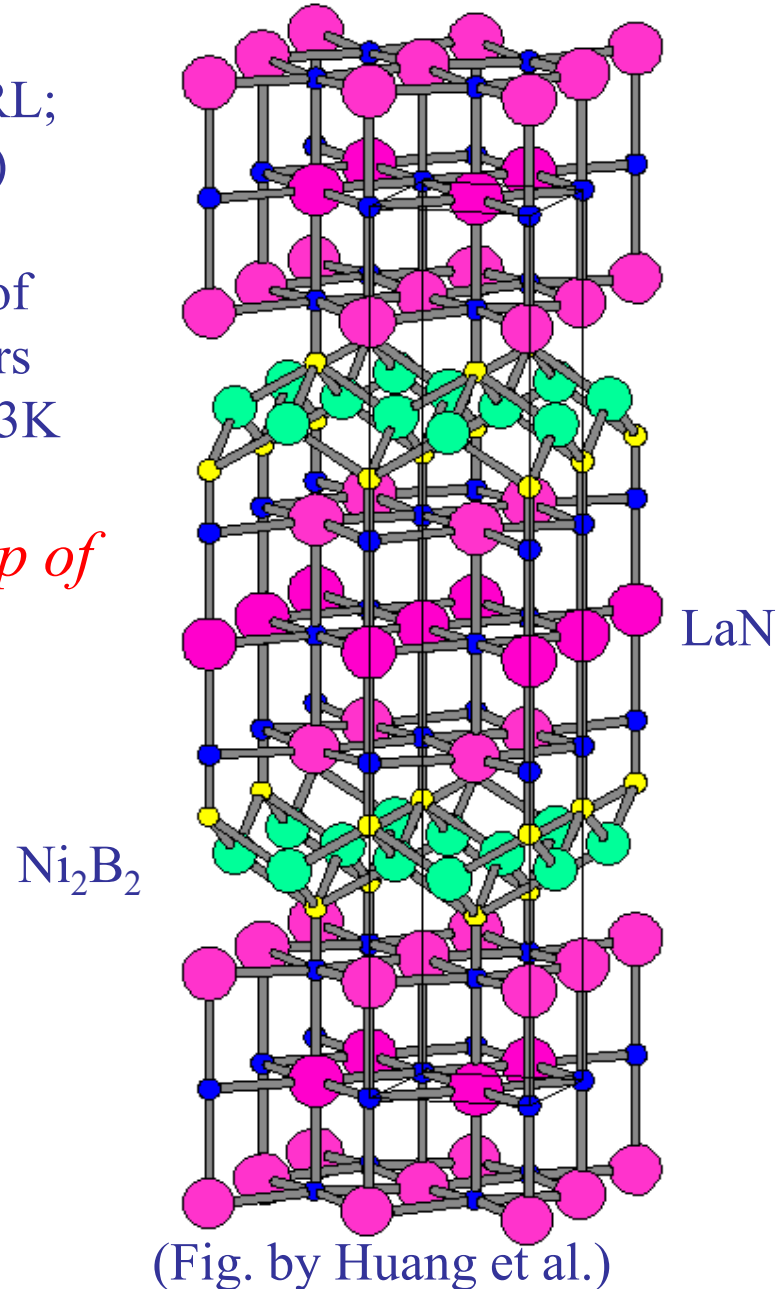
M. Opel



NEWS: 1994
(Nagarajan, PRL;
Cava, Nature)

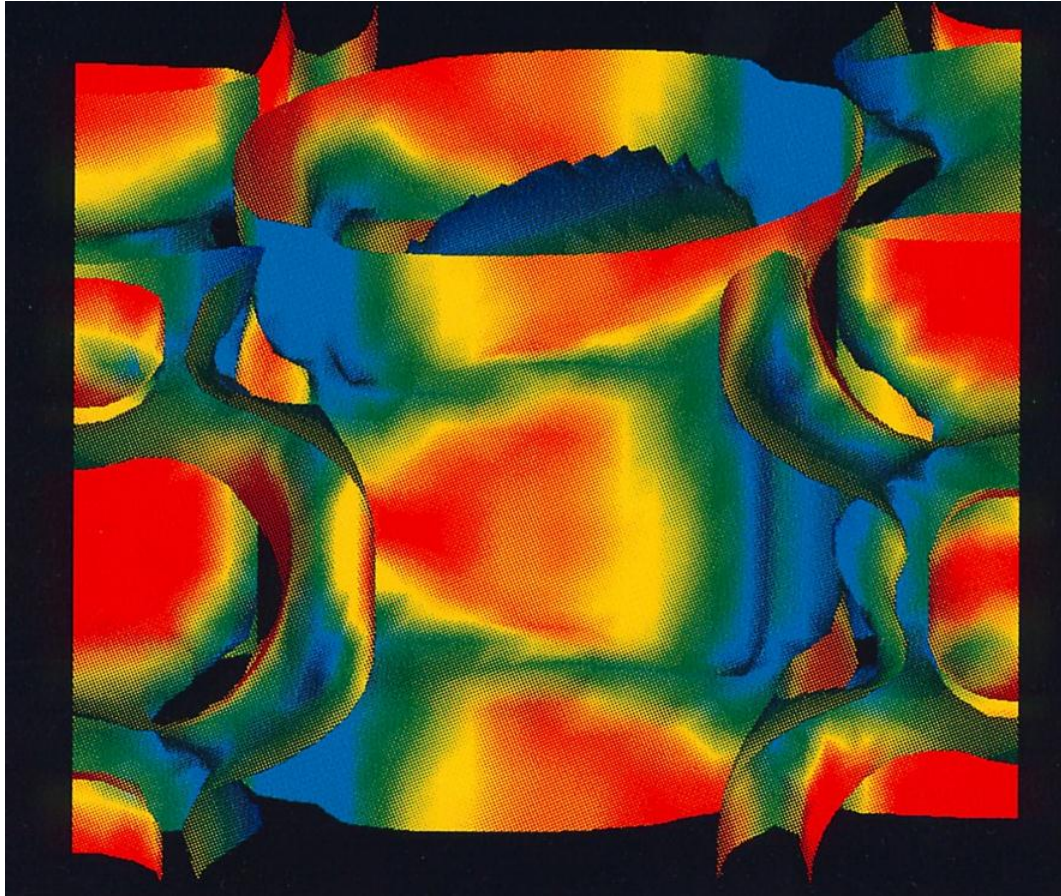
A new family of
superconductors
with T_c up to 23K

*Is 23K the tip of
the iceberg?*



ANSWER: 1994 (Pickett and Singh, PRL) **NO!**

Fermi Surface of $\text{YNi}_2\text{B}_2\text{C}$ ($T_c=16\text{K}$)



- Electronic structures are very three dimensional
- Due to strong B-C bonds
- Large electron phonon coupling is responsible for superconductivity (conventional mechanism).
- **NOT THE BASIS OF A NEW FAMILY OF HIGH TEMPERATURE SUPERCONDUCTORS**

Density Functional Theory

Standard approach: properties are governed by a wavefunction:

$$\Psi(\mathbf{r}_1, \mathbf{r}_2, \dots, \mathbf{r}_N) ; H\Psi = E\Psi$$

Given the Hamiltonian, we focus on solving for the wavefunction and extract observables as expectation values of operators with this wavefunction – for N electrons this is a $3N$ dimensional problem.

Density Functional Theory: Hohenberg-Kohn theorem tells us

- Energy and other observables of the ground state are given as functionals of the density $\rho(\mathbf{r})$ which exists in 3 dimensions only.
- The ground state density is unique and is the density that minimizes this functional.

$$E = E[\rho] ; \rho = \min_{E[\rho]} \{\rho\}$$

The functional E is proven to exist, but is not given by the theorem.

Kohn-Sham Approach

Any density N electron density can be written as the density corresponding to an N electron Slater determinant (never mind that the true wavefunction cannot).

$$\rho(\mathbf{r}) = \sum \varphi_i(\mathbf{r})^* \varphi_i(\mathbf{r}) ; i=1,2, \dots , N$$

Where the $\varphi_i(\mathbf{r})$ are the Kohn-Sham orbitals

→ variational principle for ρ yields a variational principle for the $\varphi_i(\mathbf{r})$.

Kohn and Sham then separated terms that should be large in the functional leaving a (hopefully) small remainder as the unknown functional.

$$E[\rho] = T_s[\rho] + E_{ext}[\rho] + U_{Hartree}[\rho] + E_{xc}[\rho]$$

where, like E , E_{xc} is unknown. E_{xc} is defined by this equation.

Kohn-Sham Equations

Use the variational principle to write single particle equations for the Kohn-Sham orbitals.

$$\{T_s + V_{ext} + V_{Hartree} + V_{xc}\} \varphi_i = \varepsilon_i \varphi_i$$

$$\rho(\mathbf{r}) = \sum \varphi_i(\mathbf{r})^* \varphi_i(\mathbf{r}) ; i=1,2, \dots , N$$

Here, $V_{hartree}$ and V_{xc} are functionals of the density (functional derivatives of the energy terms with respect to density), so generally these equations must be solved self-consistently.

This is straightforwardly generalizable to magnetic systems via spin-density functional theory where instead of a single function one has spin-densities, $\rho_{\uparrow}(\mathbf{r})$ and $\rho_{\downarrow}(\mathbf{r})$ for the collinear case and a four component spinor for non-collinear.

The Local Density Approximation

Generally one may write

$$E[\rho] = \int \rho(\mathbf{r}) \varepsilon_{xc}[\rho](\mathbf{r}) d^3\mathbf{r}$$

The local (spin) density approximation consists of taking $\varepsilon_{xc}[\rho]$ at each point \mathbf{r} as the value for the uniform electron gas at the density for this \mathbf{r} .

This exceedingly simple approximation works remarkably well, especially considering that the electron gasses of solids are nothing close to the uniform electron gas.

Theory of static structural properties, crystal stability, and phase transformations: Application to Si and Ge

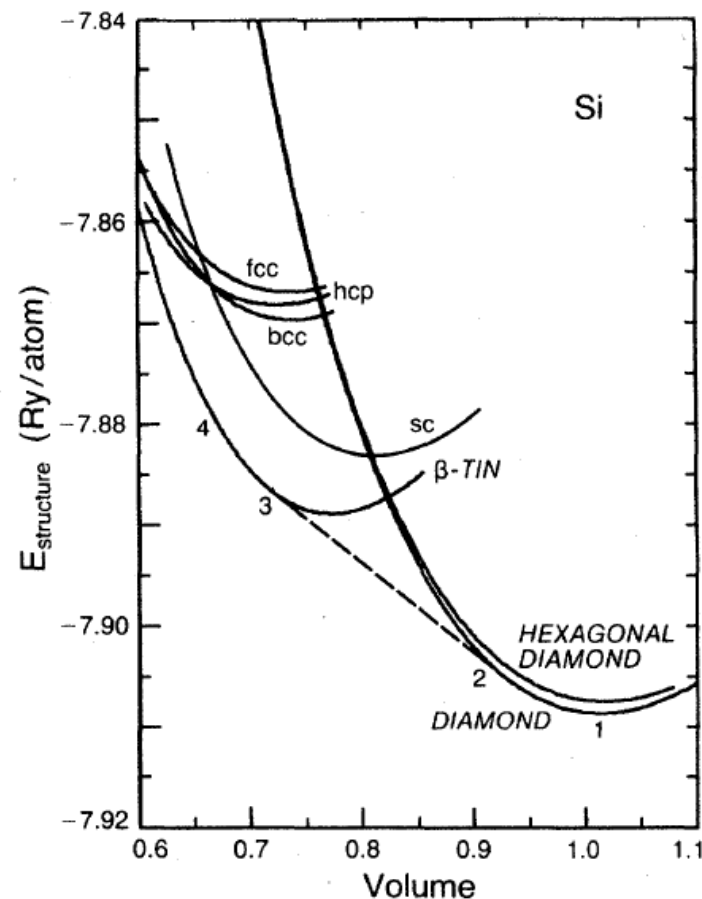
M. T. Yin* and Marvin L. Cohen

*Department of Physics, University of California, Berkeley, California 94720
and Materials and Molecular Research Division, Lawrence Berkeley Laboratory,
Berkeley, California 94720*

(Received 29 March 1982)

TABLE II. Comparison of calculated and measured static properties of Si and Ge.

	Lattice constant (Å)	Cohesive energy (eV/atom)	Bulk modulus (Mbar)
Si			
Calculation	5.451	4.84	0.98
Experiment	5.429 ^a	4.63 ^b	0.99 ^c
Ge			
Calculation	5.655	4.26	0.73
Experiment	5.652 ^a	3.85 ^b	0.77 ^c



One of many early works of this type.

Modern Density Functionals

$$E[\rho] = \int \rho(\mathbf{r}) \varepsilon_{xc}[\rho](\mathbf{r}) d^3\mathbf{r}$$

(1) Local (spin) density approximation: $\varepsilon_{xc}[\rho](\mathbf{r}) = \varepsilon_{local}(\rho(\mathbf{r}))$

- Widely used, especially for metals.

(2) Generalized gradient approximations (GGA, Langreth, Perdew):

$$\varepsilon_{xc}[\rho](\mathbf{r}) = \varepsilon_{gga}(\rho(\mathbf{r}), |\nabla\rho(\mathbf{r})|)$$

- Much improved binding energies compared to LDA (chemical accuracy).
- Not gradient expansions, but sophisticated functionals based on exact scaling relations for the inhomogeneous electron gas (electron gas in solids is very non-uniform – can't use gradient expansions).
- New versions, e.g. PBE-SOL, Wu-Cohen, give almost uniform improvement over LDA in structural properties.

Modern Density Functionals

(3) Hybrid functionals (Becke and others):

- Mixture of GGA and Hartree-Fock exchange on the Kohn-Sham orbitals.
- Common in chemistry and semiconductor physics (band gaps are better than standard LDA or GGA's).

(4) Van der Waal's Functionals (Langreth, Lundqvist):

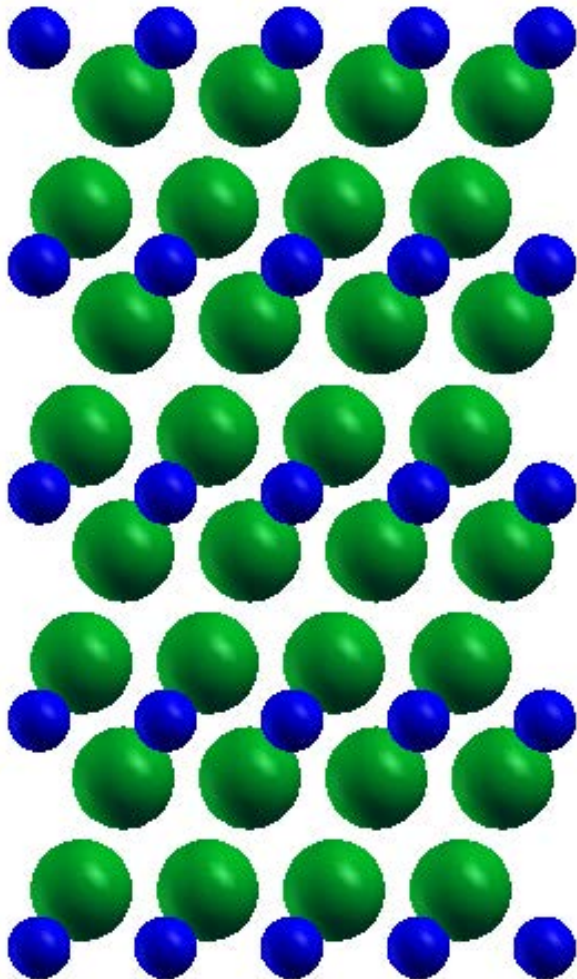
- Non-local functionals that incorporate dispersion interactions.
- Surface science, molecular systems, water, DNA, carbon materials, etc.

Salt

NaCl:

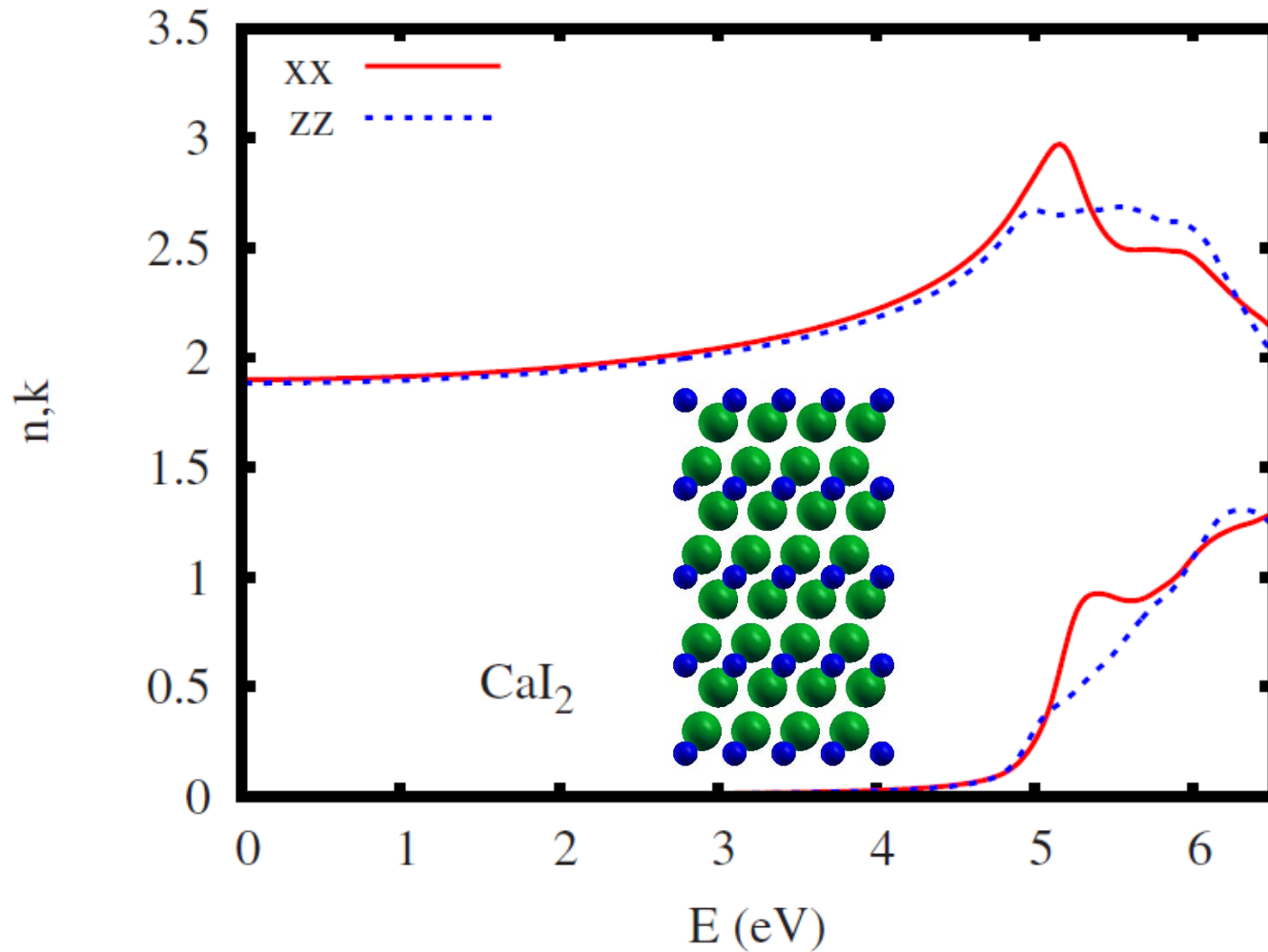
Halides (Cl, Br, I)

- Structures generally show cations in locally symmetric anion cages, but the overall lattice structures of halides are often very non-isotropic (Pauling Rules).



CaI_2 – light yield is $>100,000$ ph/MeV with Eu^{2+} activators (Hofstadter, 1964, Cherepy, 2008), but this has not proven useful because of *difficulties with crystal growth* – very anisotropic, micaceous, rhombohedral material that invariably cracks.

Optical Properties of CaI_2

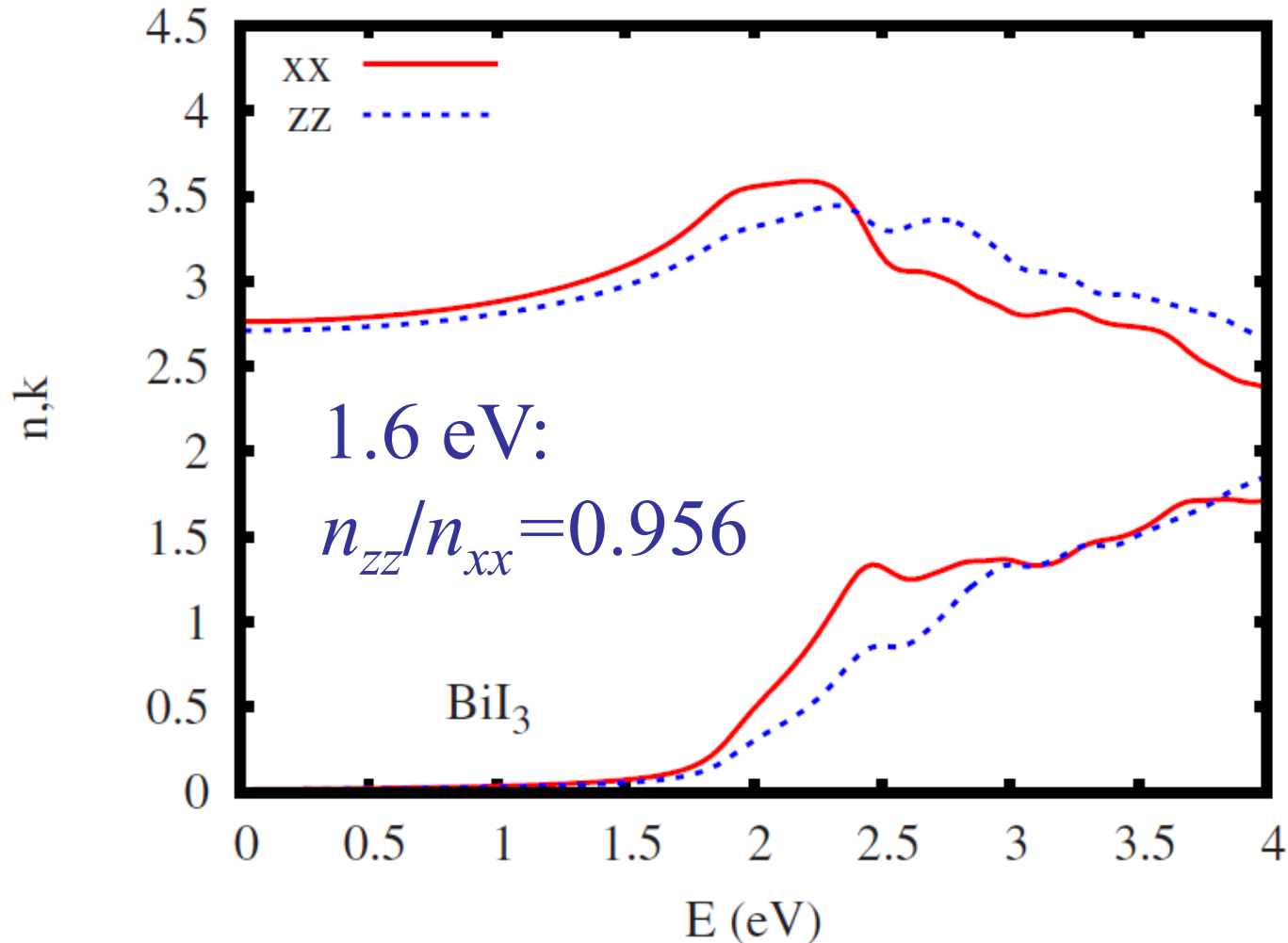


Low energy
limit:

$$n_{zz}/n_{xx} = 0.991$$

Not the expected result

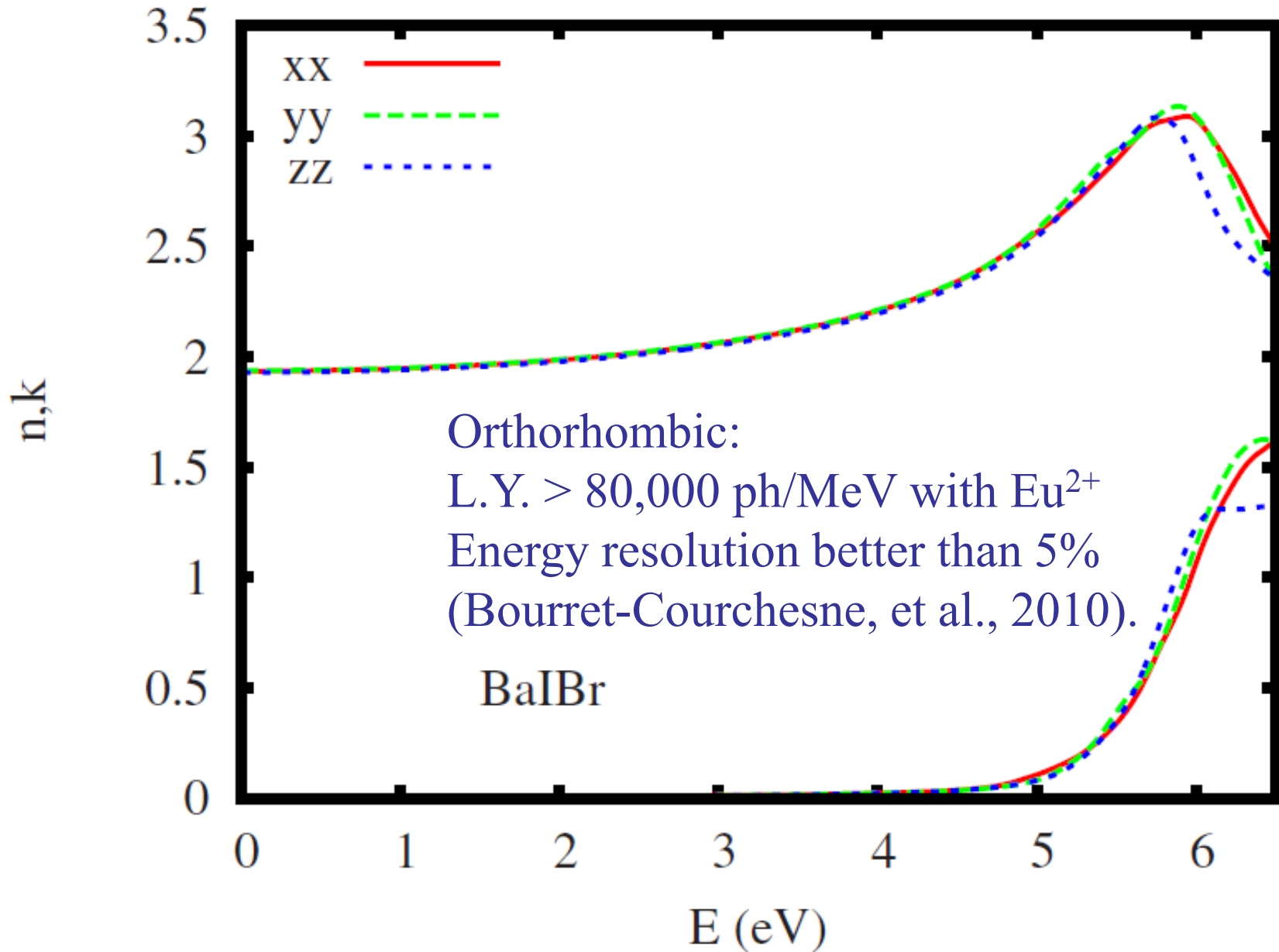
Not All Halides Are Near Isotropic



Measurements (G.E. Jellison, Jr., et al.): $n_{AV}(1.6 \text{ eV})=3.1$

First principles: $n_{AV}(1.6 \text{ eV})=3.11$ *in excellent agreement*

But we found that many are: BaI Br



Transparent Ceramics

Key:

High density ceramic.

Low light scattering due to use of cubic (isotropic) materials.

Crystal growth is not part of the process.

Casio transparent ceramic camera lens (2004).

Opportunity for lower-cost manufactured scintillators with uniform characteristics.

Predictive Theory

APPLIED PHYSICS LETTERS 92, 201908 (2008)

IEEE TRANSACTIONS ON NUCLEAR SCIENCE, VOL. 57, NO. 6, DECEMBER 2010

3827

Near optical isotropy in noncubic SrI₂: Density functional calculations

D. J. Singh^{a)}

Materials Science and Technology Division and Center for Radiation Detection Materials and Systems, Oak Ridge National Laboratory, Oak Ridge, Tennessee 37831-6114, USA

(Received 24 March 2008; accepted 1 May 2008; published online 22 May 2008)

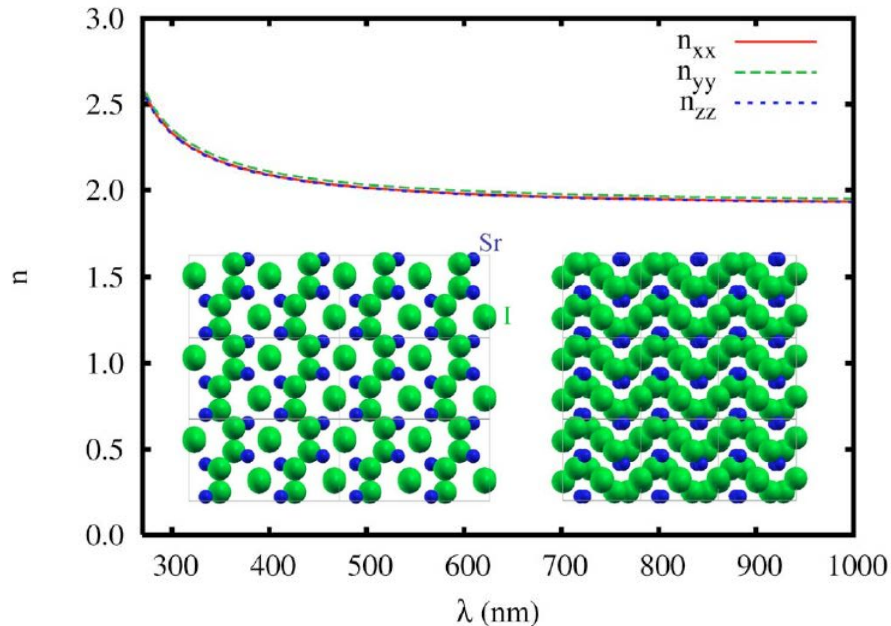


FIG. 4. (Color online) Wavelength dependent refractive index of SrI₂ as obtained with the Engel–Vosko GGA.

Fabrication and Properties of Translucent SrI₂ and Eu:SrI₂ Scintillator Ceramics

Stephen R. Podowitz, Romain M. Gaumé, Wesley T. Hong, Atfal Laouar, and Robert S. Feigelson

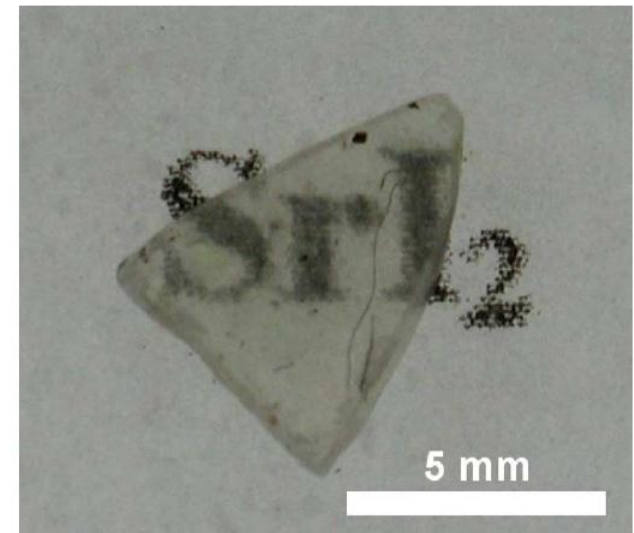


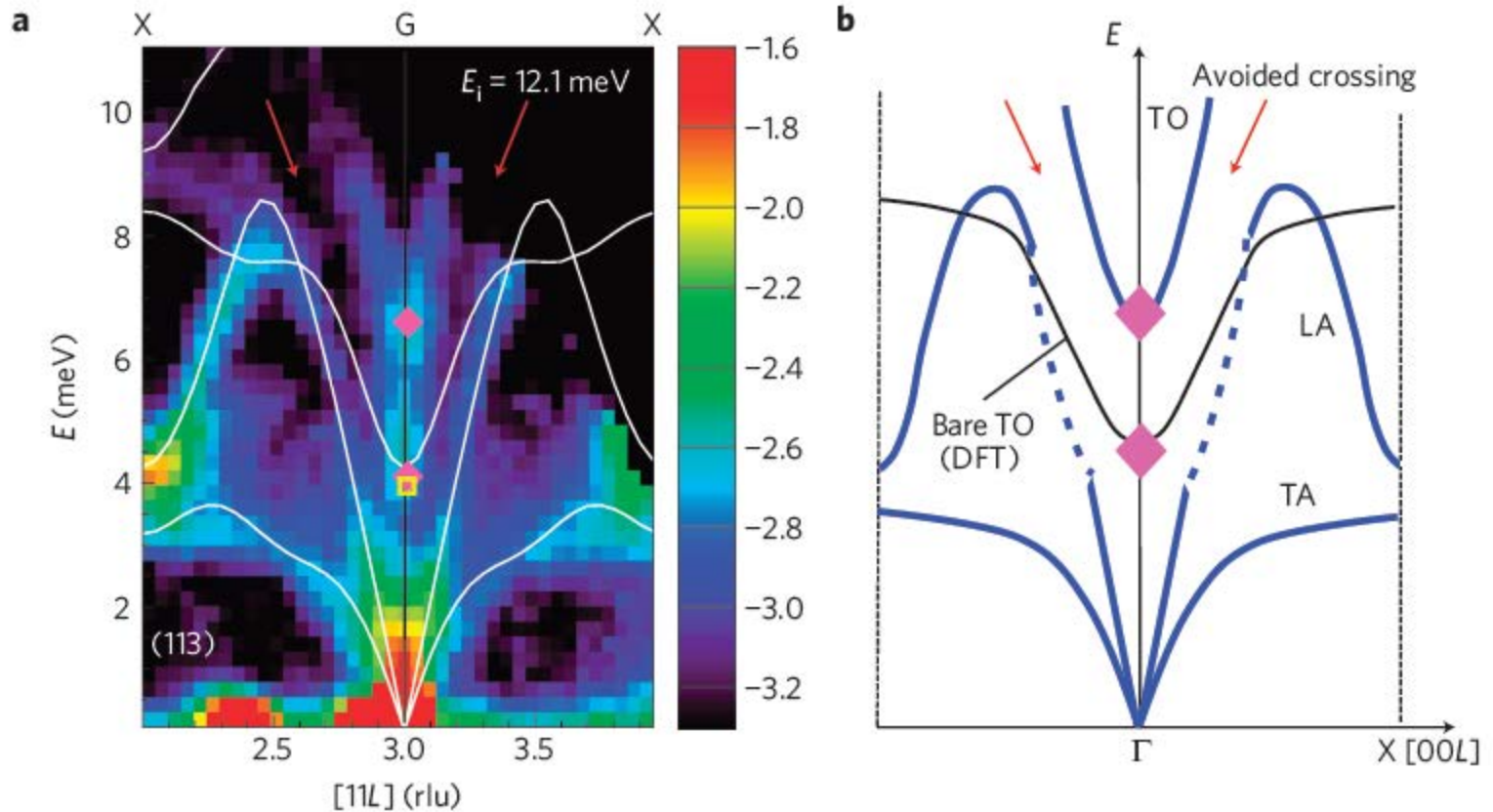
Fig. 5. Translucent ceramic sample of 0.77 mm-thick Eu:SrI₂ backlit.

First principles theory, not fit to experiment → results that can point in unanticipated directions.

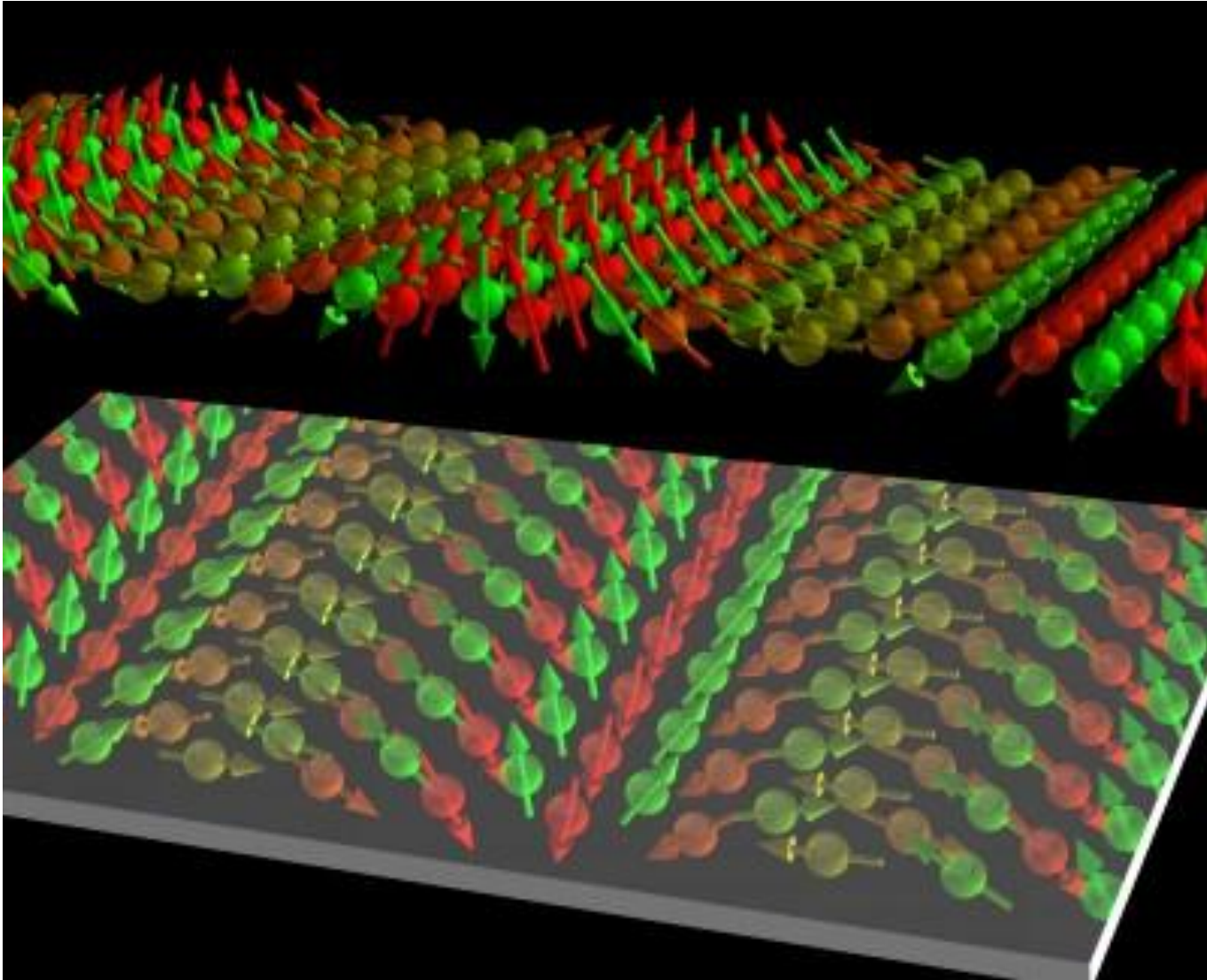
Dynamics

Giant anharmonic phonon scattering in PbTe

O. Delaire^{1*}, J. Ma¹, K. Marty¹, A. F. May², M. A. McGuire², M-H. Du², D. J. Singh², A. Podlesnyak¹, G. Ehlers¹, M. D. Lumsden¹ and B. C. Sales²

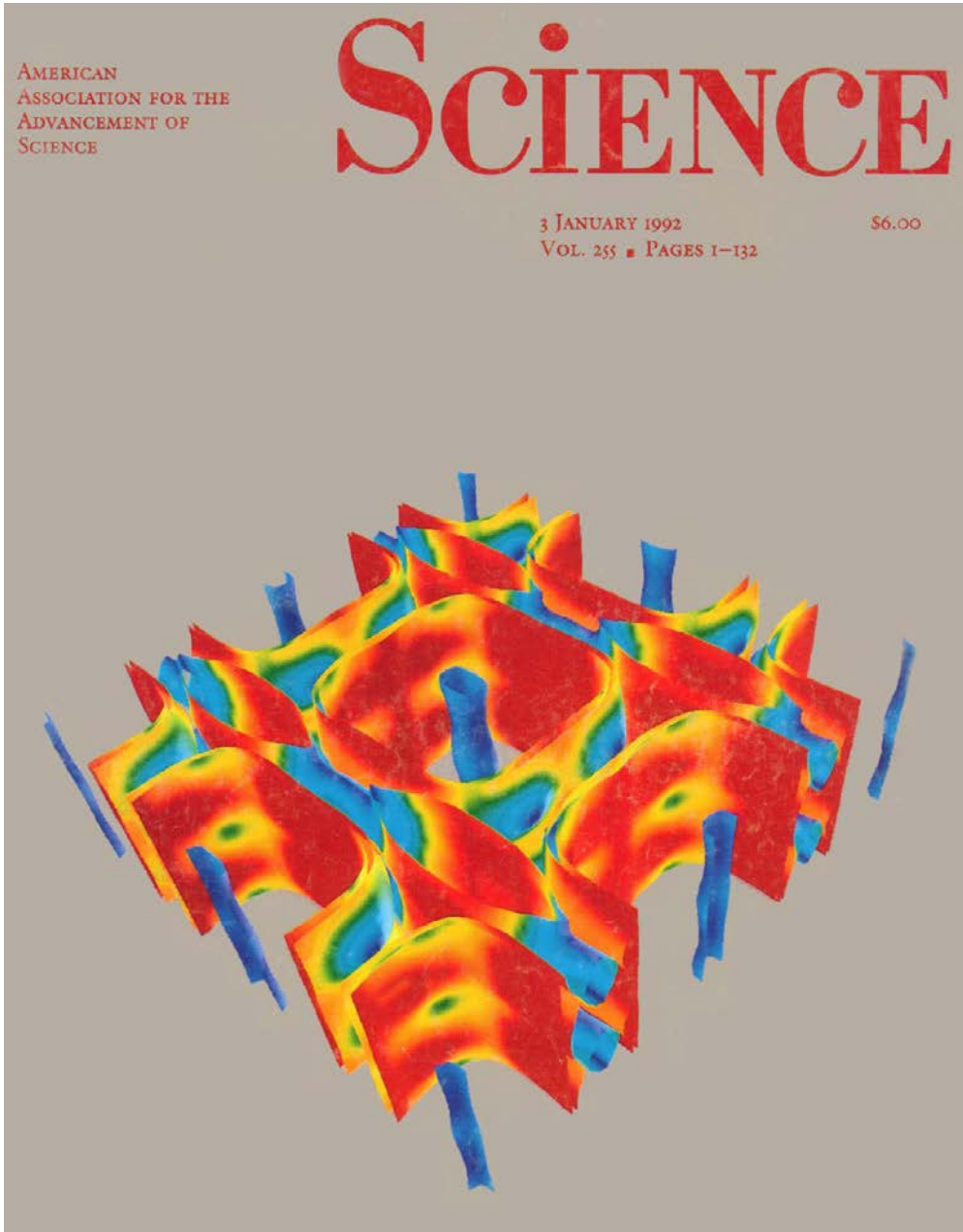


Magnetism



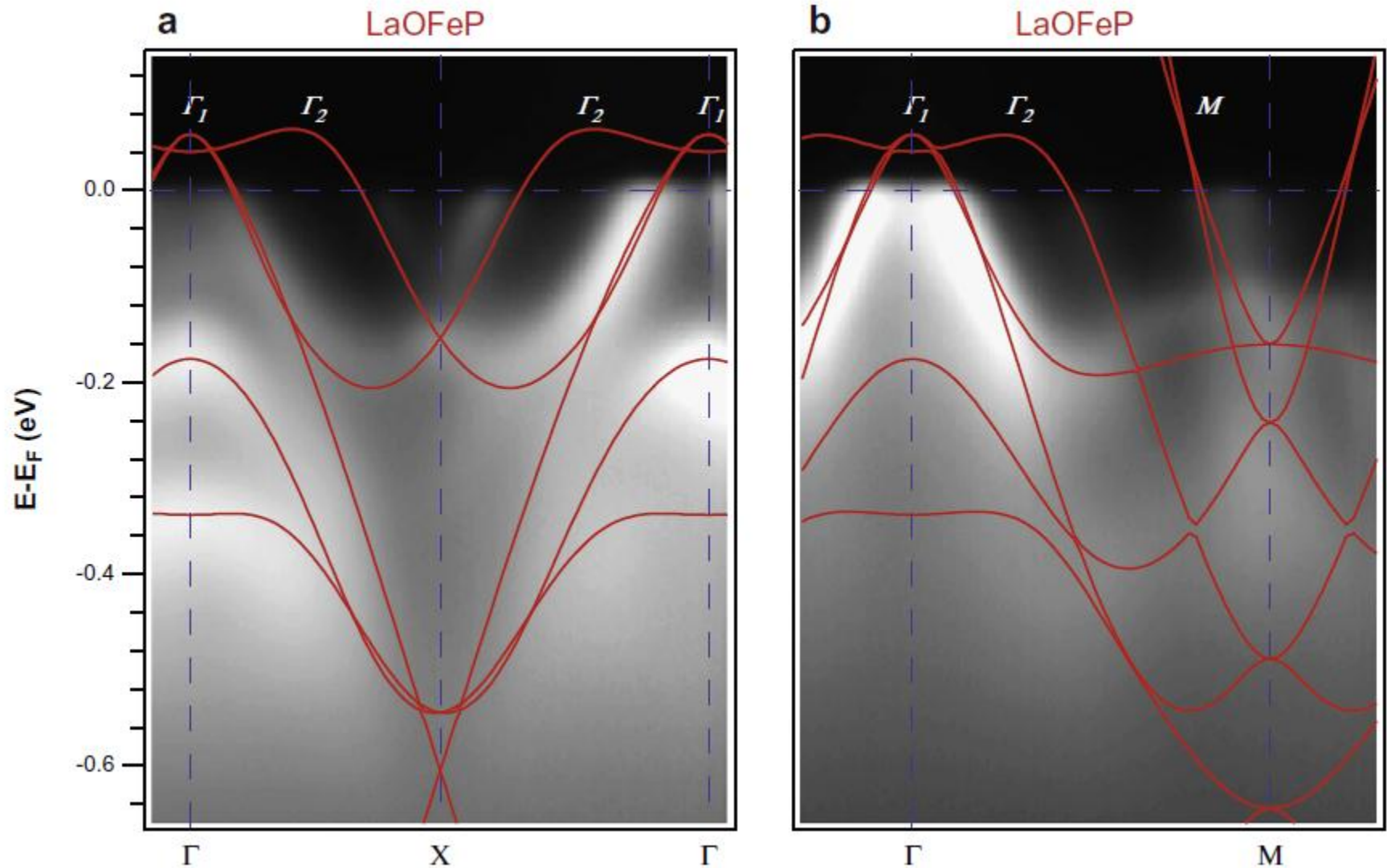
S. Blugel, Julich, Germany: Non-collinear magnetism on a thin film.

Fermi Surfaces



Based on Kohn-Sham eigenvalues, which are not fundamentally related to excitation energies in exact DFT – but this is known to be predictive and useful based on experience.

Band Structures



D.H Lu (2009)

Band Structure Related Quantities

- Optical properties.
- Excitation energies.
- Electronic transport.
- Electron-Phonon interactions.
- etc.

None of these are fundamental in DFT, but they are often quite accurate, and the inaccuracies are well established from much experience.

This is very useful because DFT is tractable, microscopic and predictive.

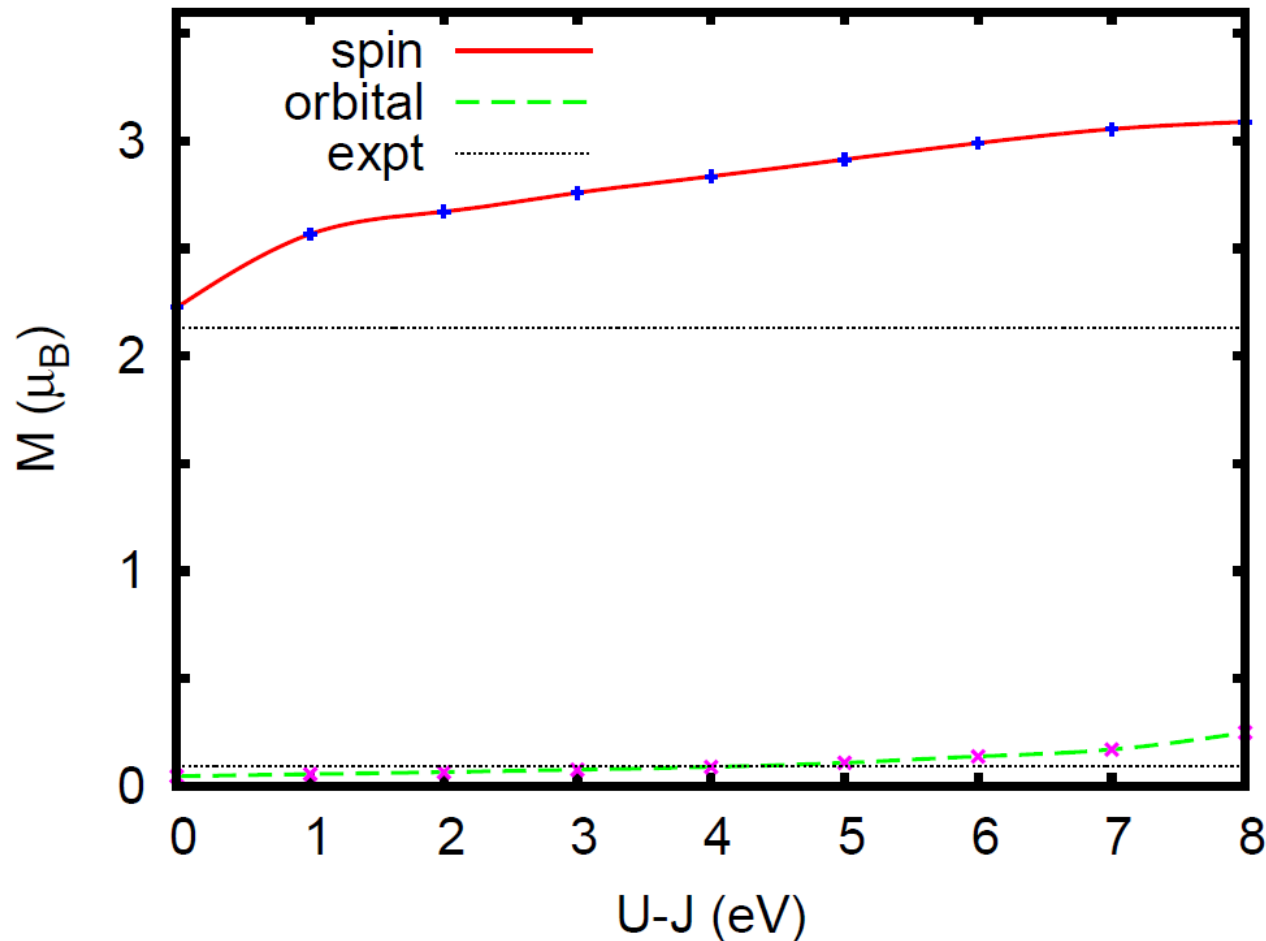
Hartree-Fock vs. Approximate DFT

- Hartree-Fock is a controlled approximation. Approximate DFT is not.
 - We can systematically improve Hartree-Fock, but with DFT we always have to “guess” about what is / is not already included. LDA+x need not be better than LDA (but it may very well be). ***Be Judicious.***
- Hartree-Fock gives poor results for materials. Modern approximate DFT is typically excellent for structures, energies etc.
- There are no metals, no stable Fermi surfaces and no Fermi liquids in Hartree-Fock. There are in DFT, perhaps too many.

Never equate DFT calculations with Hartree-Fock.

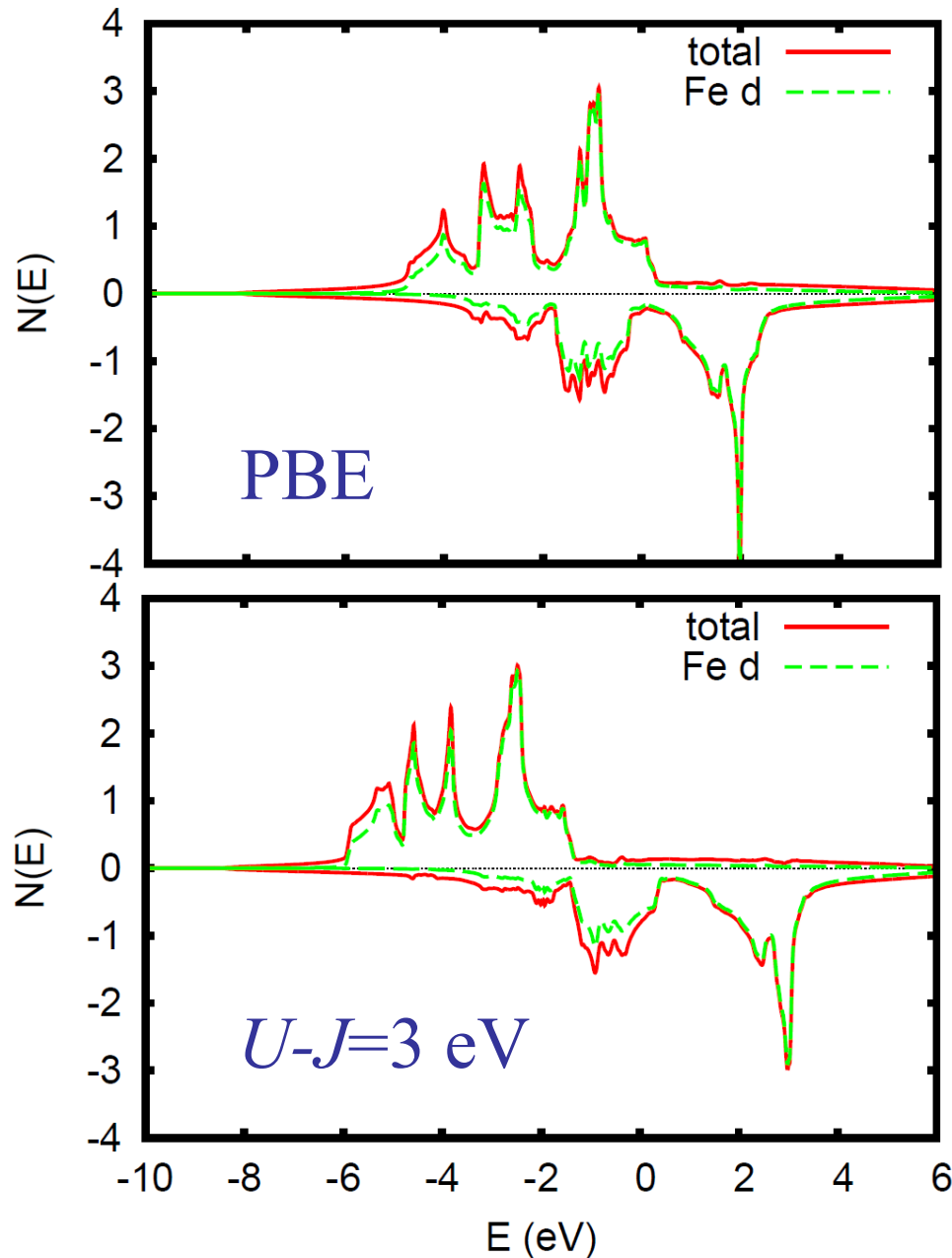
bcc Iron

- Ferromagnetic metal: $m_{spin}=2.13\mu_B$, $m_{orb}=0.09\mu_B$.
- LAPW calculations with GGA (PBE) and spin-orbit.
- LDA+U with SIC double counting.



	PBE	Expt.
m_{spin}	2.21	2.13
m_{orb}	0.05	0.09

bcc Iron (Ferromagnetic) Density of States



As U is increased go from metallic partially polarized $3d$ metal to a fully polarized metal with 5 electrons in the t_{2g} manifold \rightarrow expected ground state will become orbital ordered antiferromagnetic insulator.

References: DFT and Methods

1. H. Hohenberg and W. Kohn, *Phys. Rev.* **136**, B864 (1964); W. Kohn and L.J. Sham, *Phys. Rev.* **140**, A1133 (1965). *Foundation Papers for DFT.*
2. S. Lundqvist and N.H. March, *Theory of the Inhomogeneous Electron Gas* (Plenum, N.Y., 1983). *Excellent book on DFT.*
3. R.G. Parr and W. Yang, *Density functional theory of atoms and molecules* (Oxford, 1994). *Book with a chemical viewpoint.*
4. G.B. Bachelet, D.R. Hamann and M. Schluter, *Phys. Rev. B* **46**, 4199 (1982). *Norm conserving pseudopotentials and their use.*
5. J. Ihm, A. Zunger and M.L. Cohen, *J. Phys. C* **12**, 4409 (1979). *Total energy formalism for norm conserving pseudopotentials.*
6. D.J. Singh and L. Nordstrom, *Planewaves, Pseudopotentials and the LAPW Method, 2nd Ed.* (Springer, 2006). *Book about the LAPW method with some discussion of pseudopotentials.*
7. V. Eyert, *The Augmented Spherical Wave Method* (Springer, Berlin, 2007). *A detailed description of the ASW (closely related to LMTO) method.*
8. Richard M. Martin, *Electronic Structure of Matter* (Cambridge University Press, 2004). *Excellent overview of electronic structure methods and calculations.*

Magnetism and Superconductivity

⁴P. W. Anderson and A. H. Dayem, Phys. Rev. Letters 13, 195 (1964). See also J. Lambe, A. H. Silver, J. E. Mercereau, and R. C. Jaklevic, Phys. Letters 11, 16 (1964).

⁵A. H. Dayem and C. C. Grimes, Appl. Phys. Letters 9, 47 (1966).

⁶P. L. Richards, J. Opt. Soc. Am. 54, 1474 (1964).

⁷E. Riedel, Z. Naturforsch. 19a, 1634 (1964).

⁸N. R. Werthamer, Phys. Rev. 147, 255 (1966).

⁹I. K. Yanson, V. M. Svistunov, and I. M. Dmitrenko, Zh. Eksperim. i Teor. Fiz. 48, 976 (1965) [translation: Soviet Phys.—JETP 21, 650 (1965)]; D. N. Langenberg, D. J. Scalapino, B. N. Taylor, and R. E. Eck, Phys. Rev. Letters 15, 294, 842(E) (1965); D. N. Langenberg, D. J. Scalapino, and B. N. Taylor, Proc. IEEE 54, 560 (1966).

EFFECT OF FERROMAGNETIC SPIN CORRELATIONS ON SUPERCONDUCTIVITY*

N. F. Berk and J. R. Schrieffer

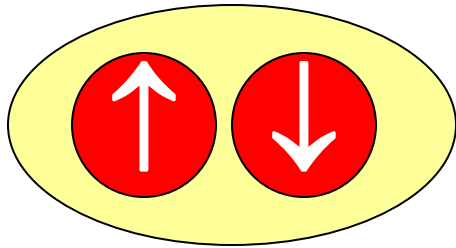
Department of Physics, University of Pennsylvania, Philadelphia, Pennsylvania

(Received 24 June 1966)

*Pd is not a superconductor because
of nearness to ferromagnetism.*

Bardeen Cooper Schrieffer - 1957

Singlet (s, d)



electron - polarization - electron

Hg, Pb, Cuprates

Singlet Channel:

*Charge fluctuations (phonons) are attractive.
Ferromagnetic fluctuations are pair breaking
Spin fluctuations in general are repulsive.*

Since electron phonon is always attractive the s -wave channel is most favored by it.

Inferred Phase Diagram

*Competition of superconductivity
and magnetism.*

T

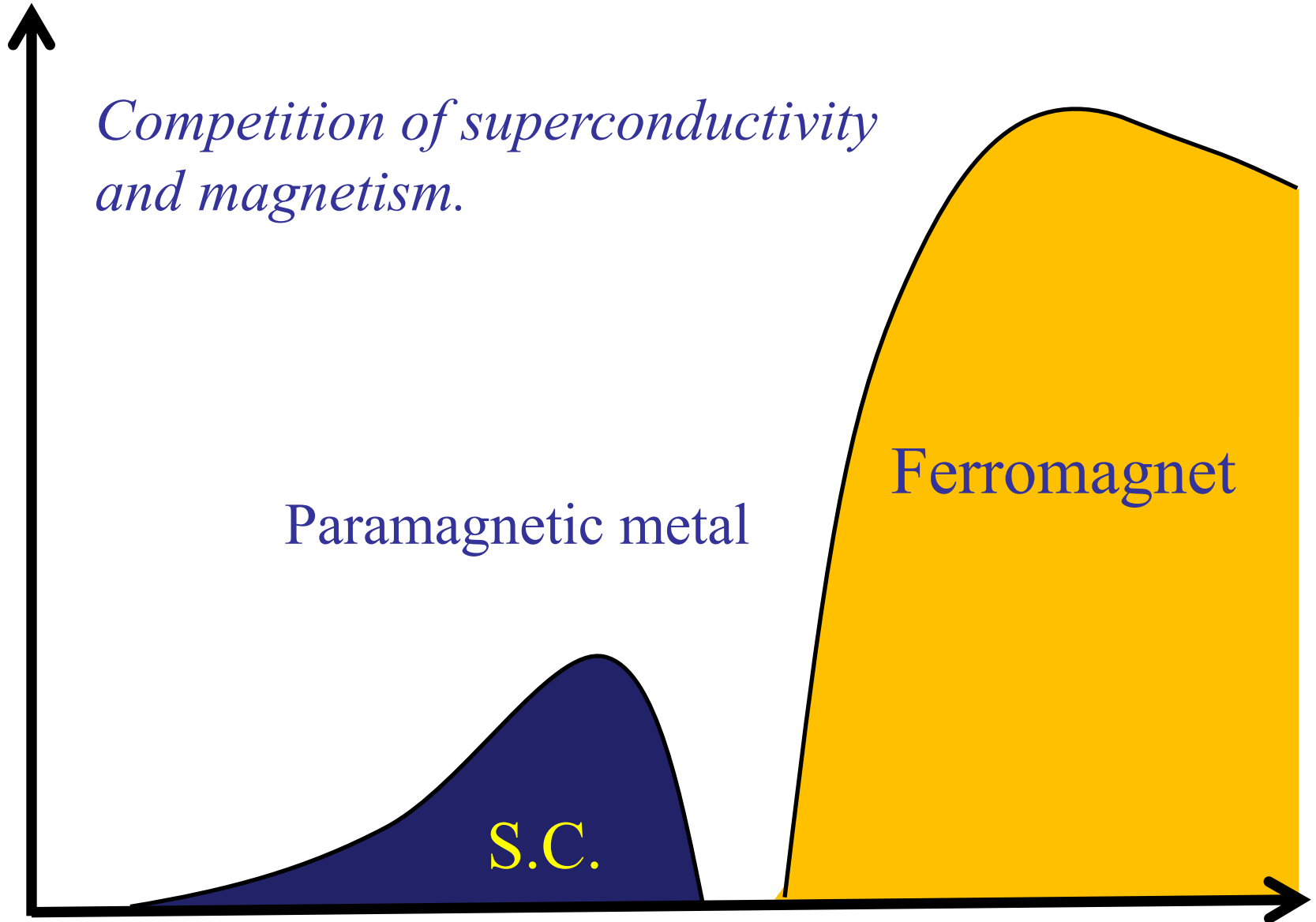
Paramagnetic metal

Ferromagnet

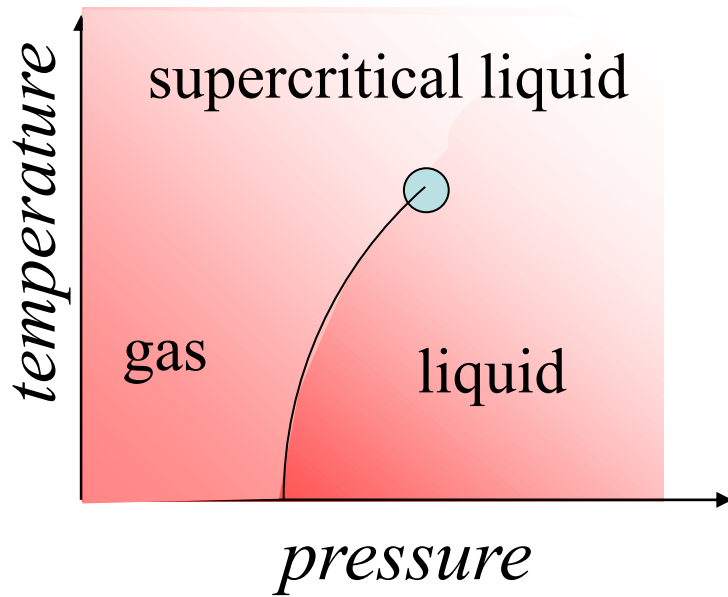
S.C.

$N(E_F)I$

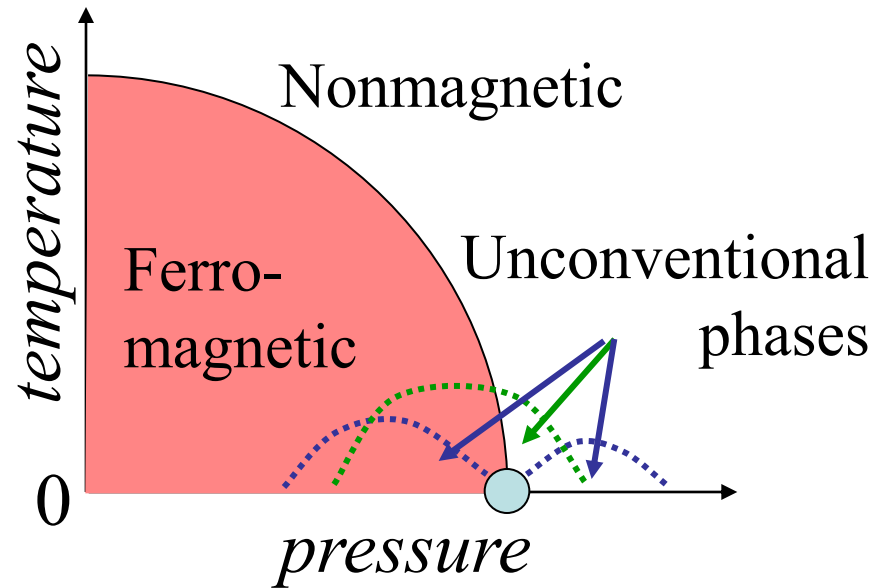
1.0



Metals Near Quantum Critical Points



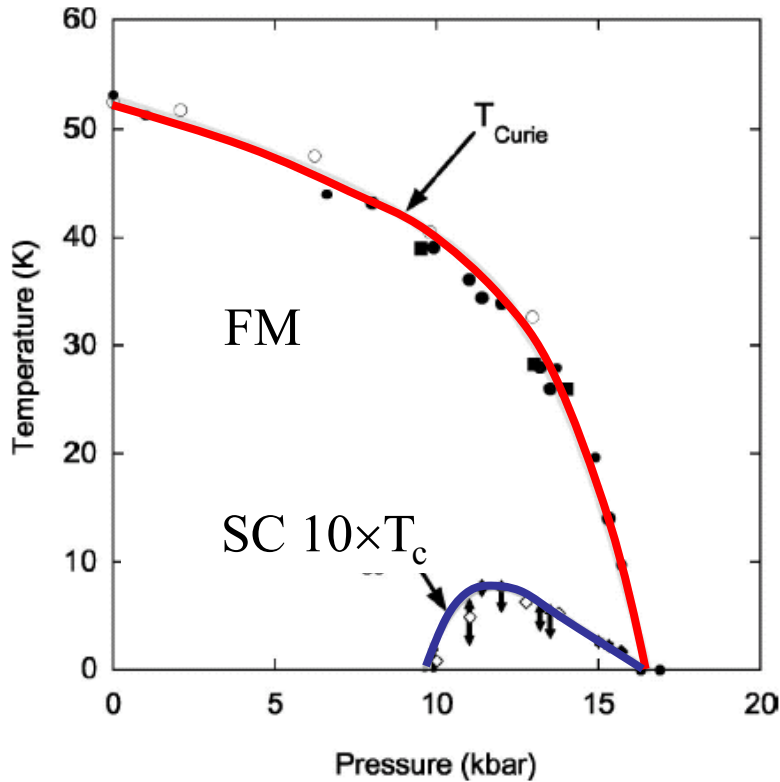
Classical criticality: Thermal density fluctuations grow indefinitely close to the Critical Point (CP).



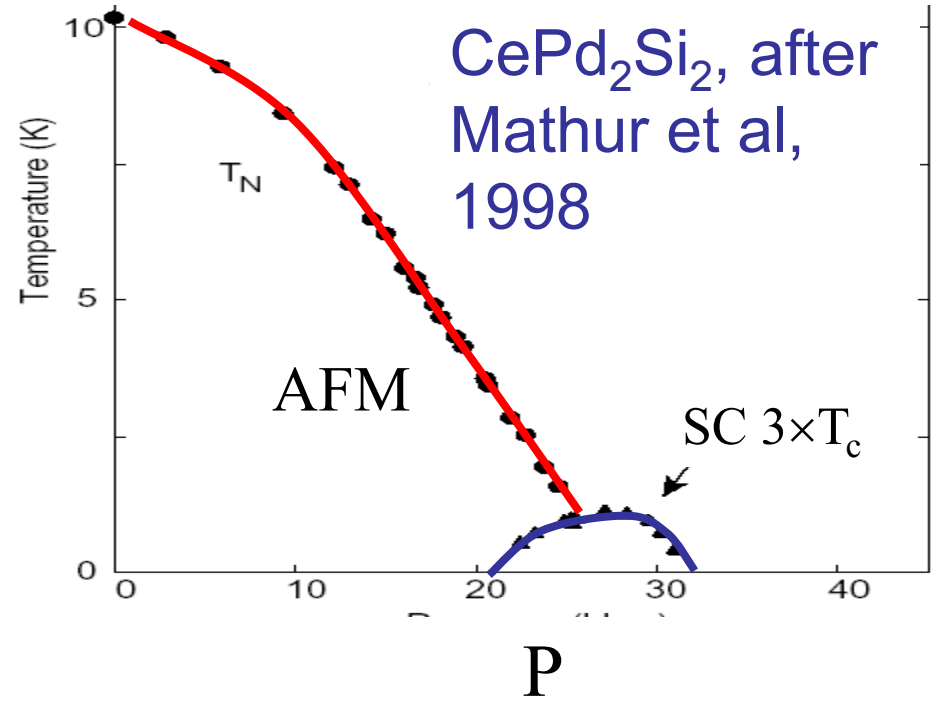
Quantum criticality: Quantum density fluctuations grow indefinitely close to the Quantum Critical Point (QCP).

Interesting things happen near critical points: In this region fluctuations are important and DFT does badly.

Something Different?



UGe_2 , after Huxley et al, 2001
and Saxena et al, 2000

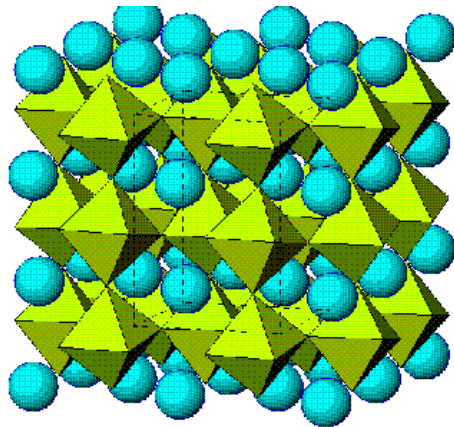


Interesting things may happen near critical points: In this region fluctuations are important and DFT does badly.

“Strontium Ruthenate”

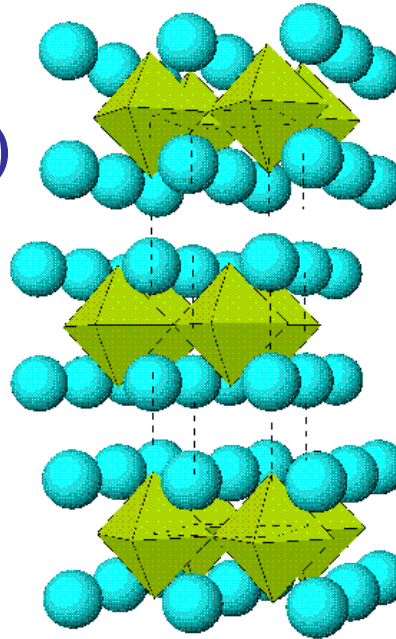


Ru^{4+} (4 d-electrons)



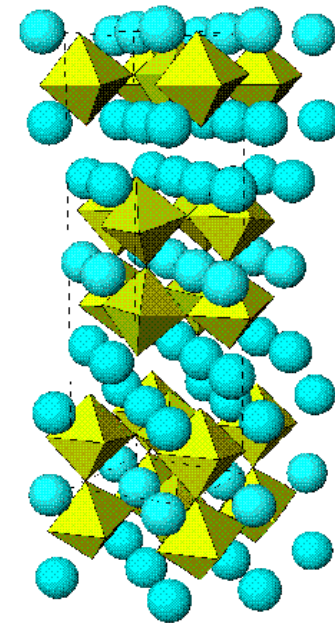
$n = \infty$

Ferromagnet



$n = 1$

Triplet
superconductor



$n = 2$

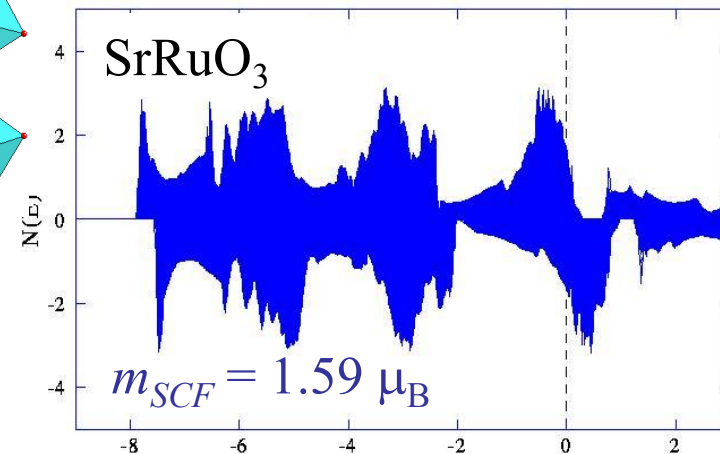
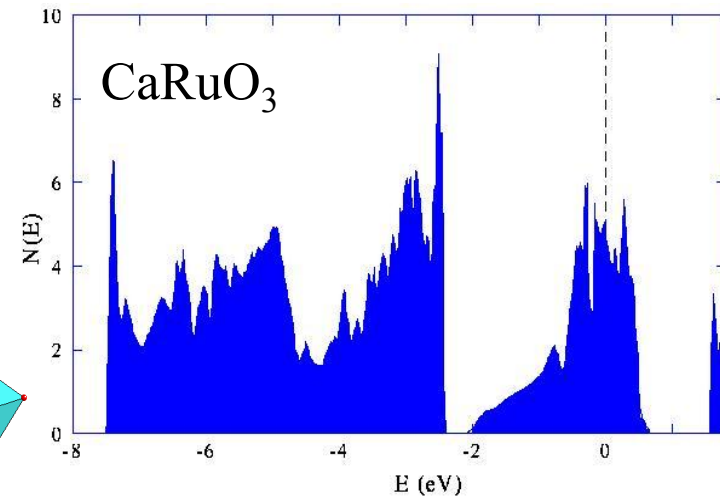
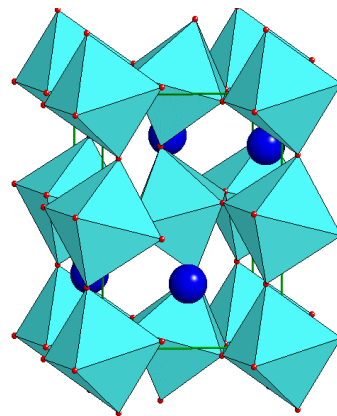
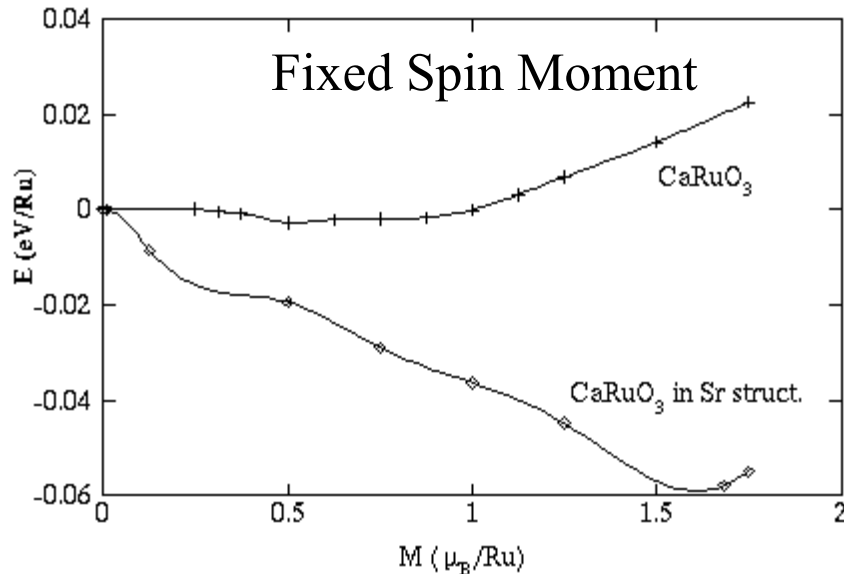
Metamagnetic
quantum critical
point

Magnetic Order in $\text{Sr}_{1-x}\text{Ca}_x\text{RuO}_3$

Experiment:

- SrRuO_3 is FM $T_C \sim 165\text{K}$.
- T_C fall smoothly with x , reaching 0 near $x=1$.
- CaRuO_3 was reported AFM, but now thought PM.

LSDA: Octahedral Tilt Broadens DOS.



Itinerant Stoner Explanation

STONER PICTURE

$$\Delta E = \frac{1}{2} \int_0^m [m' dm' / N(m')] - I_{TOT} m^2 / 4$$

$$\Delta E = - I_{TOT} m^2 / 4 = - \sum_{\alpha} I_{\alpha} m_{\alpha}^2 / 4$$

with $I_{TOT} = \sum_{\alpha} I_{\alpha} \nu_{\alpha}^2$

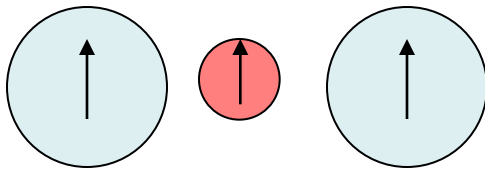
and $N = \sum_{\alpha} N_{\alpha} \nu_{\alpha}$

For SrRuO₃

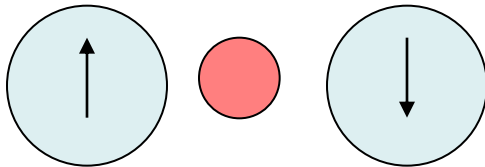
- $I_{TOT} = 0.41 \text{ eV}$

- $I_{Ru} = 0.35 \text{ eV}$

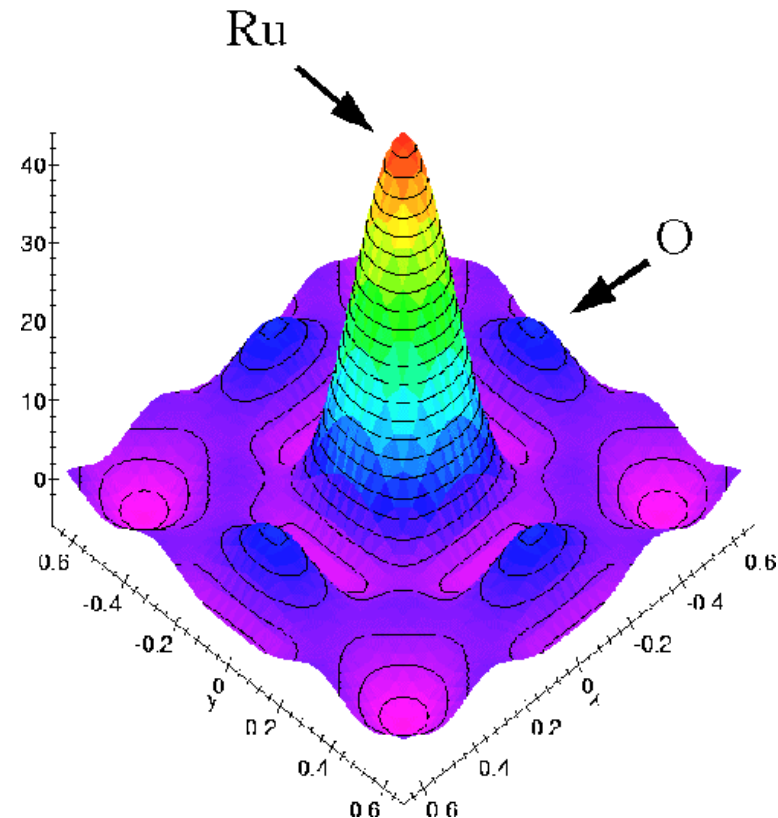
→ Significant on-site O contribution
- Favors Ferromagnetism.



- Over Antiferromagnetism.



Also band KE.



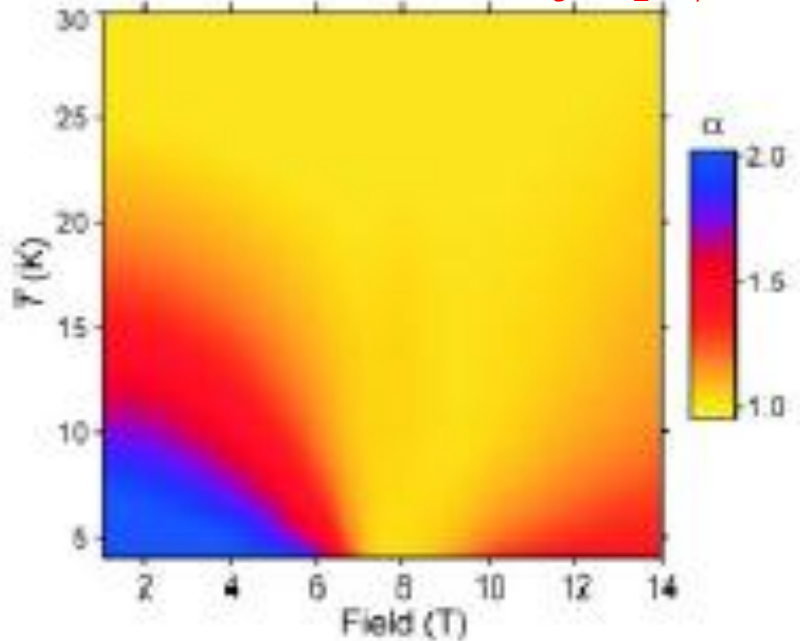
Nagler and Chakoumakos, ORNL

Quantum Critical Points and the LDA

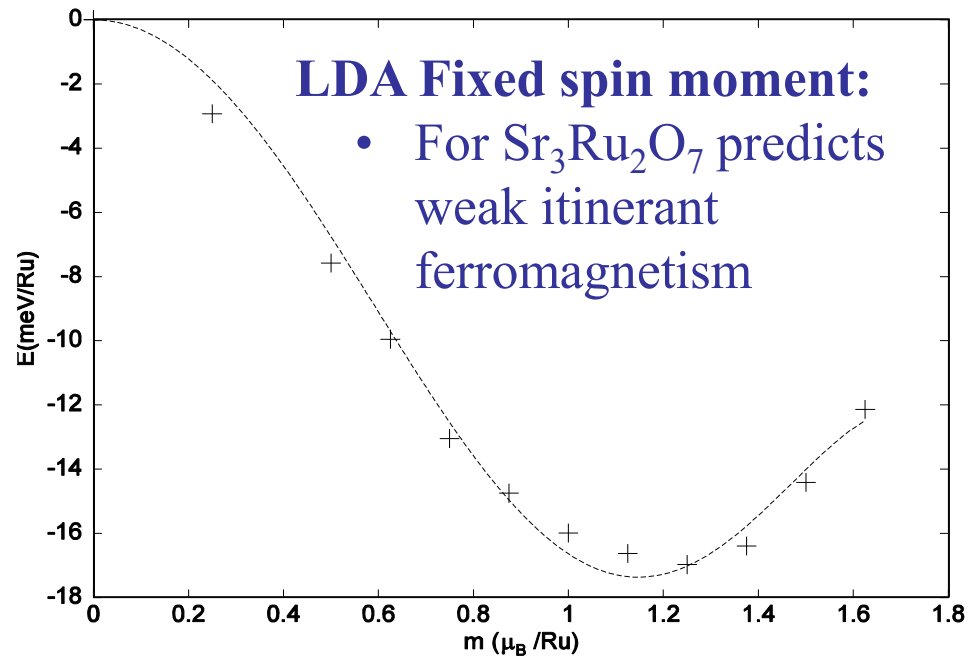
Density Functional Theory: LDA & GGA are widely used for first principles calculations but have problems:

- Mott-Hubbard: Well known poor treatment of on-site Coulomb correlations.
- Based on uniform electron gas. Give mean field treatment of magnetism: Fluctuations missing (generally small, but important near quantum critical points)

Resistivity exponent in $\text{Sr}_3\text{Ru}_2\text{O}_7$



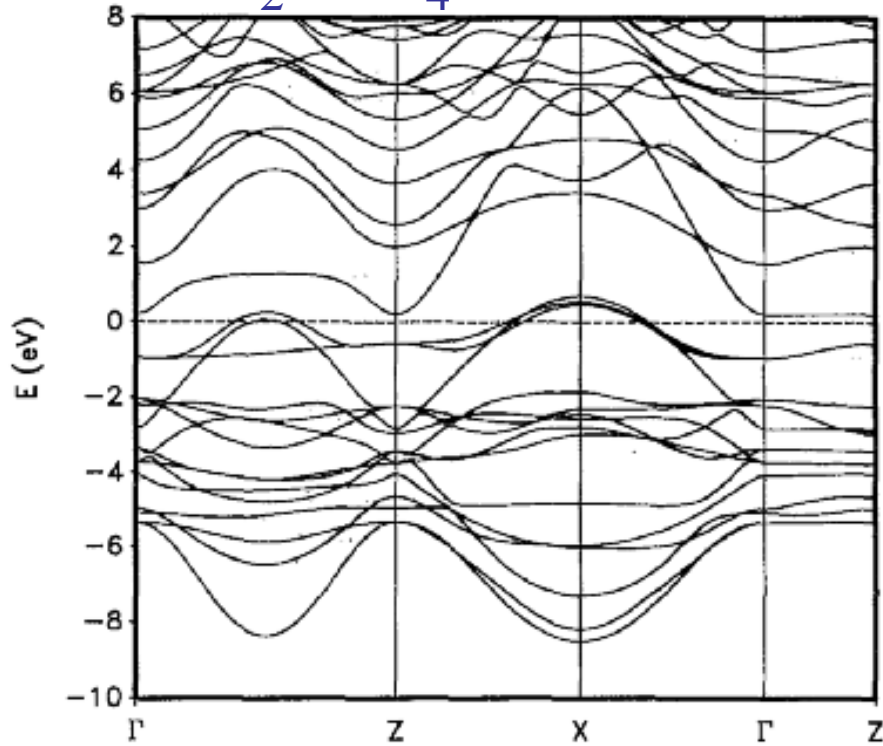
Grigera *et al.*, Science (2001).



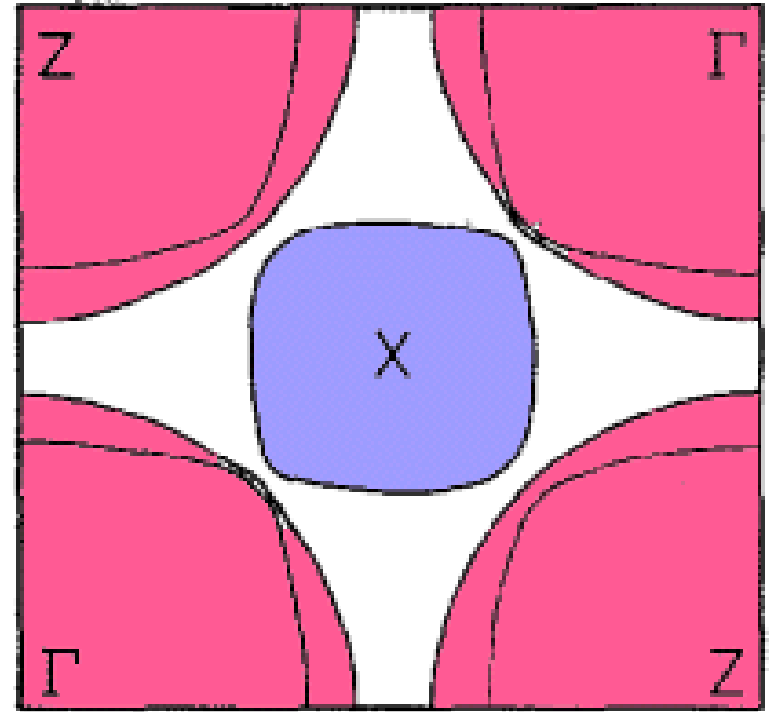
LDA overestimate of ferromagnetic tendency is a signature of quantum critical fluctuations – neglected fluctuations suppress magnetism

Electronic Structure of Sr_2RuO_4

Sr_2RuO_4 - $I4/mmm$



• 3 t_{2g} derived bands at E_F : d_{xy} , d_{xz} , d_{yz} .



- Highly 2D electronic structure.
- FS agrees in detail with dHvA.
- Mass renormalizations ~ 4

What are the pairing interactions on the FS? Unconventional symmetry \rightarrow not electron-phonon.

\rightarrow Spin-fluctuations?

SPIN-FLUCTUATIONS

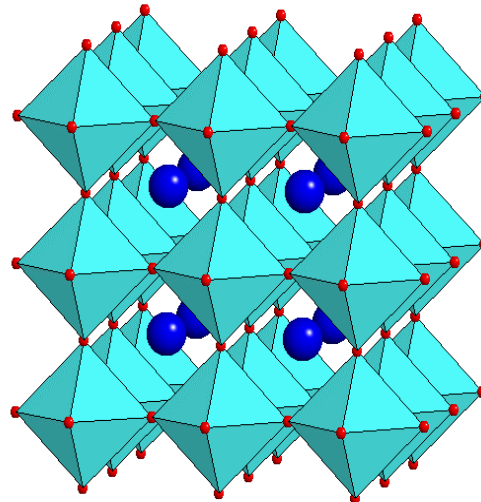
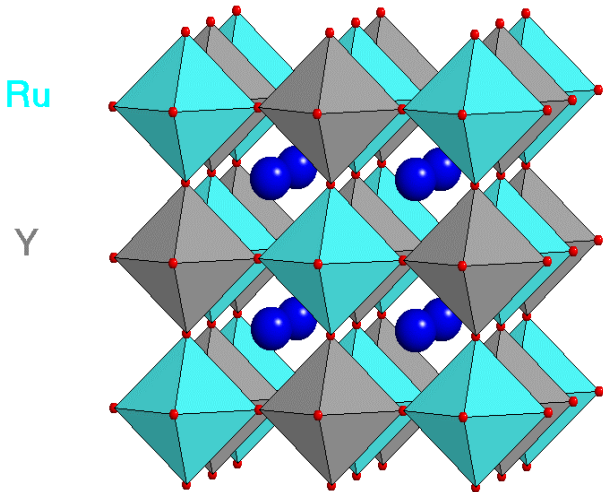
Ingredients:

1. On-Site Stoner (O) - Ru-O hybridization

Sr_2YRuO_6 - no shared O
 $\text{Sr}_2\text{RuYO}_6 \rightarrow \text{AFM}$

SrRuO_3 - shared O
 $\rightarrow \text{FM}$

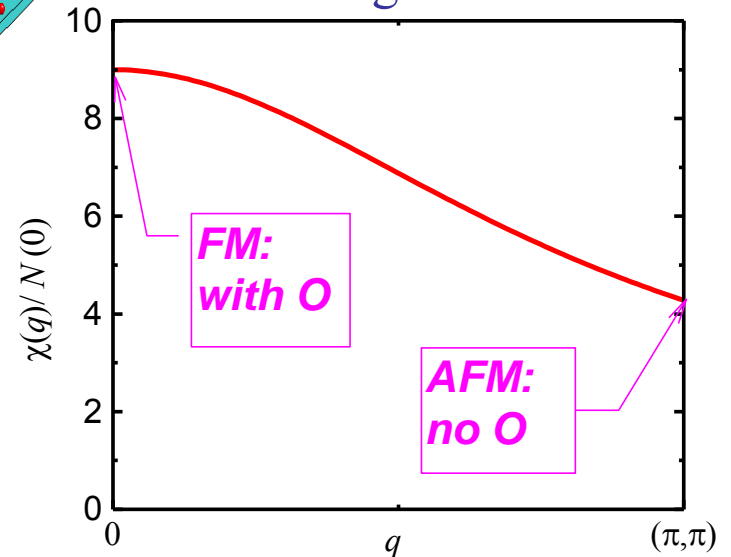
Sr_2RuO_4 - shared O
 $\rightarrow \text{FM}$ fluc.



- Shared O in RuO_2 planes will favor FM fluctuations.

- Can model by smooth background using calculations of
 - I_{Ru} and I_O .
 - Projections of $N(E_F)$.
 - Taking full O contribution at $\mathbf{k}=(0,0)$ and no O contribution at $\mathbf{k}=(\frac{1}{2},\frac{1}{2})$.

Ferromagnetic Part



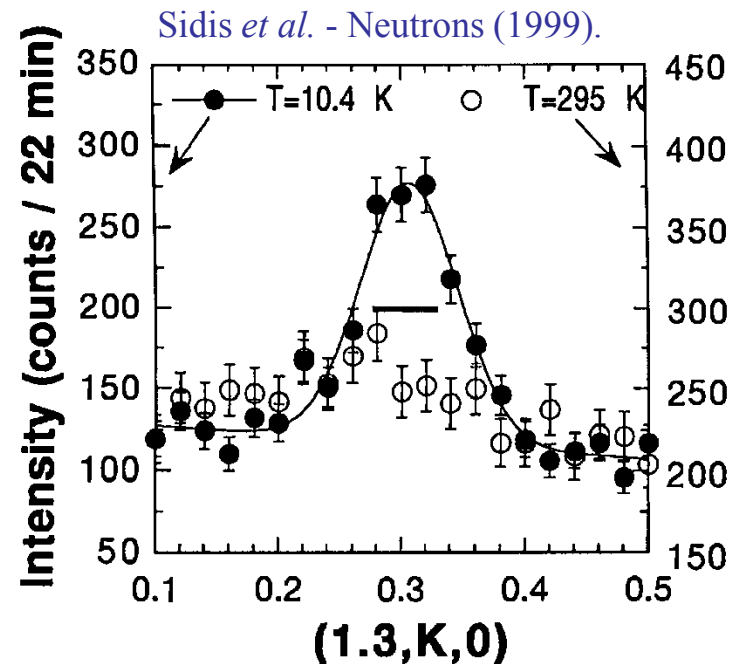
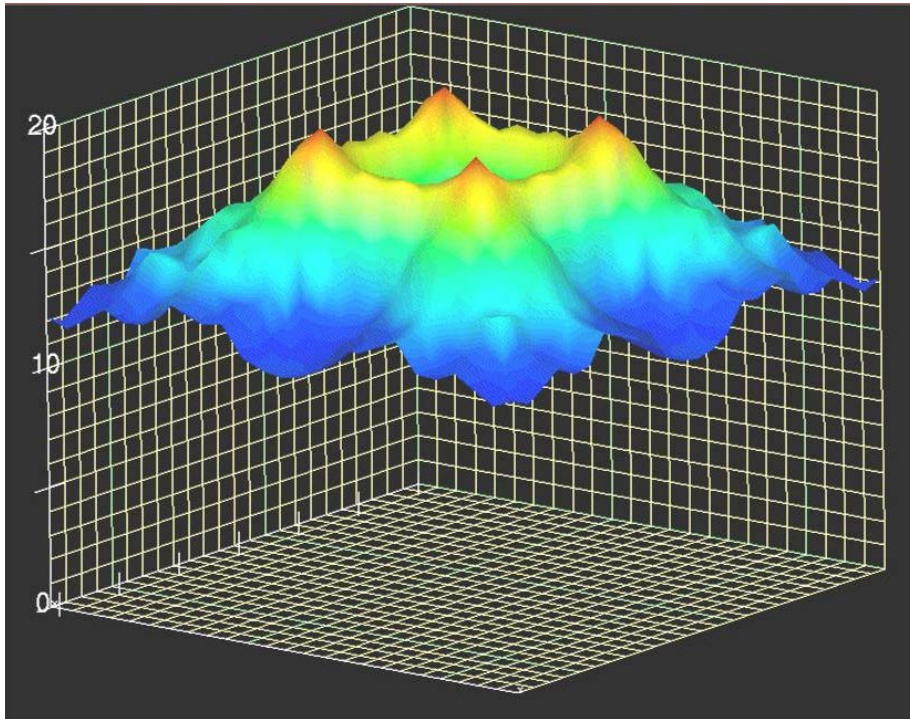
SPIN-FLUCTUATIONS (CON'T)

2. Nesting:

$$\chi(\mathbf{q}) = \frac{\chi_0(\mathbf{q})}{1 - I(\mathbf{q})\chi_0(\mathbf{q})}$$

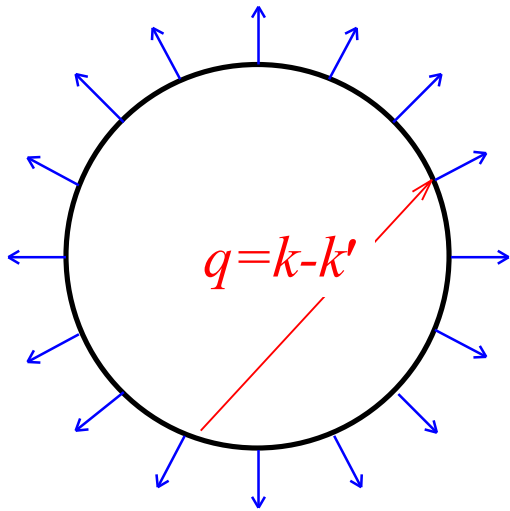
Previous slide had $I(q)$ from Stoner but no \mathbf{q} dependence in χ_0

Fermi Surfaces: Simple and 2-dimensional \rightarrow strong nesting.



SUPERCONDUCTIVITY

e.g.



Triplet works in BCS gap equation provided that the pairing at small \mathbf{q} is dominant (s.f. are attractive for triplet).

- Non- s depends on q dependence in $V(q)$.
- Generally higher ℓ needs more structure in $V(q)$.
- The details of the Fermi surface and $V(q)$ are crucial.

Singlet:

$$V(\mathbf{q}) = - \frac{I^2(q)\chi_0(\mathbf{q})}{1 - I^2(\mathbf{q})\chi_0(\mathbf{q})}$$

Triplet:

$$V(\mathbf{q}) = \frac{I^2(q)\chi_0(\mathbf{q})}{1 - I^2(\mathbf{q})\chi_0(\mathbf{q})}$$

Note signs

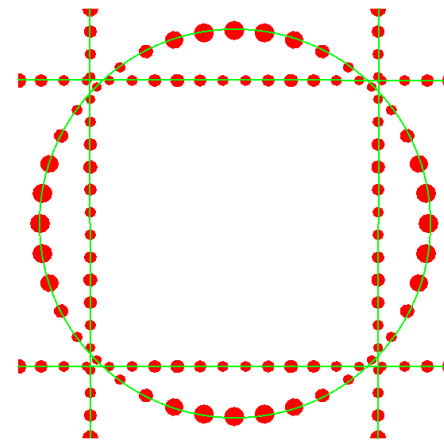
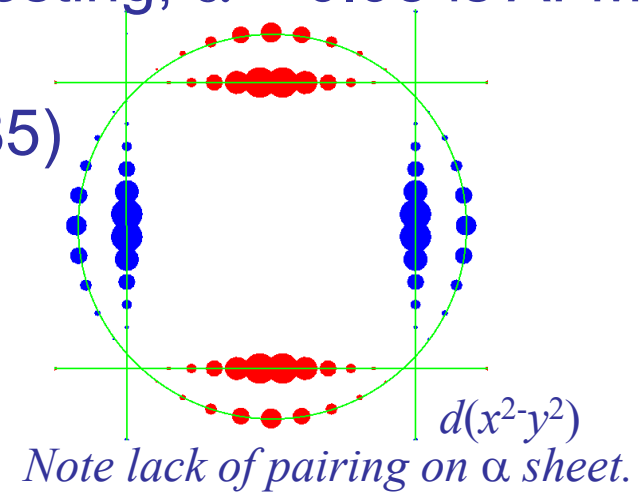
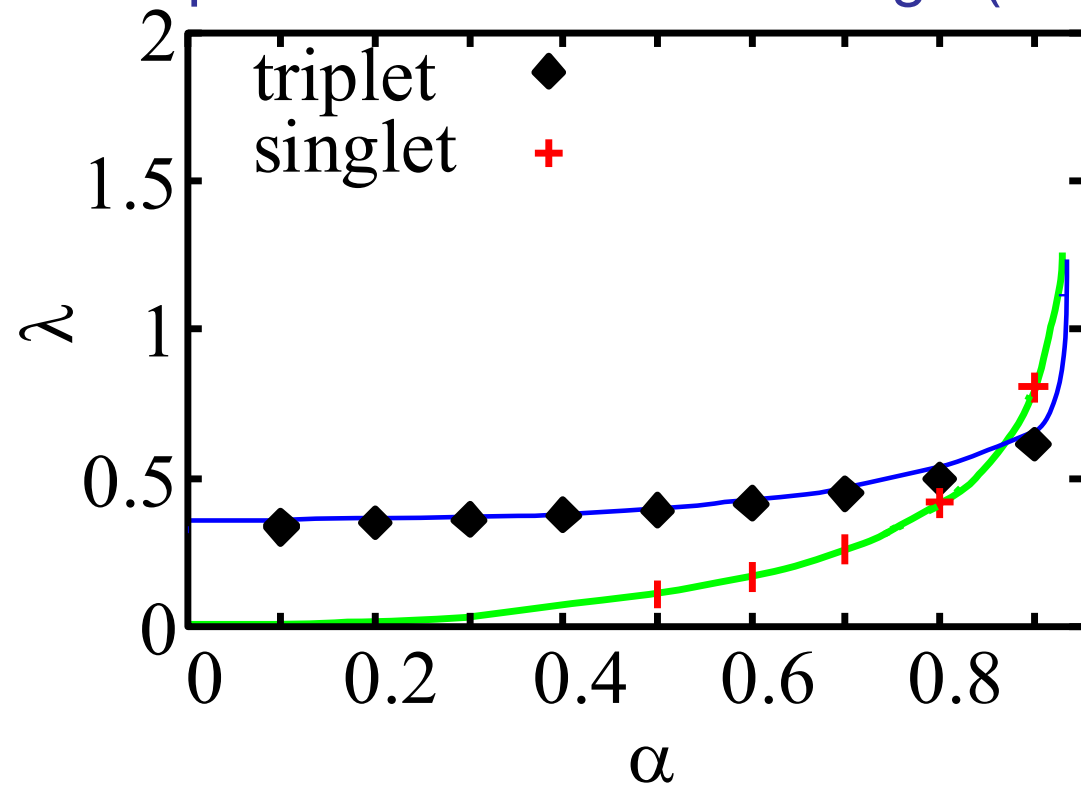
SUPERCONDUCTIVITY (Con't)

What we did:

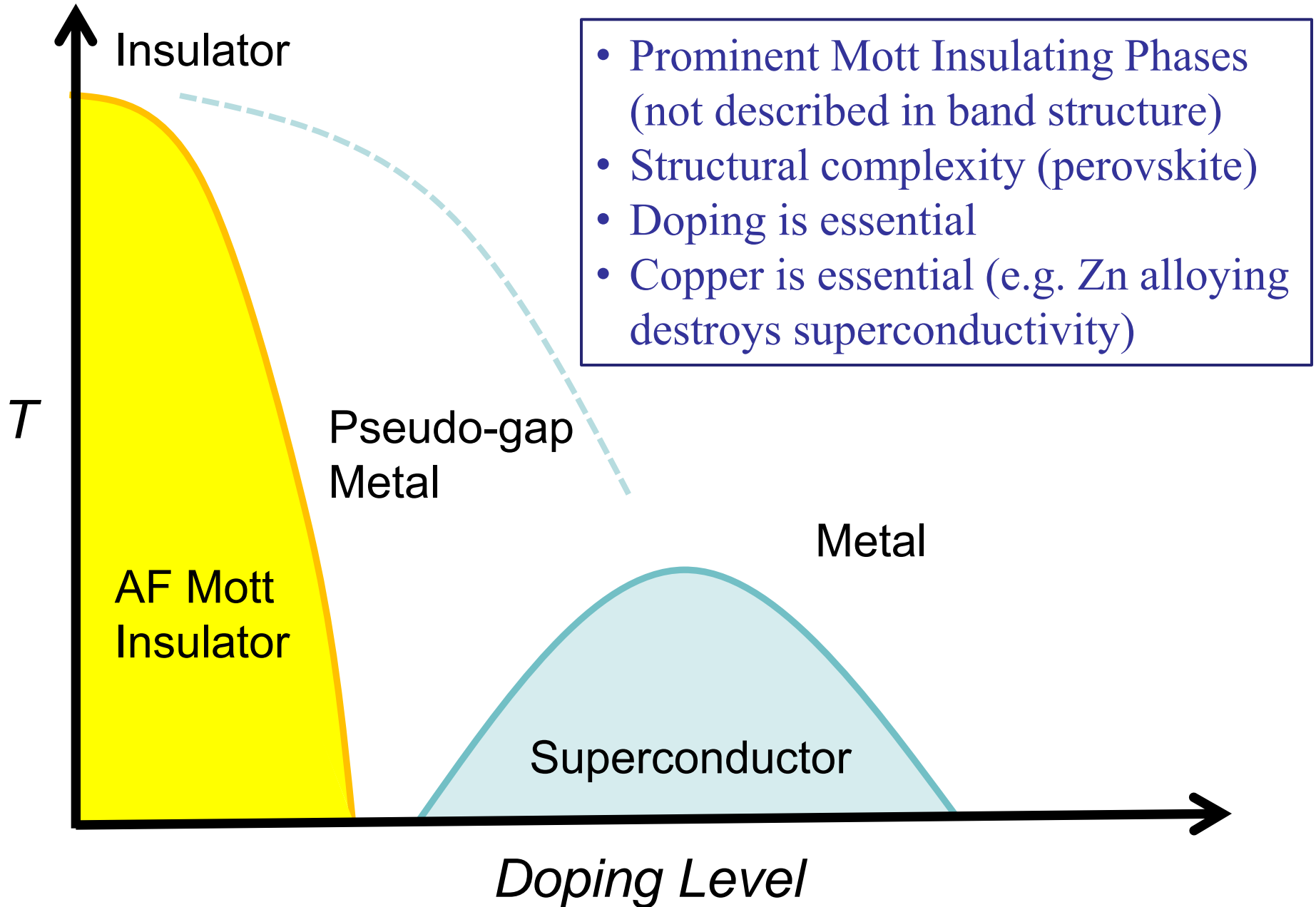
- Calculate matrix elements $V_{\mathbf{k},\mathbf{k}'}$ for a set of \mathbf{k},\mathbf{k}' on the FS.
- Set-up gap equation -- diagonalize V .
- Use $\chi_0(q) = N(0) + \alpha\chi_{\text{nesting}}(\mathbf{q})$. -- *i.e.* FM Stoner + adjustable strength nesting -- $\alpha = 0$ means no nesting; $\alpha = 0.98$ is AFM.

Result:

- Triplet wins over a wide range ($\alpha < .85$)



A Brief Introduction to Cuprates



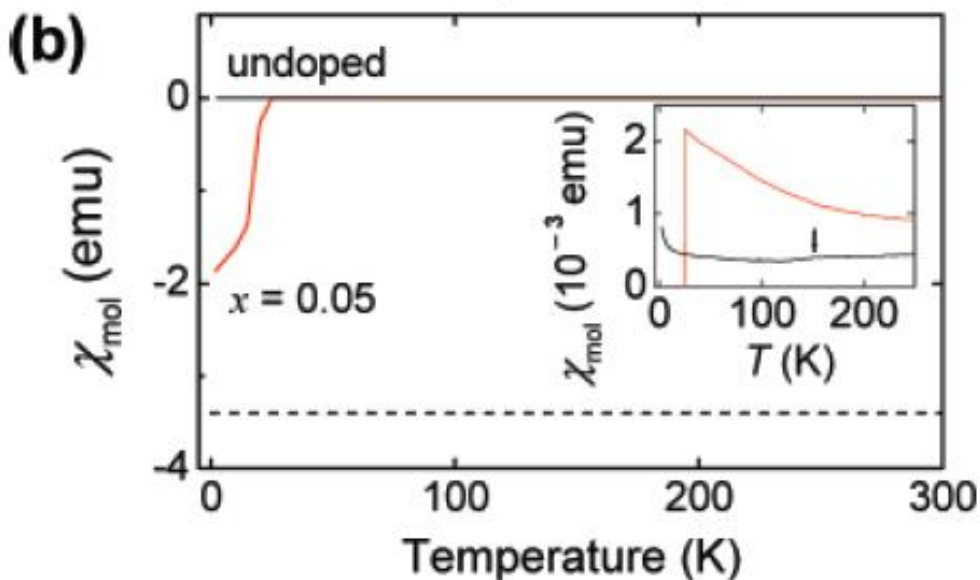
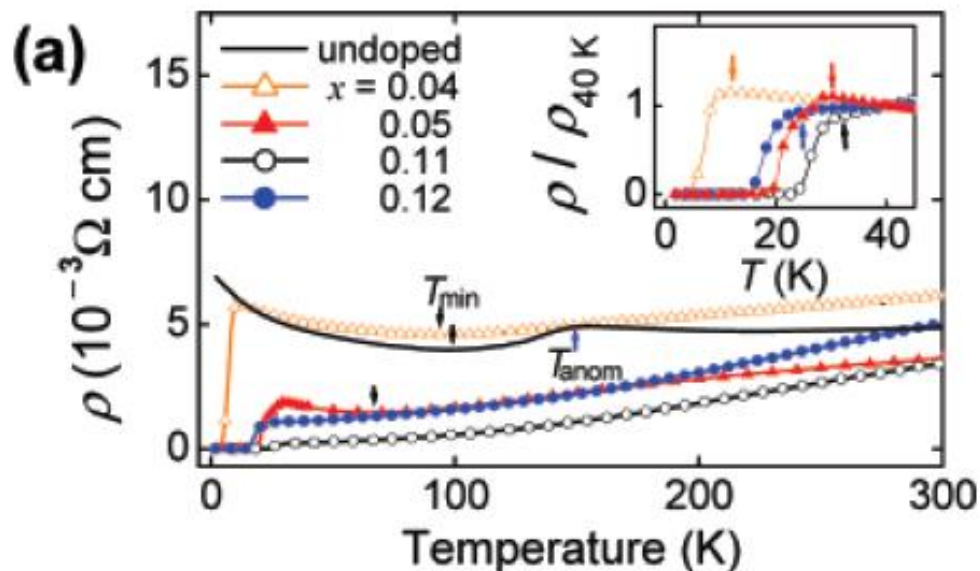
Discovery of Superconductivity in Fe-As Compounds

Kamihara *et al.*, JACS, 2006

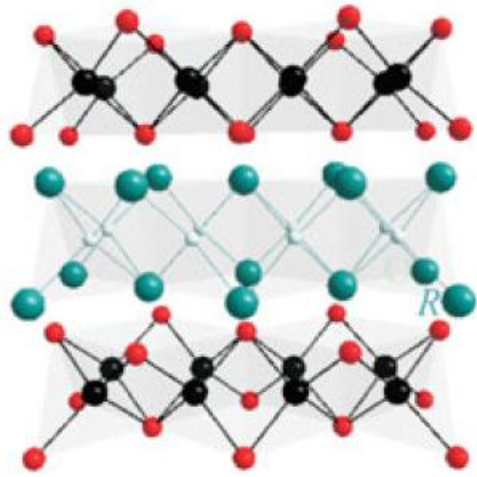
LaFePO, $T_c \sim 4\text{K}$

Kamihara, Watanabe and Hosono, JACS, Feb. 2008

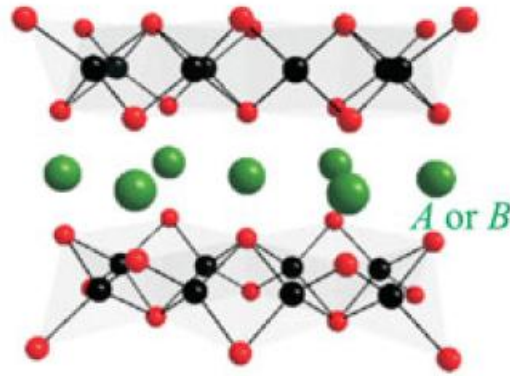
LaFeAsO_{1-x}F_x $T_c=26\text{K}$



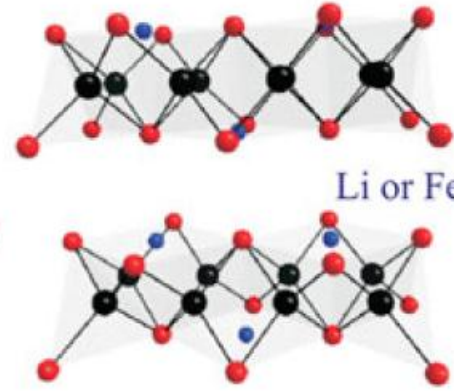
A Big Family of High T_c Superconductors



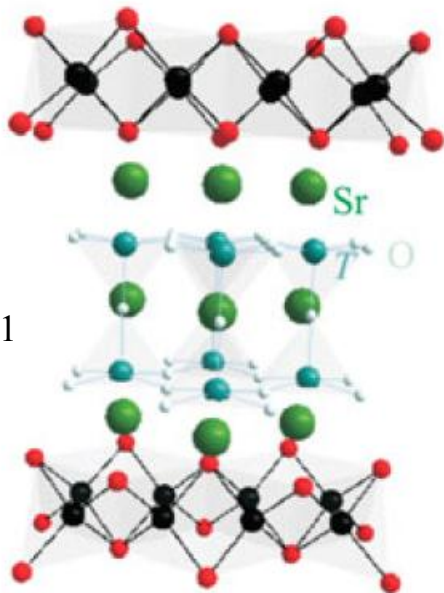
1111



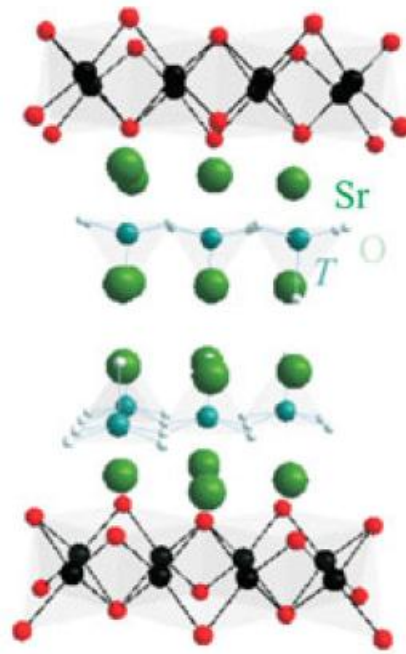
122



111, 11



32522



42622

Common Features:

- High T_c .
- Near magnetism.
- Fe square lattice.
- Near divalent Fe.
- Tetrahedral coordination.

A Word About Structure

- Large size of As^{3-} , Se^{2-} relative to Fe^{2+} leads to tetrahedral structures with anion contact (edge shared tetrahedra). Tendency to high symmetry, small unit cells without structural distortion.
- Cuprates, etc. are based on corner shared units, with resulting tendency to complex structure distortions. The interplay with properties greatly complicates the physics.



PRL 96, 107007 (2006)

PHYSICAL REVIEW LETTERS

week ending
17 MARCH 2006

Experimental Proof of a Structural Origin for the Shadow Fermi Surface of $\text{Bi}_2\text{Sr}_2\text{CaCu}_2\text{O}_{8+\delta}$

A. Mans,¹ I. Santoso,¹ Y. Huang,¹ W. K. Siu,¹ S. Tavaddod,¹ V. Arpiainen,² M. Lindroos,² H. Berger,³ V. N. Strocov,⁴ M. Shi,⁴ L. Patthey,⁴ and M. S. Golden¹

¹*van der Waals-Zeeman Institute, University of Amsterdam, NL-1018XE Amsterdam, The Netherlands*

²*Department of Physics, Tampere University of Technology, PO Box 692, FIN-33101 Tampere, Finland*

³*Ecole Polytechnique Fédérale de Lausanne, Institut de Physique de la Matière Complexe EPFL Bt. PH CH-1015*

⁴*Swiss Light Source, Paul Scherrer Institute, CH-5232 Villigen, Switzerland*

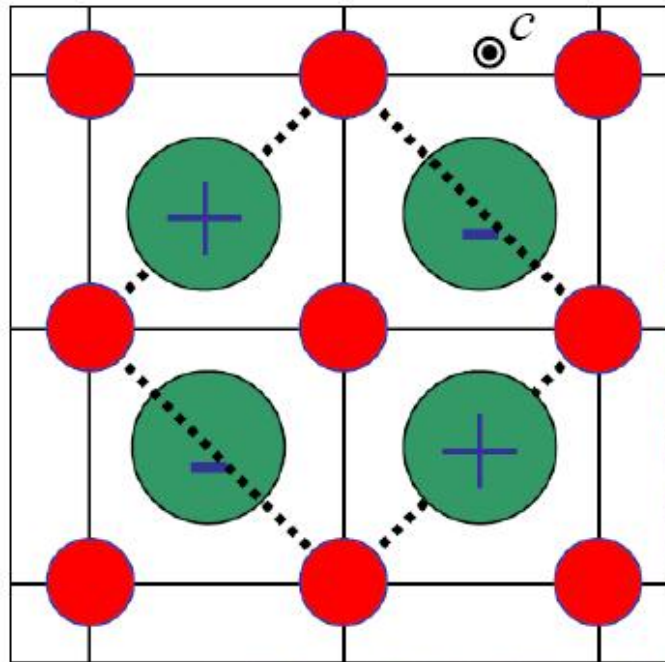
(Received 3 August 2005; published 16 March 2006)

In summary, by proving the microscopic structural origins of the shadow bands in the $\text{Bi}2212$ and $\text{Bi}2201$ families of cuprate superconductors, we have finally been able to close this chapter in the rich and complex tale of the high T_c superconductors.

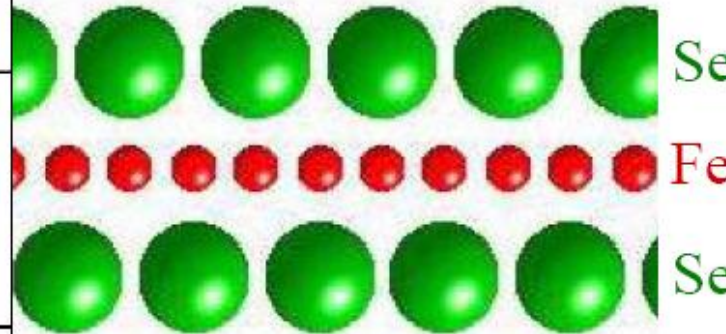
Bi-2212 – Zandbergen et al.

FeSe - The “Simplest” Fe-Superconductor

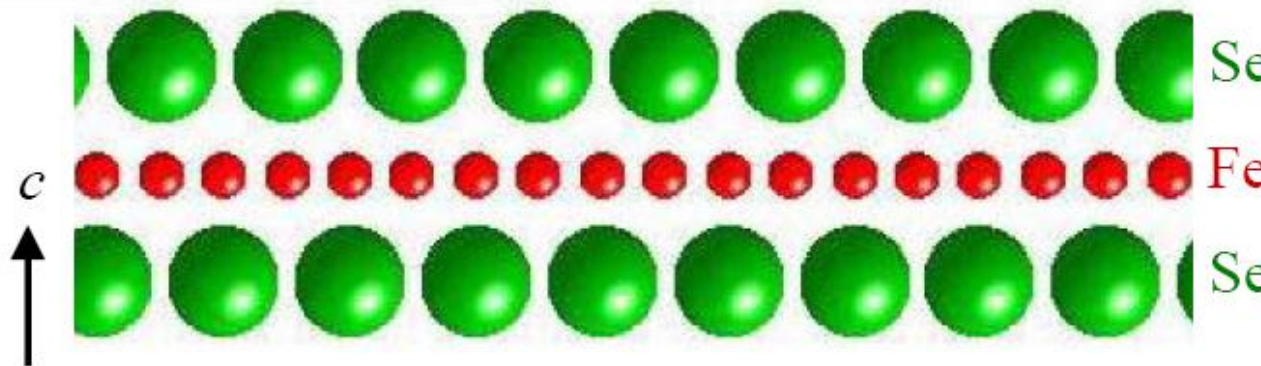
- Simple tetragonal structure, four atoms per unit cell (Hagg and Kindstrom, Z. Phys. Chem. (1933).



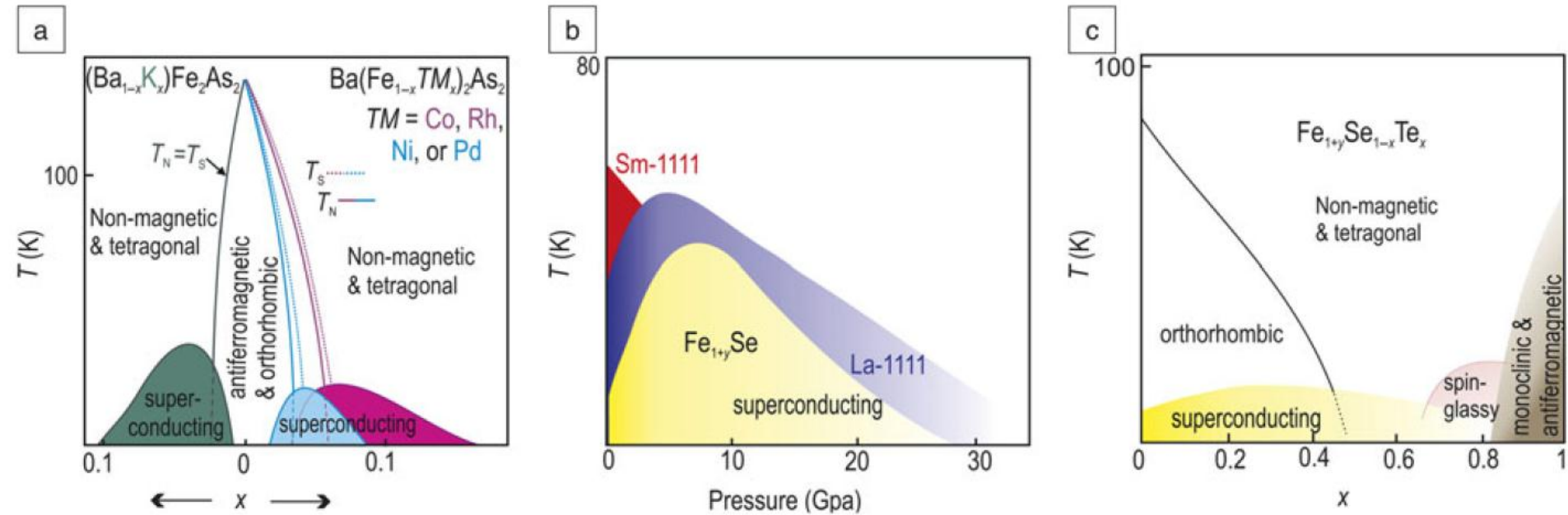
- Actual material is Fe_{1+x}Se , with extra Fe in holes of Se lattice.
- LiFeAs is similar, but extra sites are filled with Li.



$$d_{\text{Fe-Fe}} = 2.66 \text{ \AA}$$



Some Phase Diagrams



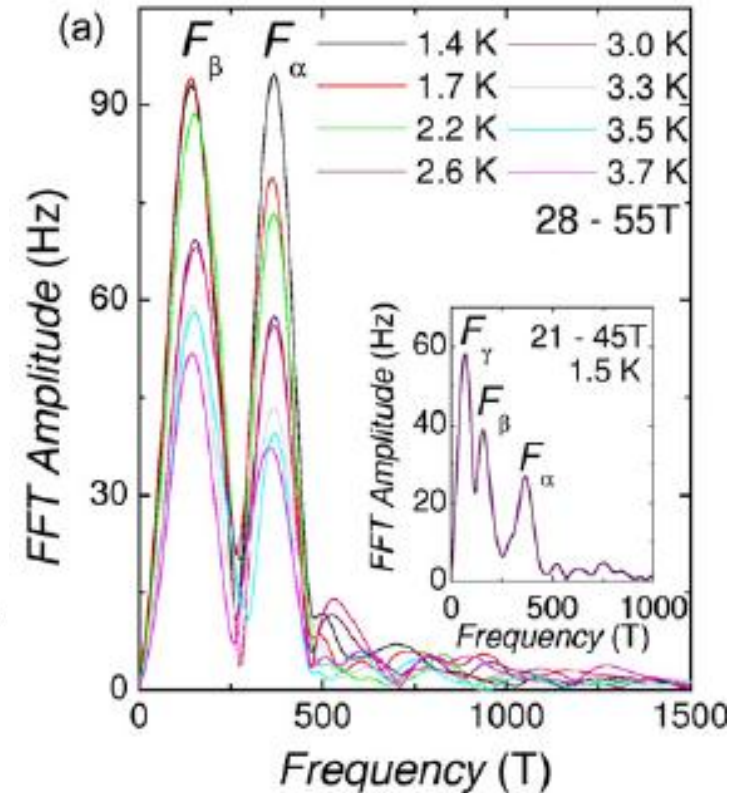
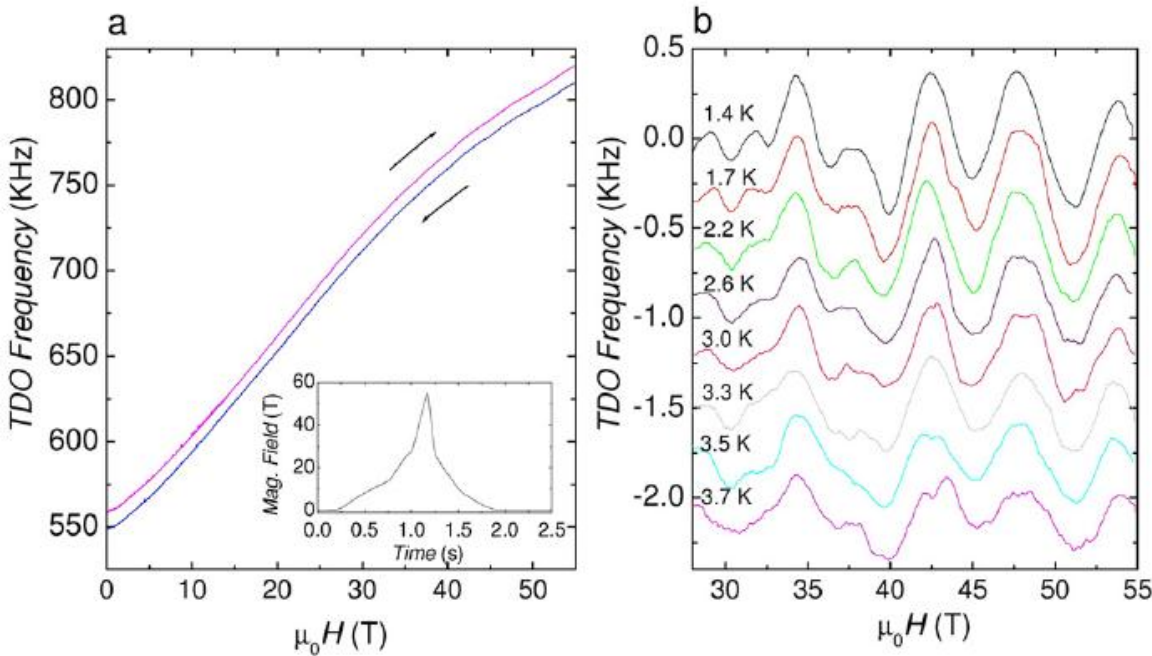
Sefat *et al.*, MRS Bull. **36**, 216 (2011)

Not List:

- Doping is not essential.
- Not in proximity to Mott phases.
- Magnetic order & superconductivity not incompatible (compete).
- Orthorhombicity occurs without magnetic order, but not always, and highest T_c is tetragonal (but large orthorhombic regions).
- Maximum T_c in different families is not so different (factor of ~ 2).

Metallic Antiferromagnetic State

SrFe_2As_2 (Sebastian *et al.*)

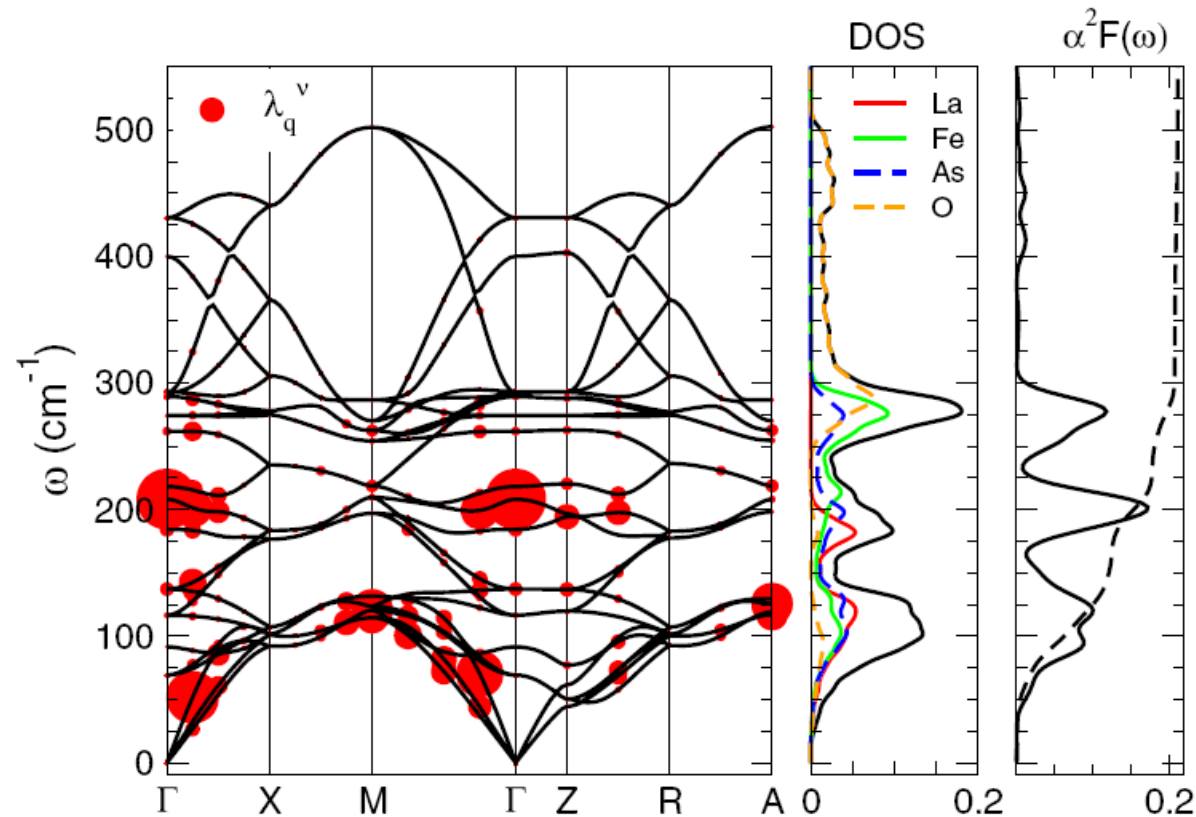


Shubnikov – de Hass measured by tunnel diode method.

SDW state has quantum oscillations reflecting a Fermi surface and is therefore a metal.

Phonons and Electron-Phonon Interaction

- First principles calculations allow direct calculation of pairing interaction, and almost first principles calculation of T_c .
- Calculations show weak coupling, no superconductivity ($\lambda_{ep} \sim 0.2$).



- Fe/As phonons are below 300 cm^{-1} .
- Corresponding Ni compounds, LaNiPO, LaNiAsO, BaNi₂As₂ ... are electron-phonon superconductors!
- Fe compounds are not electron-phonon superconductors.

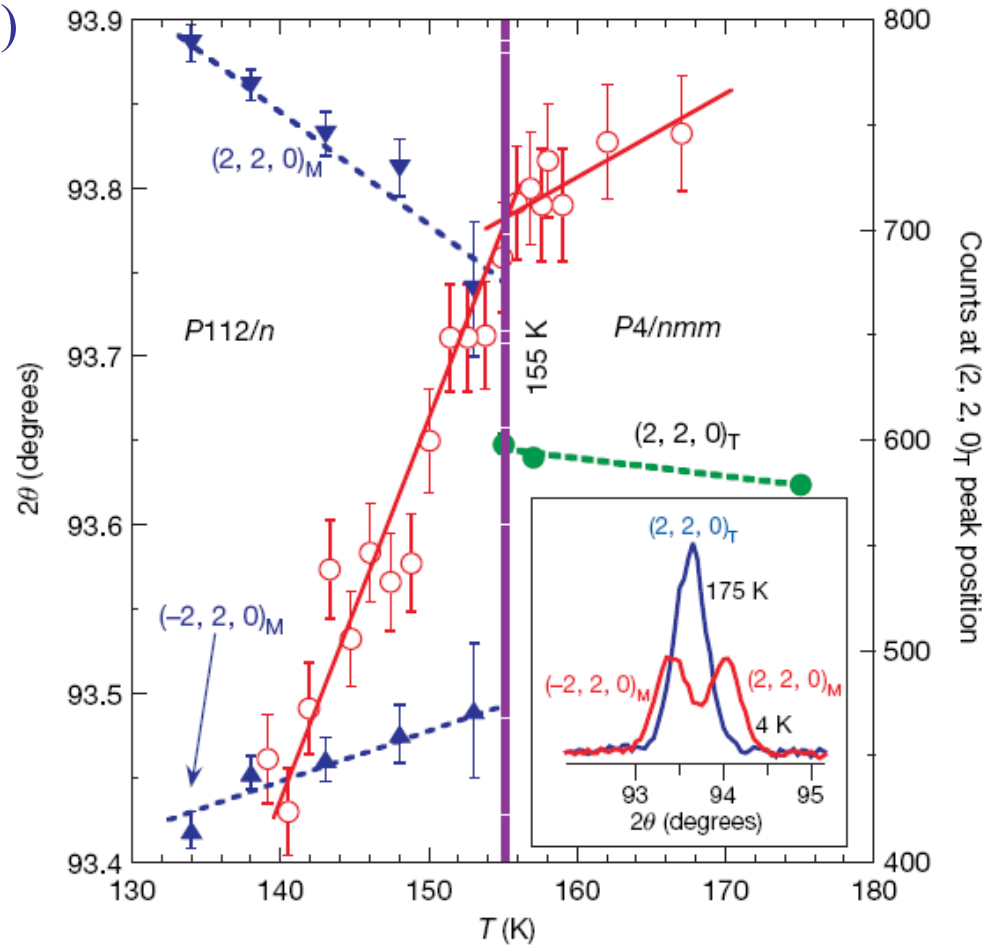
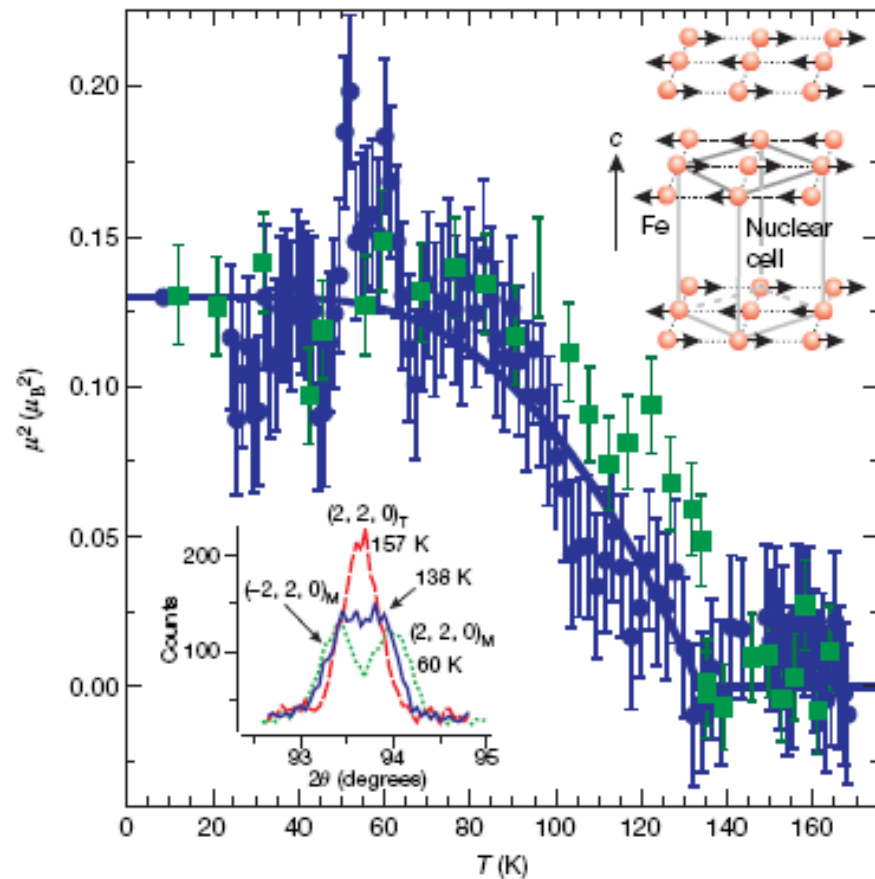
Neutron Scattering – Magnetism & Structure

LaFeAsO:

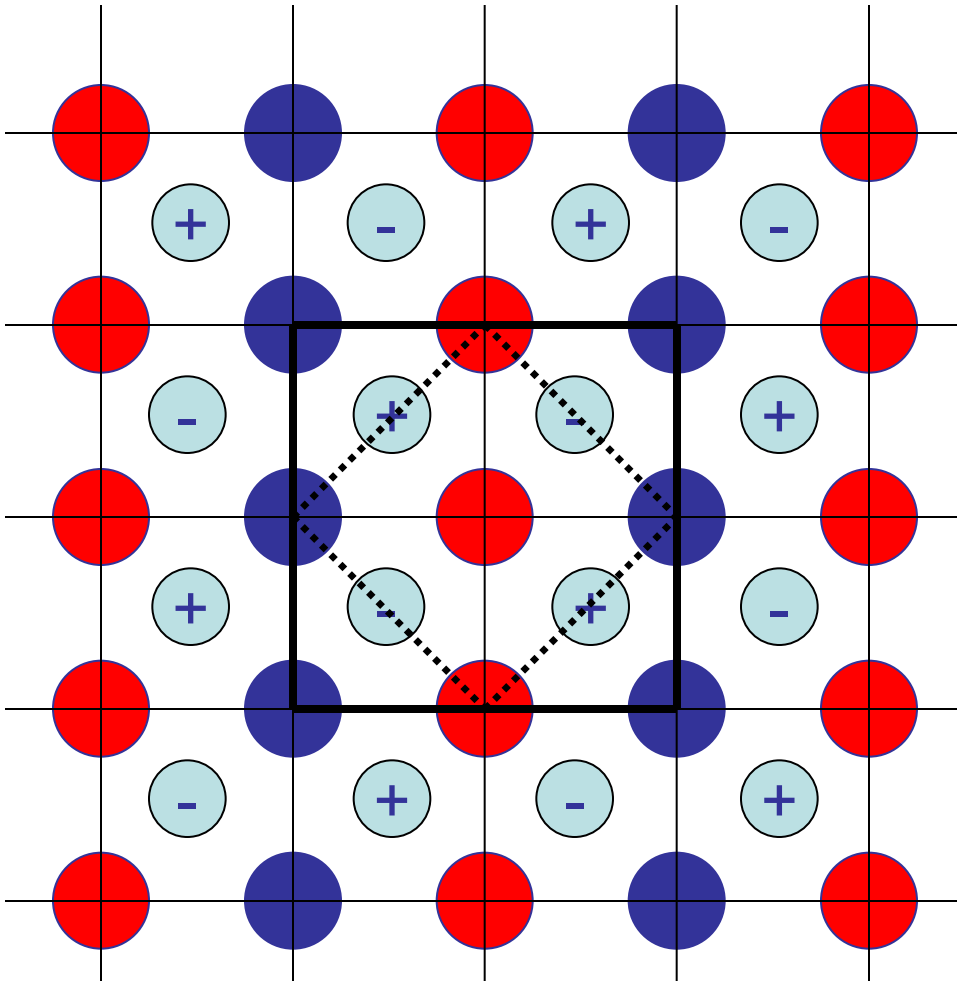
Ordered $m(\text{Fe}) = 0.36 \mu_B$

(other compounds so far are between 0.3 and 1 μ_B)

C. de la Cruz et al., Nature **453**, 899 (2008)



In-plane SDW structure



1 D Chains of parallel spin Fe atoms.

Hund's Coupling

- Hund's coupling in 3d ions is strong (Stoner $I \sim 0.8$ eV)
- Spin-fluctuations are then expected to couple to electronic states in the d -band going up to high energy (i.e. the d -band width) – may be observable in spectroscopy. Drude weight seems reduced in optics.

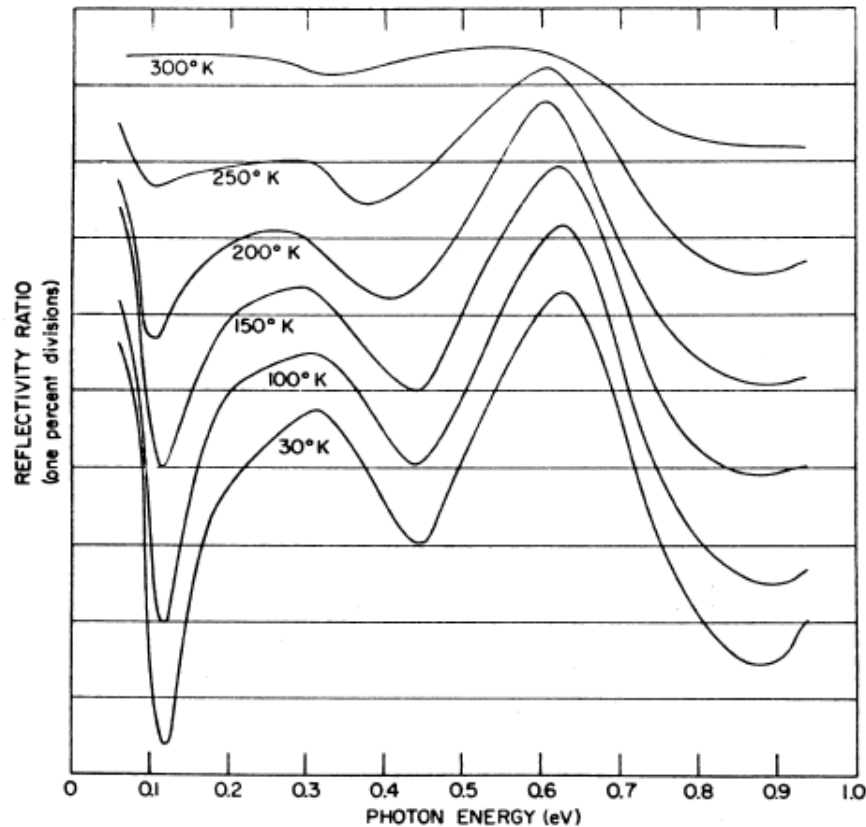
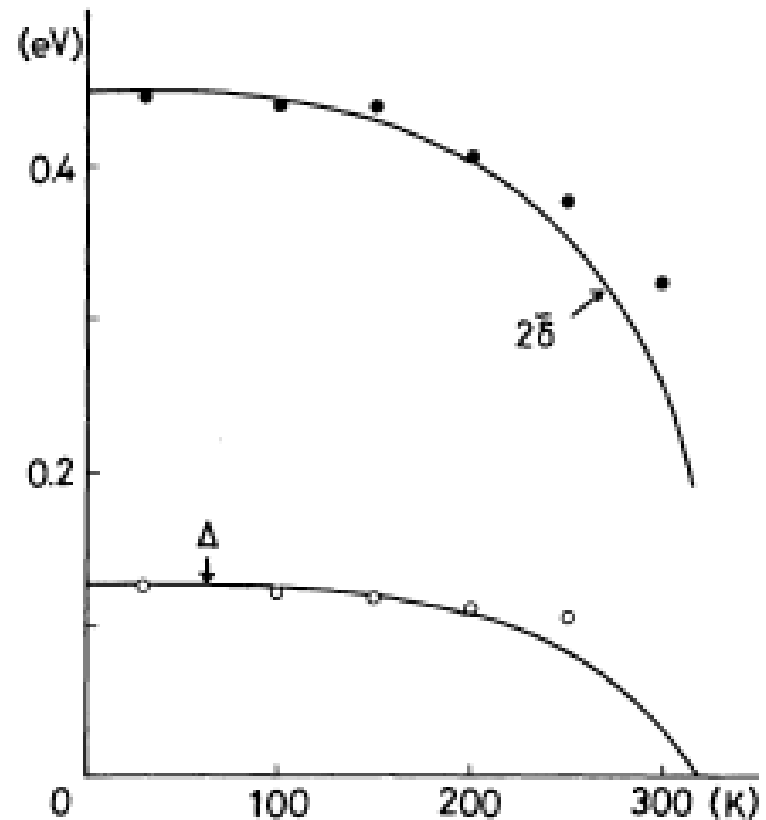


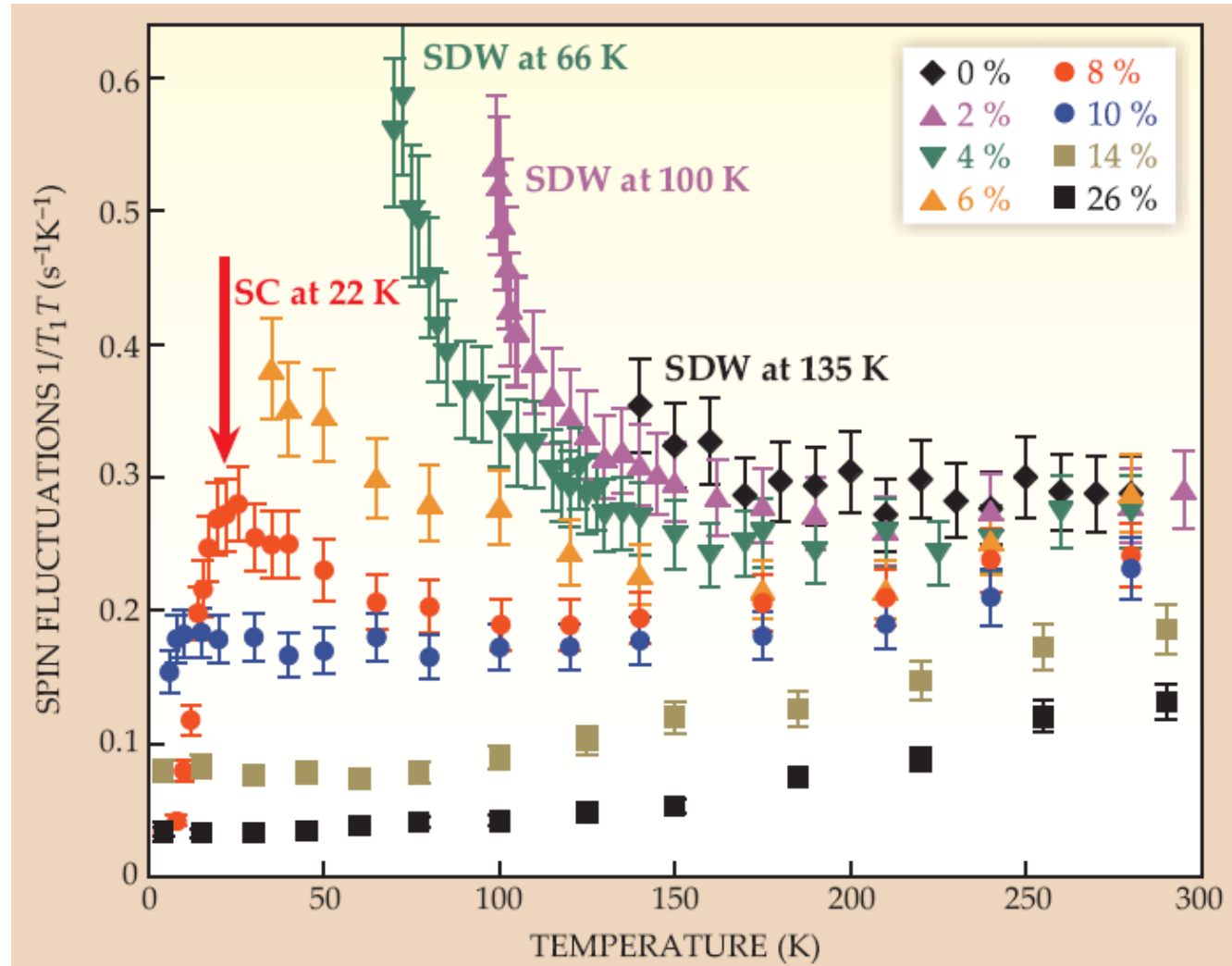
Fig. 3. The temperature dependent reflectivity of chromium normalized to $T=400$ K.

Cr metal: Machida et al., JPSJ (1984).



NMR: Connection of SDW and SC States

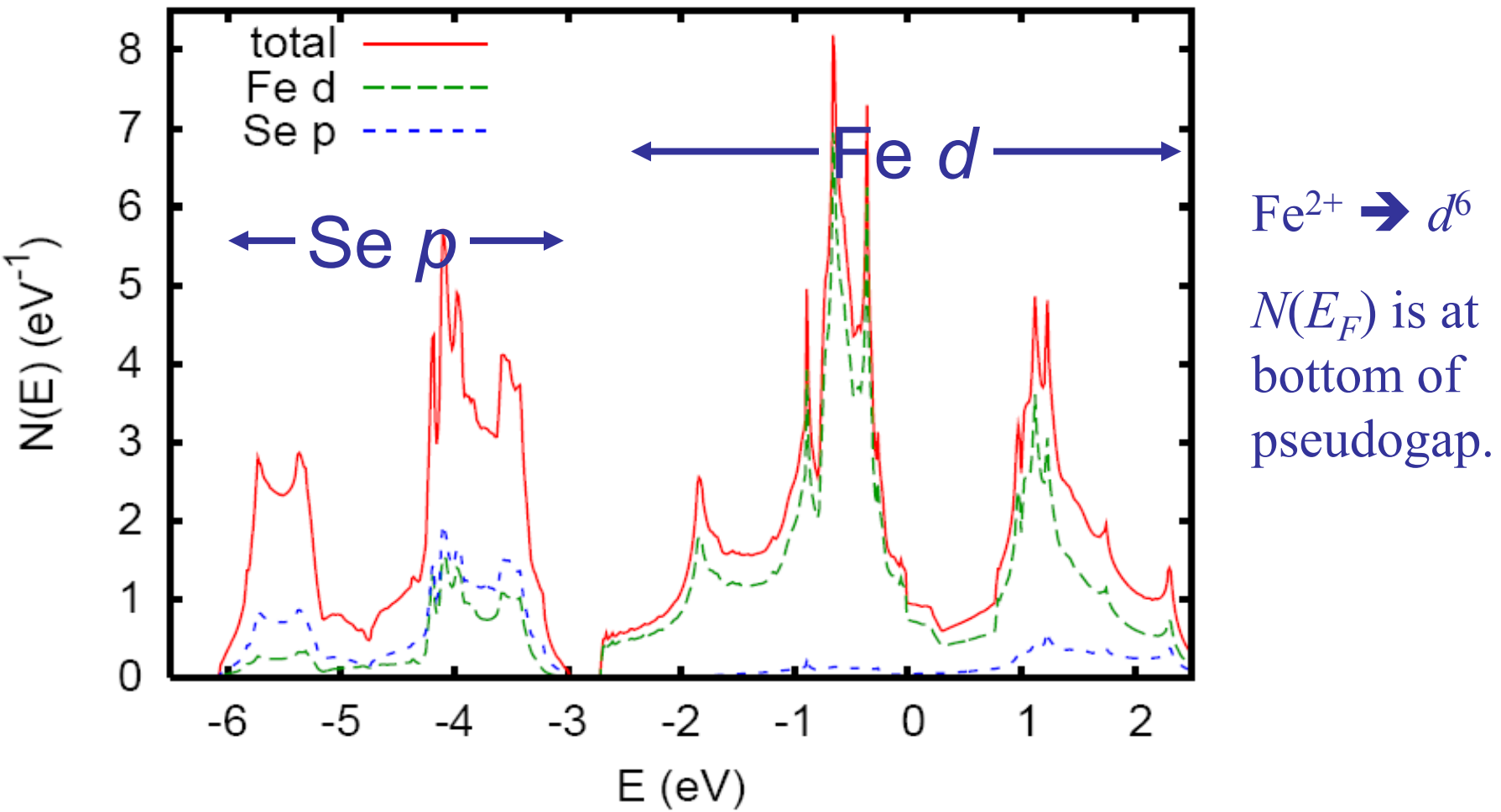
$1/T_1T$ shows strong spin fluctuations (constant for ordinary F.L.)



Ning, et al., JPSJ 78, 013711 (2009).

LDA Electronic Structure of FeSe

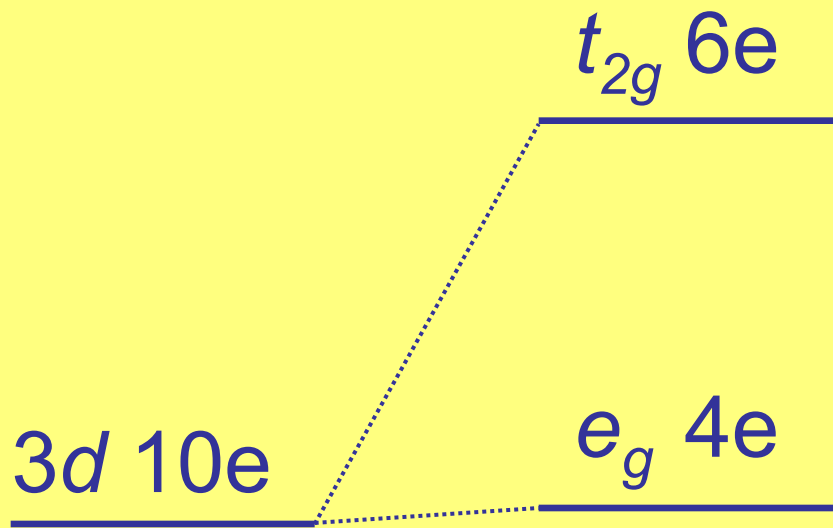
- A rather ionic material – Fe^{2+} and Se^{2-} with some hybridization, as in an oxide \rightarrow metallic sheets of Fe^{2+} modified by interaction of anions.
- Pauling electronegativities: Fe = 1.83; Se = 2.55; As = 2.18.



Formation of Band Structure

- Bands from -2 eV to +2 eV are derived from Fe^{2+} d -states.
- Fe^{2+} has 6 d -electrons.

Tetrahedral Crystal Field Scheme:

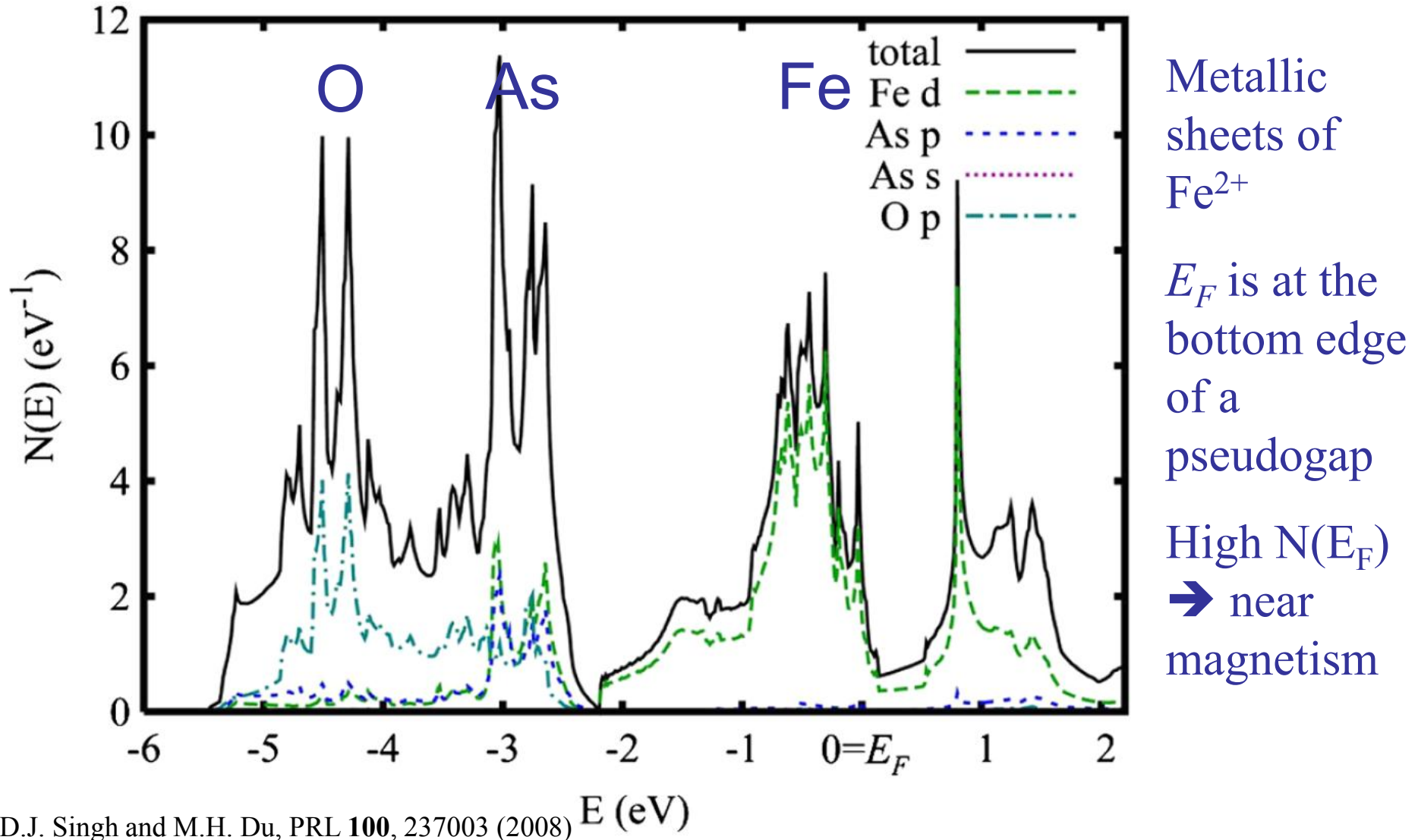


Does not correspond to the calculated electronic structure.

Key is the short Fe-Fe bond length → direct Fe-Fe interactions.

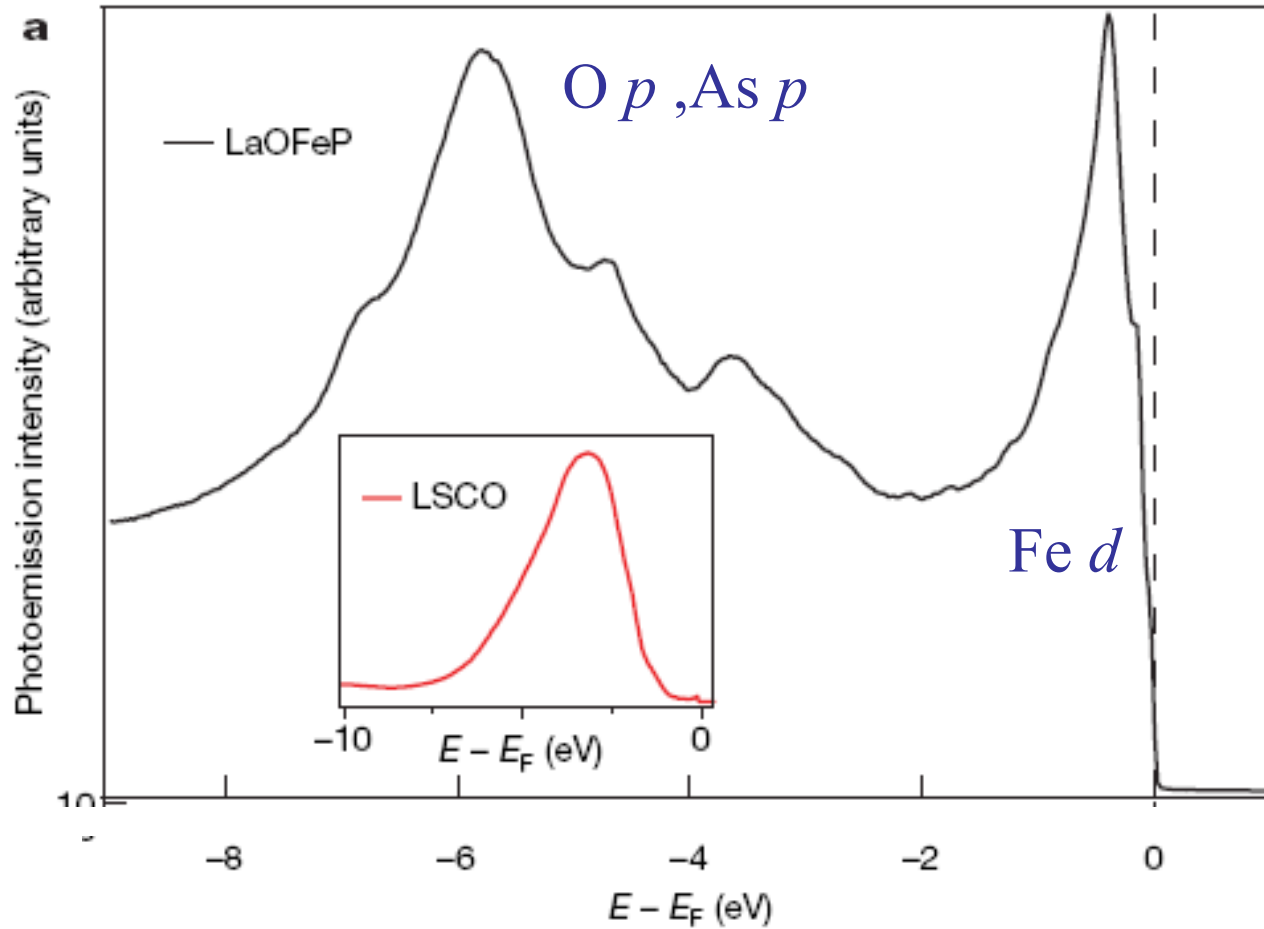
Arsenide Electronic Structure: LaFeAsO

- LaFeAsO: Rather ionic electronic structure: O^{2-} , As^{3-} , La^{3+}
- Bands near E_F are derived from Fe with little As admixture



Metallic Character

Photoemission: LaFePO (D.H. Lu et al.)

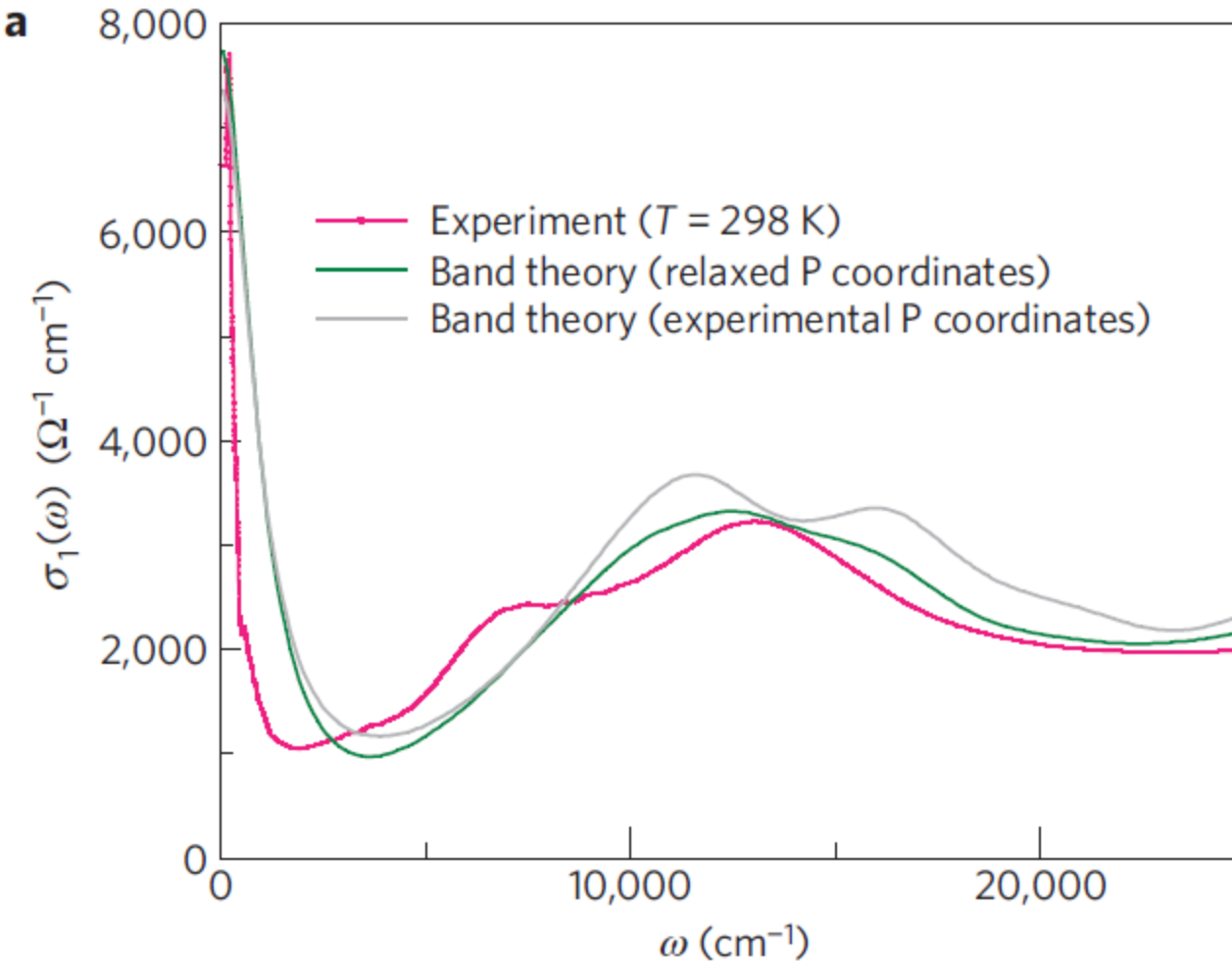


Very prominent Fermi edge (not like cuprates).

Fe d bands are narrower (by ~ 2) compared to LDA.

Optics

LaFePO (M.M. Qazilbash et al.)



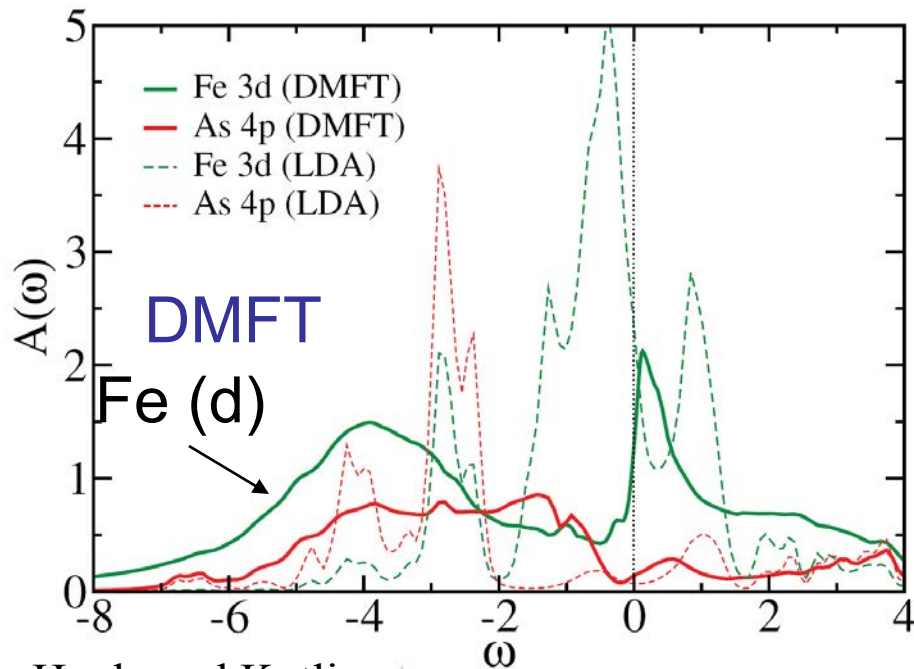
Drude has lower weight than in band calculation.

Re-distribution of spectral weigh in d-bands.

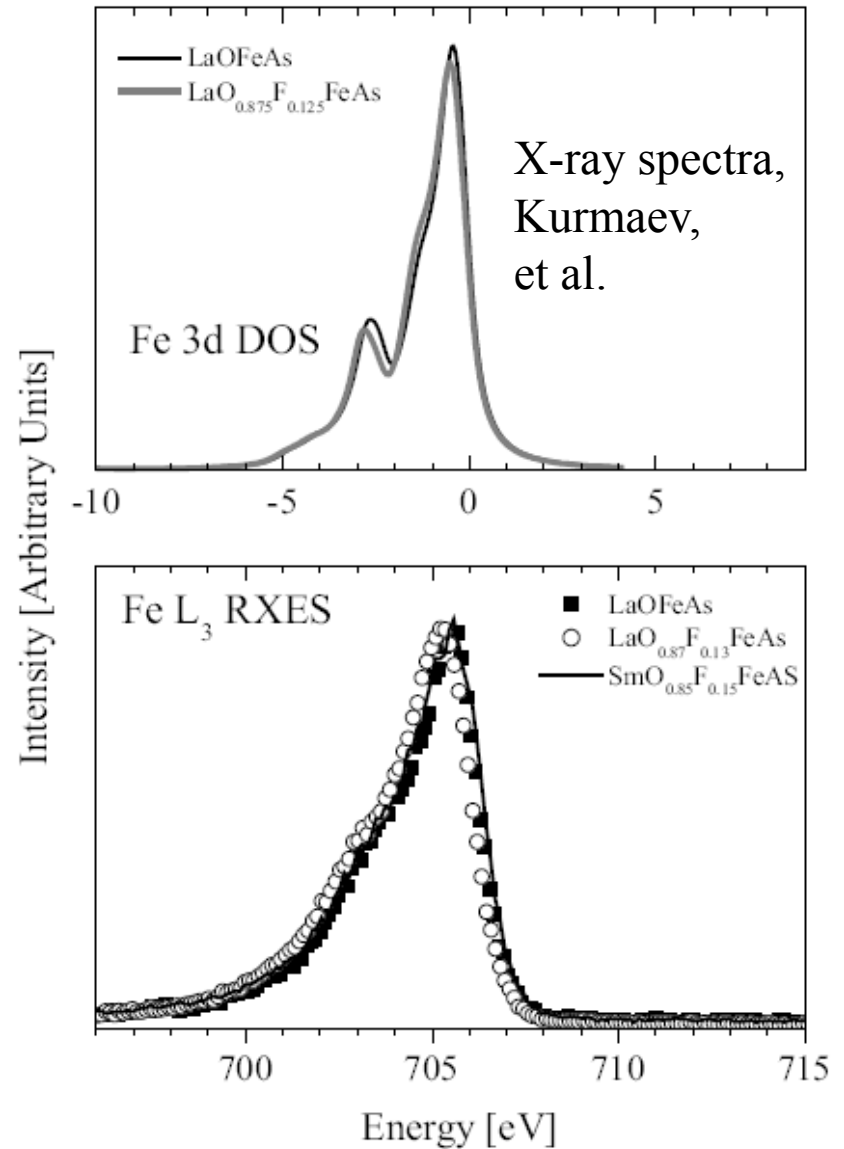
No Hubbard bands.

Coulomb Correlations

- LDA and correlated approaches give different predictions.
- So far Hubbard bands are not seen; strong Fe d character is seen at Fermi edge.
- There is however a renormalization of ~ 2 in band width c.f. LDA.



Haule and Kotliar

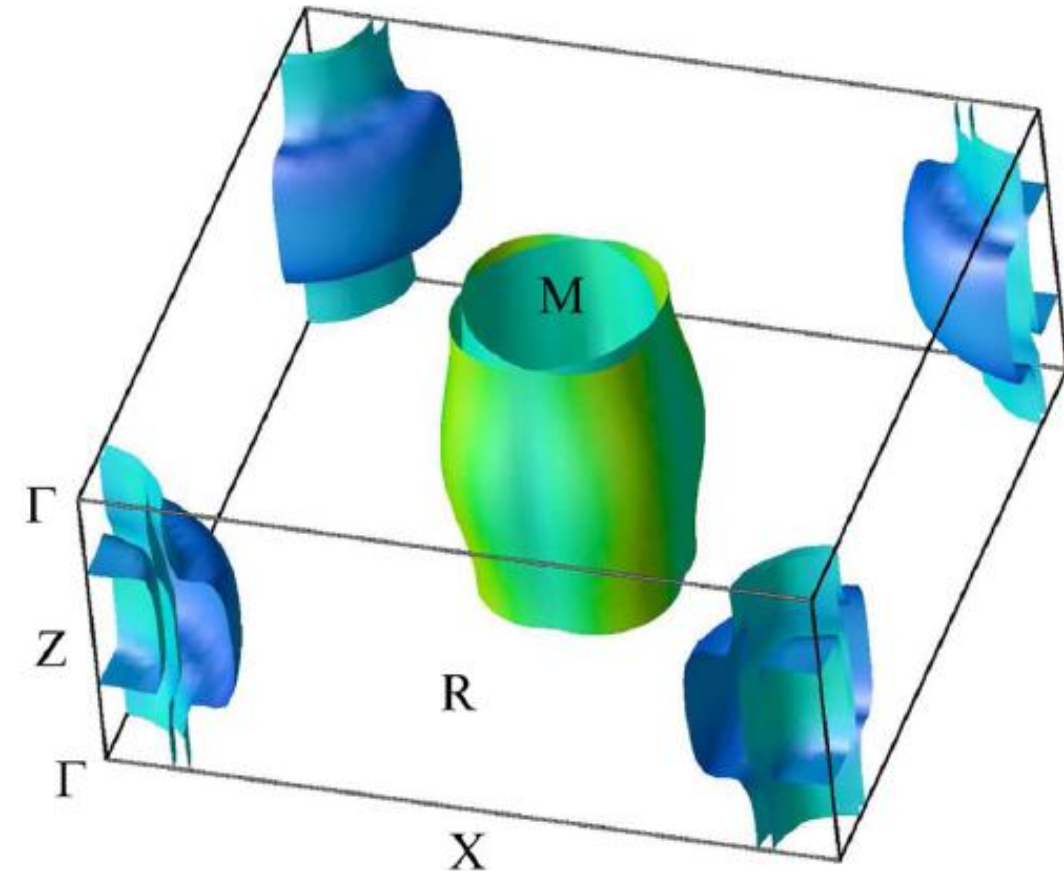


Density Functional Study of $\text{LaFeAsO}_{1-x}\text{F}_x$: A Low Carrier Density Superconductor Near Itinerant Magnetism

D.J. Singh and M.-H. Du

Materials Science and Technology Division, Oak Ridge National Laboratory, Oak Ridge, Tennessee 37831-6114, USA

(Received 4 March 2008; published 12 June 2008)



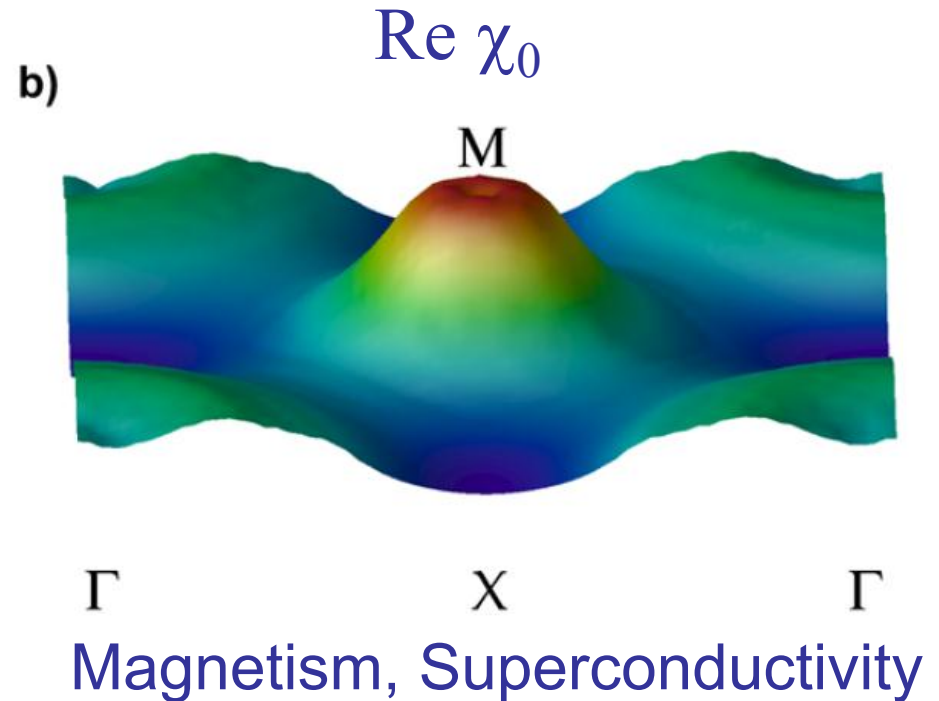
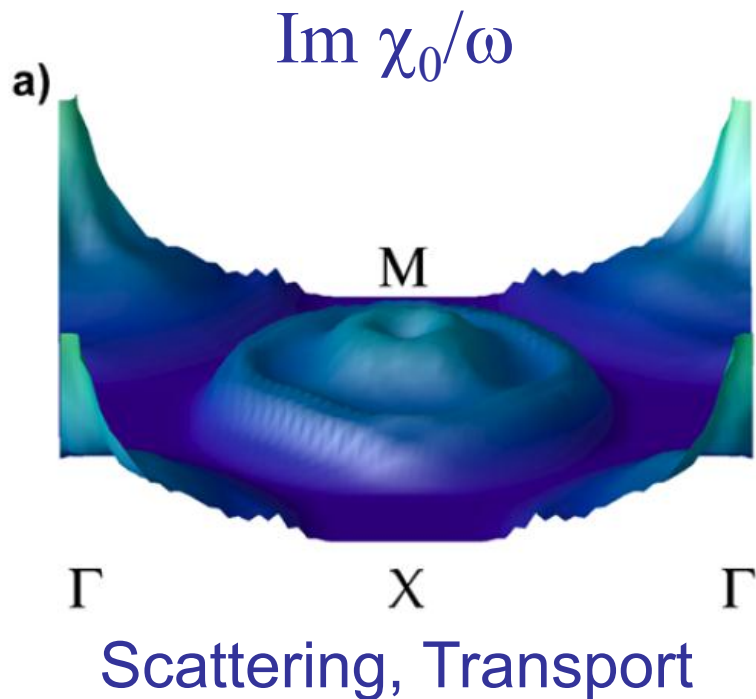
Fermi Surface of
 LaFeAsO
(not spin polarized)

Low carrier density:
 $n_e = n_h = 0.13 / \text{Fe}$

Band anisotropy: $\langle v_x^2 \rangle / \langle v_z^2 \rangle \sim 15 \rightarrow$
a modest value that is favorable for applications.

Lindhard Function (Metal Physics)

- LaFeAs(O,F) neglecting matrix elements:



Note the pronounced peak at the zone corner.

Spin Fluctuations and Superconductivity

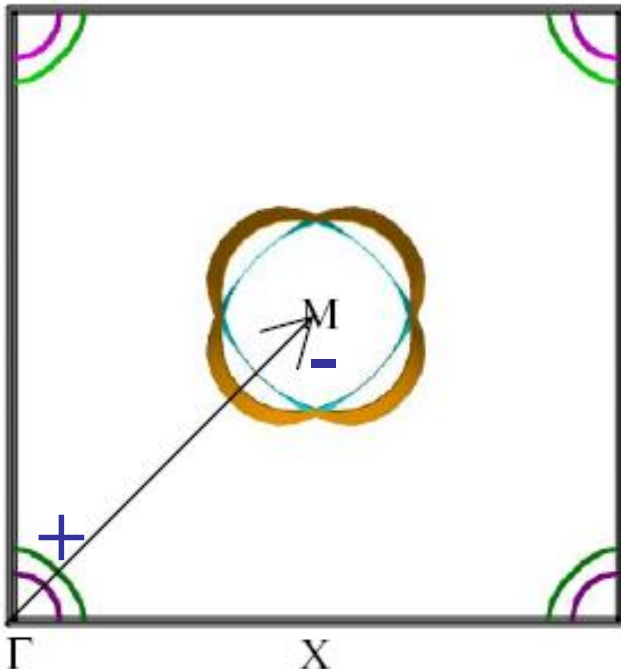
One way to proceed (weak coupling):

- Calculate matrix elements $V_{\mathbf{k},\mathbf{k}'}$ for a set of \mathbf{k},\mathbf{k}' on the FS.
- Set-up gap equation -- diagonalize V .

Berk-Schrieffer-Fay-Appel weak coupling theory, 1966-1980:

Singlet:

$$V(\mathbf{q}) = - \frac{I^2(\mathbf{q})\chi_0(\mathbf{q})}{1 - I^2(\mathbf{q})\chi_0^2(\mathbf{q})}$$



In a singlet channel there is a minus sign for spin fluctuations (repulsive), which then favors opposite order parameters on the electron and hole sheets \rightarrow s +/- state.

Note prior work, Aronov & Sonin (1972); Kuroki and Arita (2001)

Does not have an obvious strongly q-dependent interaction for nodes in a FS.

Electron doped LaFeAsO

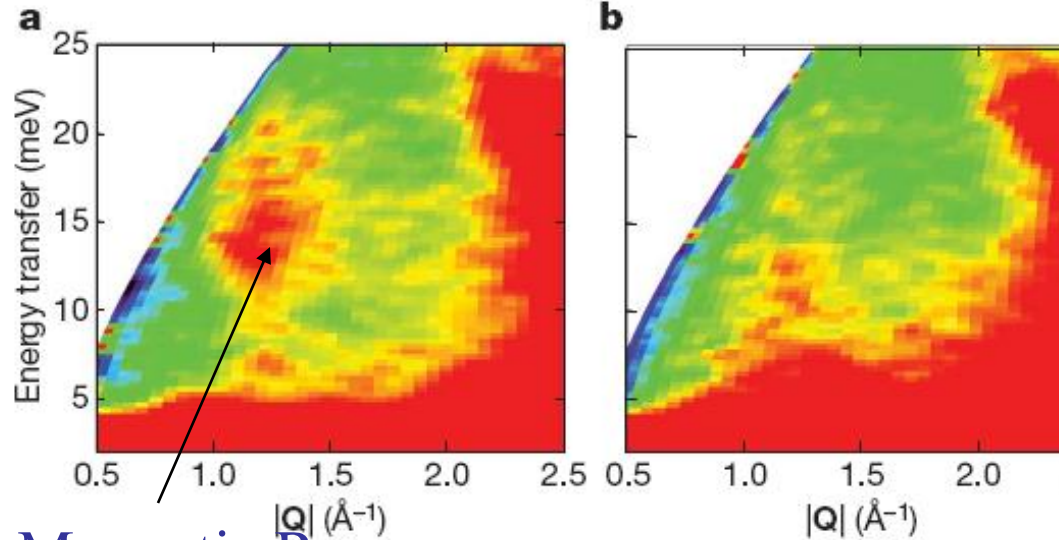
LETTERS

Unconventional superconductivity in $\text{Ba}_{0.6}\text{K}_{0.4}\text{Fe}_2\text{As}_2$ from inelastic neutron scattering

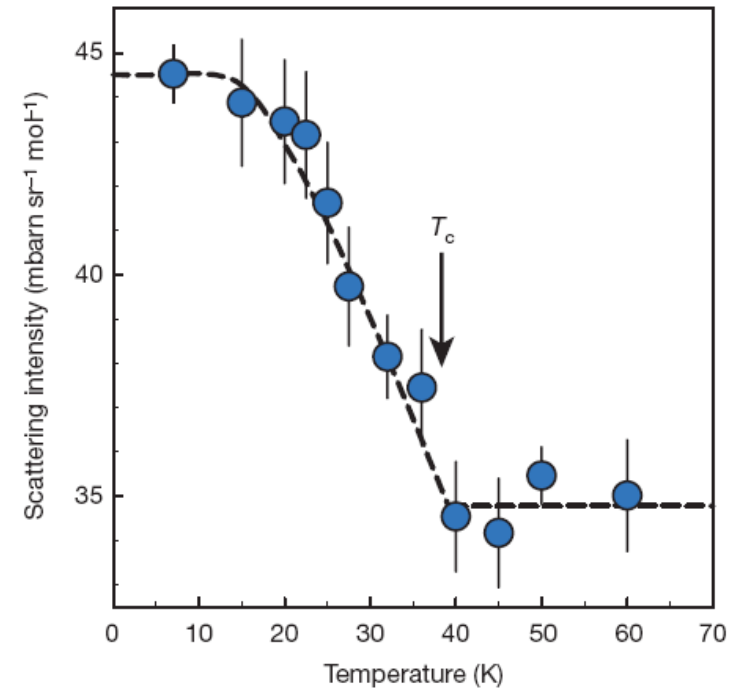
A. D. Christianson¹, E. A. Goremychkin^{2,3}, R. Osborn², S. Rosenkranz², M. D. Lumsden¹, C. D. Malliakas^{2,4}, I. S. Todorov², H. Claus², D. Y. Chung², M. G. Kanatzidis^{2,4}, R. I. Bewley³ & T. Guidi³

$T=7\text{K}$

$T=50\text{K}$



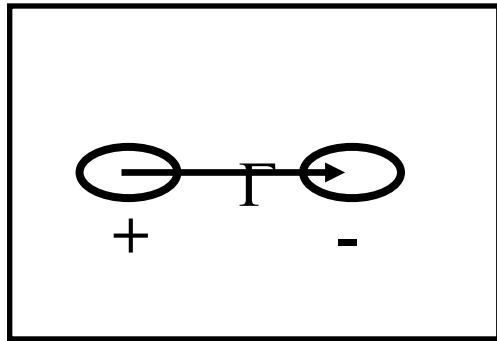
Magnetic Resonance



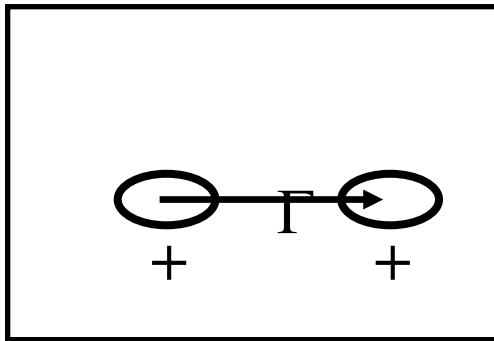
Sign changing gap with q corresponding to (π, π)

Small Fermi Surfaces in General

- Does superconductivity arise in general if one has small Fermi surfaces with nesting driven spin fluctuations? – Answer seems to be no.



p-wave state (triplet): spin-fluctuation pairing interaction has + sign → Pair breaking for the state shown.



s-wave state (singlet): spin-fluctuation pairing interaction has – sign → Pair breaking for the state shown.

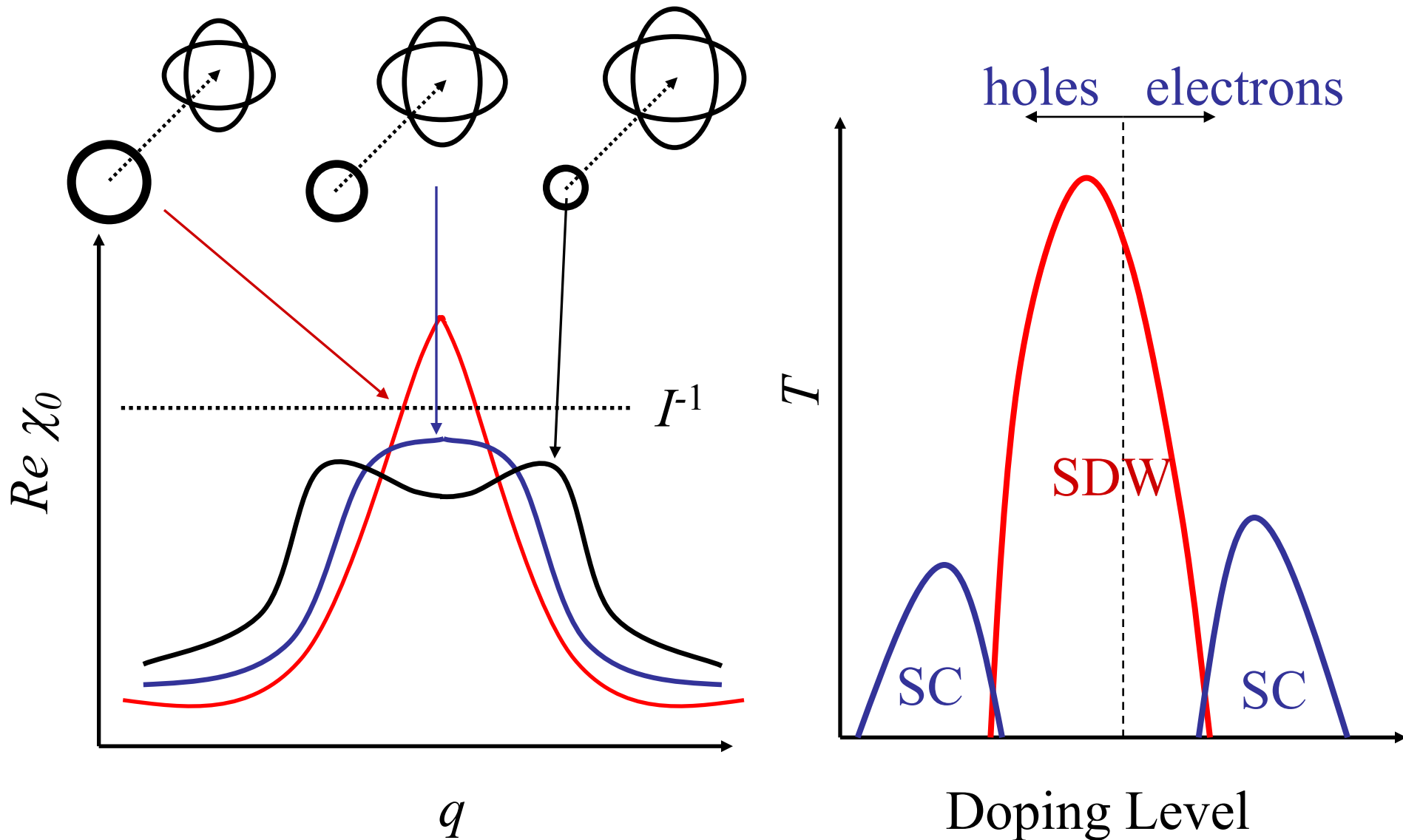
e.g. small pockets on Na_xCoO_2 (Johannes et al., 2004).

In such cases, look for chemistry with strong electron phonon and low Stoner parameter, to obtain Kohn anomaly and e-p superconductivity or maybe strange states, e.g. odd frequency.

Normal Metallic State

- Low carrier density semi-metal (dis-connected small Fermi surfaces).
- Less anisotropic than cuprates, even $\text{YBa}_2\text{Cu}_3\text{O}_7$.
- High $N(E_F)$.
 - Near itinerant magnetism in general.
 - Expect short coherence length relative to T_c .
 - Expect high superfluid density.
- Electron-Phonon interaction is weak ($\lambda \sim 0.2$, $T_c = 0$)

Nesting, Doping and the Lindhard Function



Disorder affects both magnetism and superconductivity

Neutron Scattering – Structure Details

LaFeAsO (Tetragonal → Orth/Mono):

Table 2 | Properties of LaOFeAs at 4 K

a, Refined structure parameters					
Atom	Site	x	y	z	B (Å ²)
La	2e	1/4	1/4	0.1426(3)	0.54(6)
Fe	2f	3/4	1/4	0.5006(12)	0.16(4)
As	2e	1/4	1/4	0.6499(4)	0.23(7)
O	2f	3/4	1/4	-0.0057(17)	0.69(7)

$$z_{\text{As}}(4\text{K}) = 1.308 \text{ \AA}$$

$$z_{\text{As}}(175\text{K}) = 1.317 \text{ \AA}$$

LaFeAsO_{0.92}F_{0.08} (Tetragonal):

Table 3 | Properties of LaO_{0.92}F_{0.08}FeAs at 10 K (first line), 35 K (second line) and 175 K (third line)

a, Refined structure parameters					
Atom	Site	x	y	z	B (Å ²)
La	2c	1/4	1/4	0.1448(3)	0.40(5)
		1/4	1/4	0.1458(3)	0.50(5)
		1/4	1/4	0.1446(3)	0.73(5)
Fe	2b	3/4	1/4	1/2	0.32(4)
		3/4	1/4	1/2	0.41(4)
		3/4	1/4	1/2	0.65(4)
As	2c	1/4	1/4	0.6521(4)	0.41(7)
		1/4	1/4	0.6515(4)	0.40(6)
		1/4	1/4	0.6527(4)	0.69(7)
O/F	2a	3/4	1/4	0	0.53(6)
		3/4	1/4	0	0.62(6)
		3/4	1/4	0	0.71(6)

$$z_{\text{As}}(10\text{K}) = 1.323 \text{ \AA}$$

$$z_{\text{As}}(175\text{K}) = 1.331 \text{ \AA}$$

Non-magnetic LDA calc.
(LaFeAsO – Tetragonal)

$$z_{\text{As}}(\text{LDA}) = 1.159 \text{ \AA}$$

A huge difference!



Structure and Magnetism

- As height is too low by >0.1 Å in non-magnetic LSDA calculations.
- SDW is too robust in DFT.
- Using GGA and including magnetism one can obtain much better As height. In that case magnetism is extremely robust ($m \sim 2\mu_B$) contrary to experiment.
- Discrepancy in As height persists in the paramagnetic (superconducting) doped phases.

Metals Where the LSDA Overestimates Ferromagnetism

Class 1: Ferromagnets where the LDA overestimates the magnetization.

	m (LDA, μ_B /f.u.)	m (expt., μ_B /f.u.)
ZrZn ₂	0.72	0.17
Ni ₃ Al	0.71	0.23
Sc ₃ In	1.05	0.20

Class 2: Paramagnets where the LDA predicts ferromagnetism

	m (LDA, μ_B /f.u.)	m (expt., μ_B /f.u.)
FeAl	0.80	0.0
Ni ₃ Ga	0.79	0.0
Sr ₃ Ru ₂ O ₇	1.1	0.0
Na _{0.7} CoO ₂	0.30	0.0

c.f. “Normal” Materials

	m (DFT, μ_B /f.u.)	m (expt., μ_B /f.u.)
bcc Fe	2.17	2.12
SrRuO ₃	1.59	1.6

Renormalization and The Fluctuation Dissipation Theorem

Relates fluctuation amplitude to dissipation term, i.e. spin fluctuation spectrum:

$$\xi^2 = \frac{4\hbar}{\Omega} \int d^3q \int \frac{d\omega}{2\pi} \frac{1}{2} \text{Im} \chi(\mathbf{q}, \omega)$$

Landau functional approach (after Moriya, Shimizu, others) is based on the magnetic moment dependence of the total energy *without* fluctuations

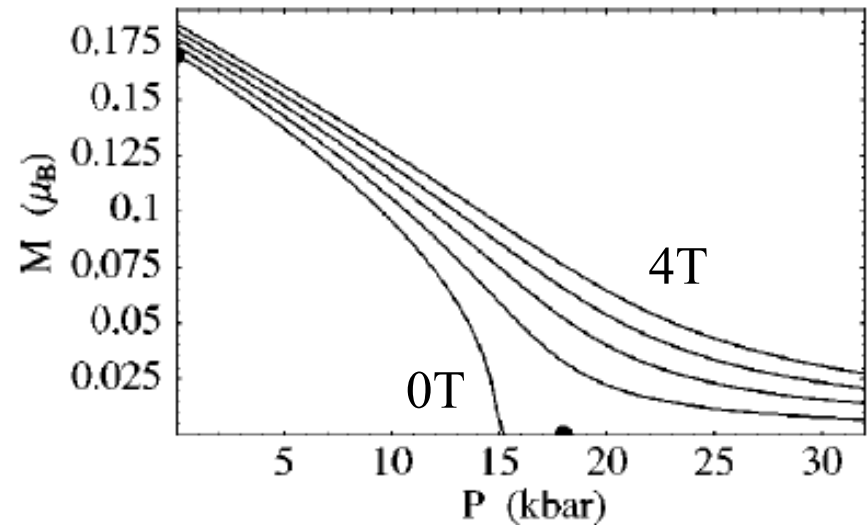
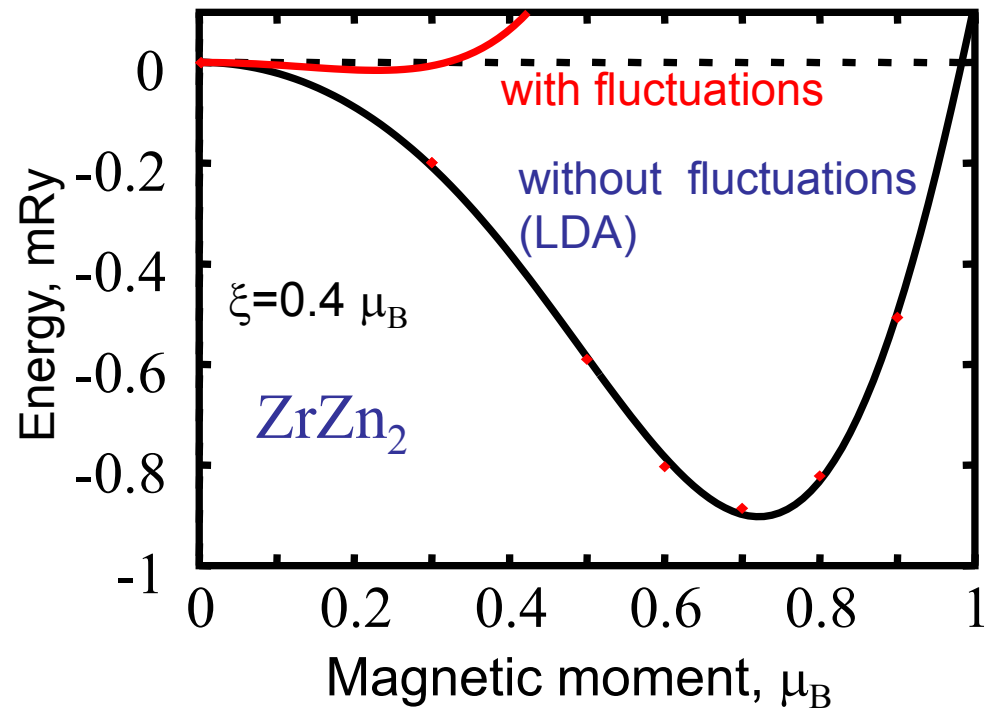
$$\Delta E(M) = aM^2 + bM^4 + cM^6 \quad a^{-1} / 2 = \chi, \text{ susceptibility}$$

Spin fluctuations renormalize this dependence, i.e. $a \rightarrow \alpha$, etc. via integration of the Landau functional with Gaussian of rms width ξ .

- 1. Large renormalization \rightarrow large fluctuation amplitude.**
- 2. Large amplitude requires large integral \rightarrow Im χ large over wide range of \mathbf{q} and ω .**

Example: ZrZn_2 (Weak Itinerant Ferromagnet)

Bare LDA moment of $\sim 0.7 \mu_B$ to $\sim 0.2 \mu_B$ by fluctuations $\xi \sim 0.4 \mu_B$

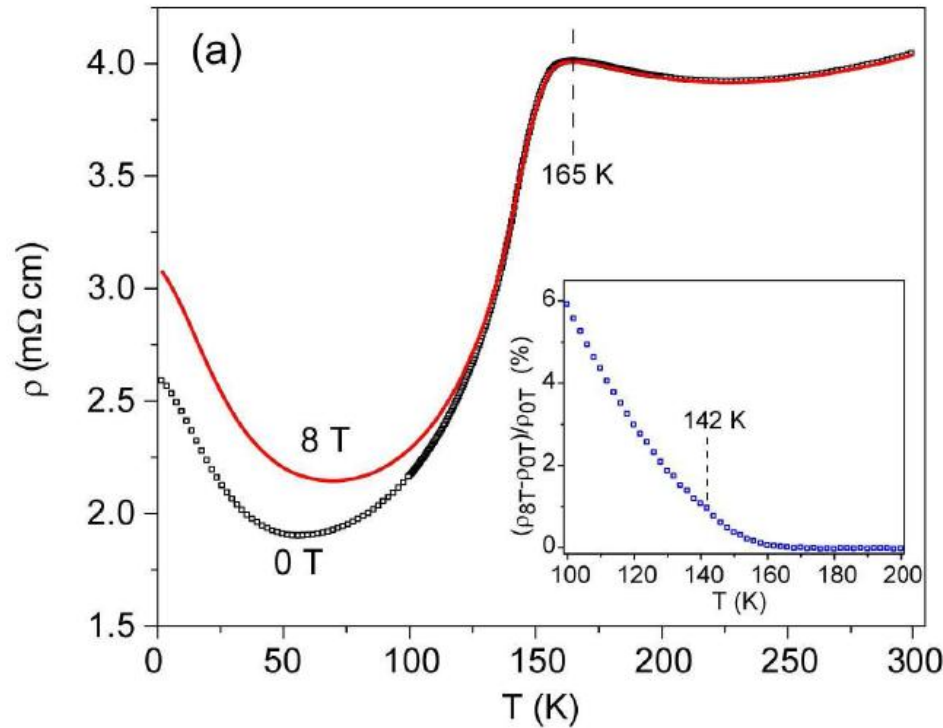


I.I. Mazin and D.J. Singh, Phys. Rev. B **69**, 020402 (2004).

Resistivity in LaFeAsO

McGuire *et al.* (cond-mat):

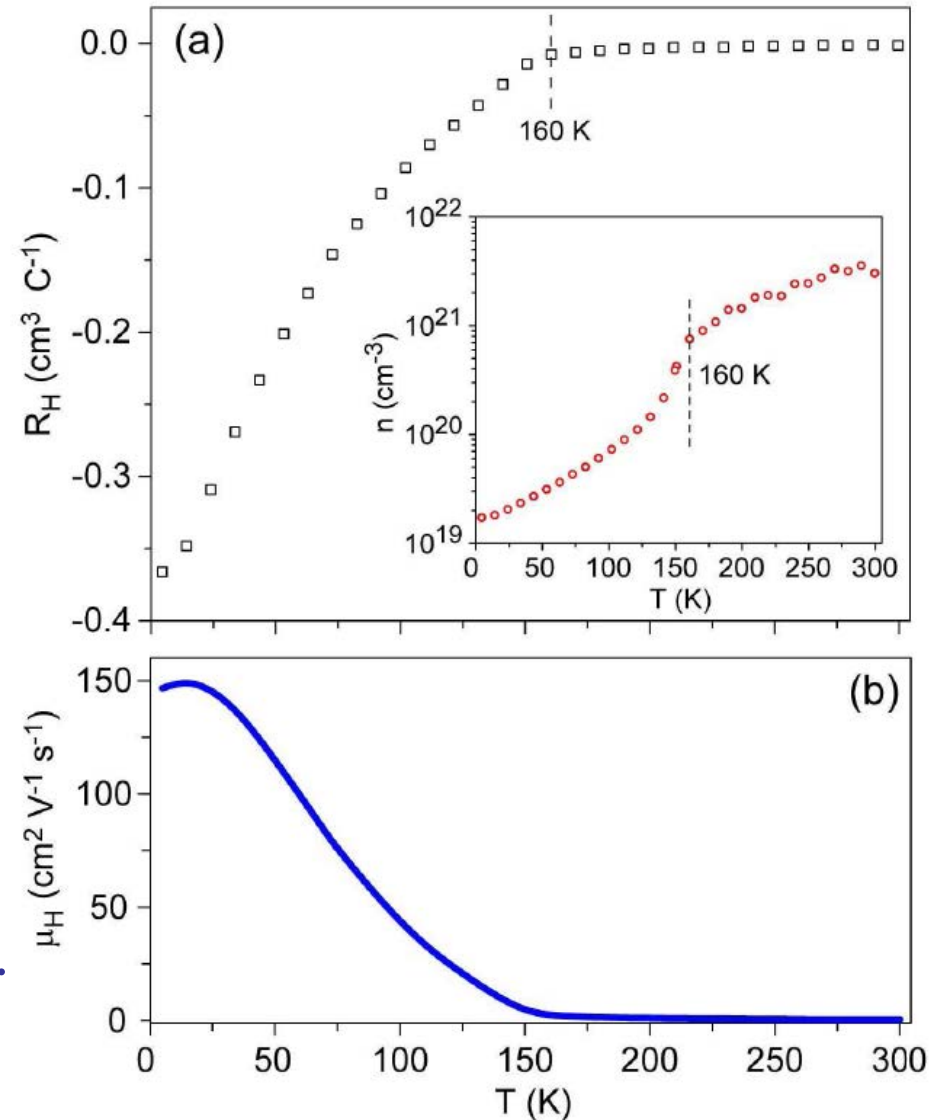
Resistivity:



Evidence of strong interplay of magnetic ordering and Fermi surface.

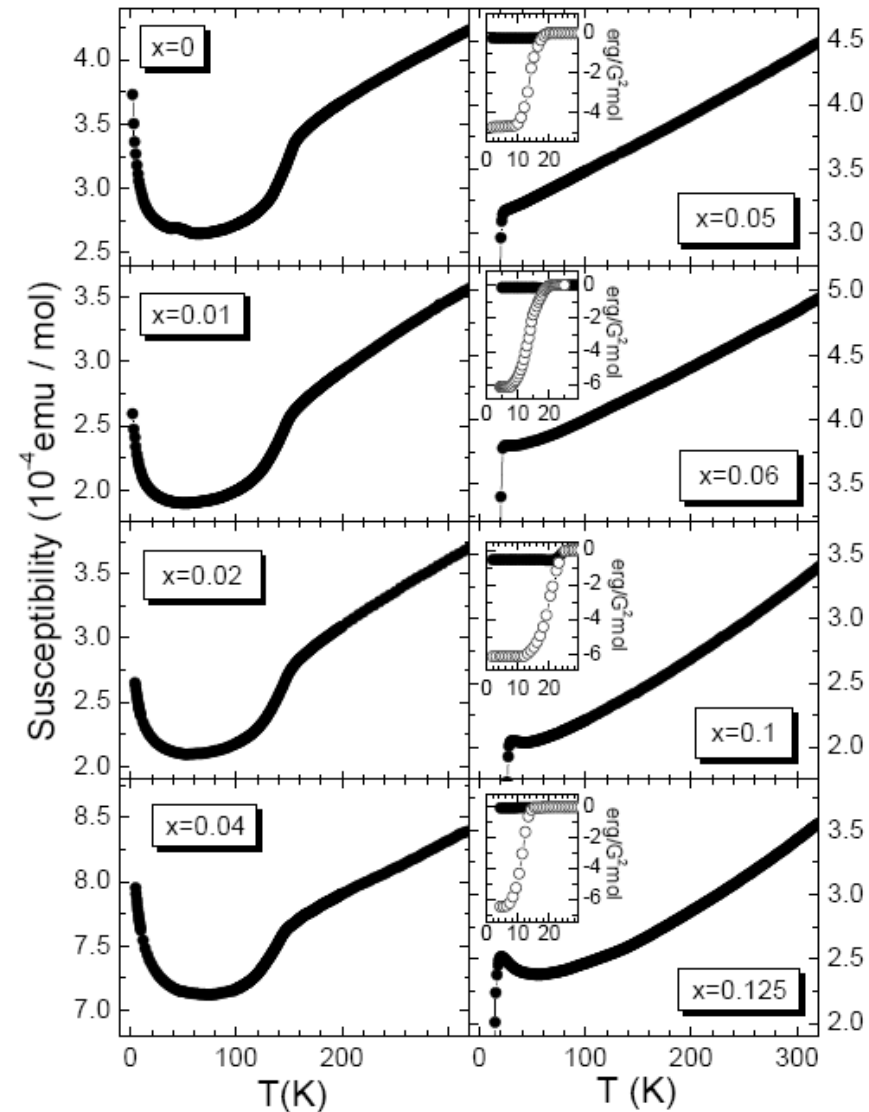
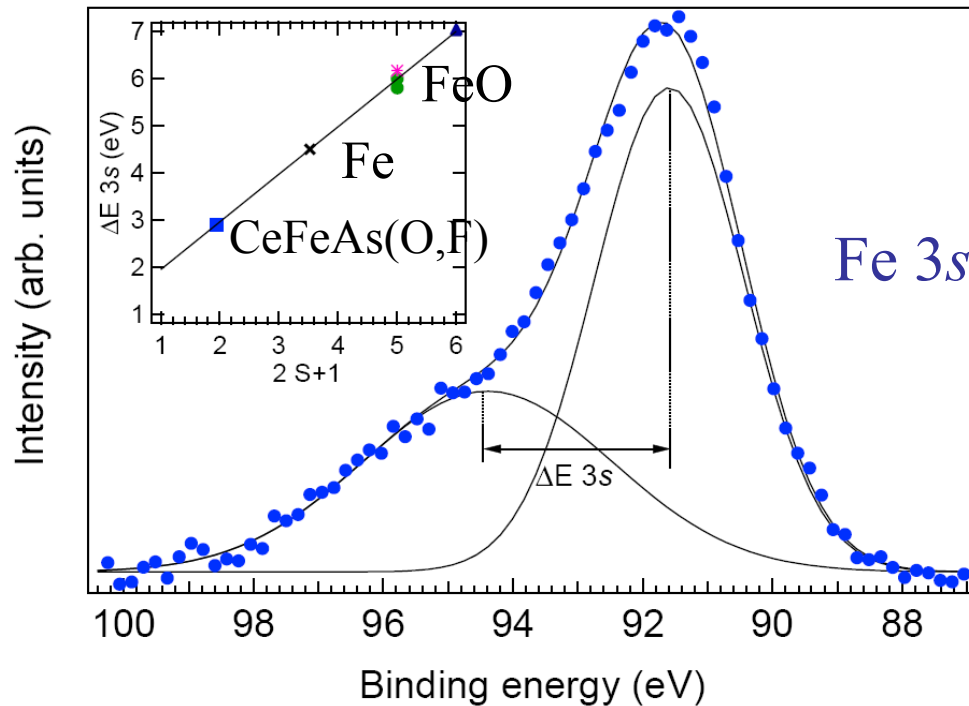
Evidence of spin fluctuations.

Hall:



Strong Spin Fluctuations in Normal State

- Transport data.
- Susceptibility - $\chi(T)$.
- Spectroscopy.
- Scattering.
- Overly magnetic in LDA.
- Precursor structural transition.

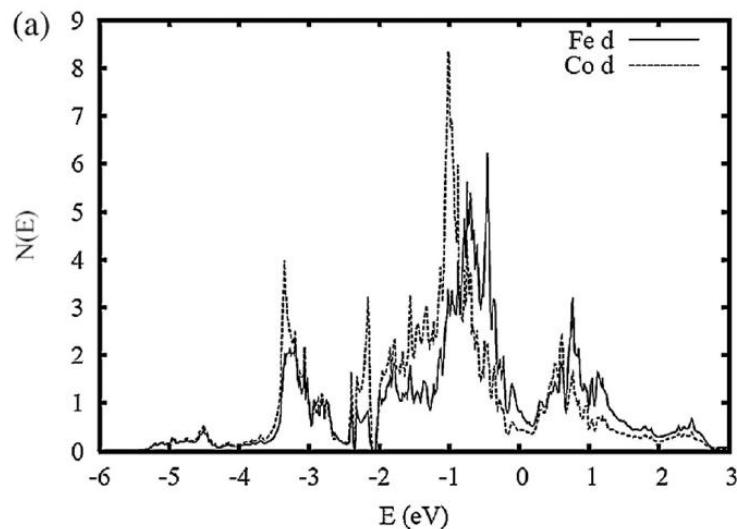
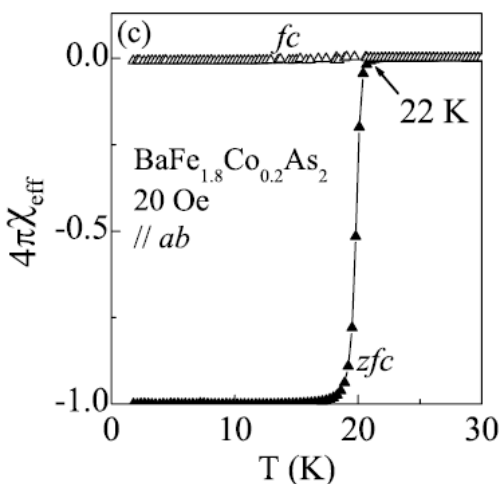


R. Klingeler et al., cond-mat
LaFeAsO_{1-x}F_x

Bondino et al. (2008); c.f. NbFe₂

Superconductivity in Metal Doped Materials

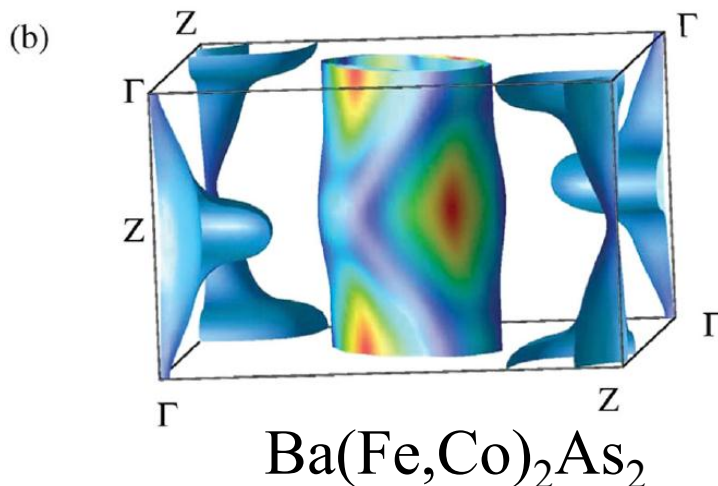
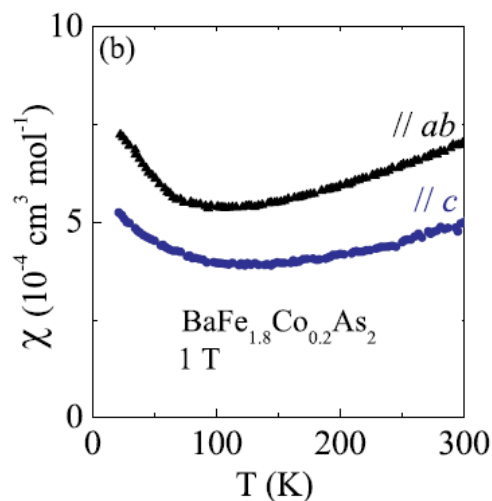
- Superconductivity requires destruction of SDW by doping.
- Remarkably, doping with Co or Ni works (*c.f.* cuprates).



Calculations show that alloy behaves very much in a rigid band sense.

Fe-Co-Ni behave very similarly apart from electron count.

Mn and Cr show strong spin dependent hybridization (different).



Is iron essential?

ThCr₂Si₂ Structure

JOURNAL OF SOLID STATE CHEMISTRY **56**, 278–287 (1985)

The Most Populous of All Crystal Structure Types—the Tetragonal BaAl₄ Structure

W. B. PEARSON

*Departments of Physics and of Chemistry, University of Waterloo,
Waterloo, Ontario, Canada, N2L 3G1*

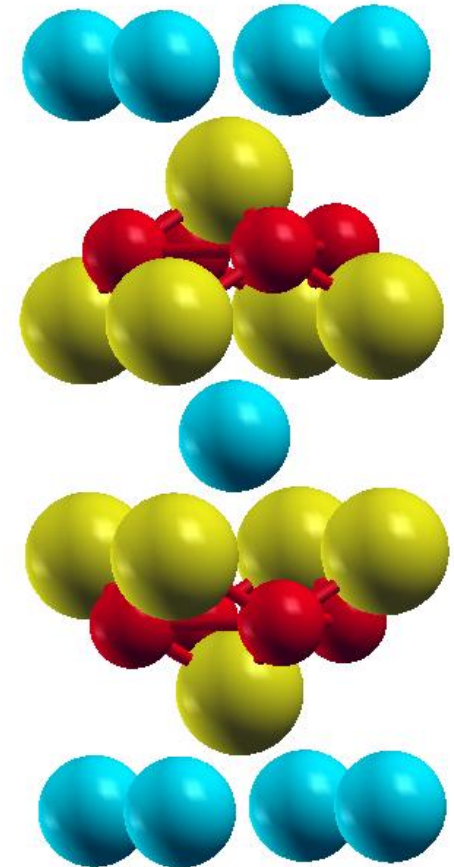
Received April 9, 1984; in revised form August 3, 1984

The BaAl₄ (ThCr₂Si₂) *tI10* structure, *MN₂X₂*, is not only the most populous of all known structure types, being adopted by some 400 phases, but is representative of a new group of metallurgically

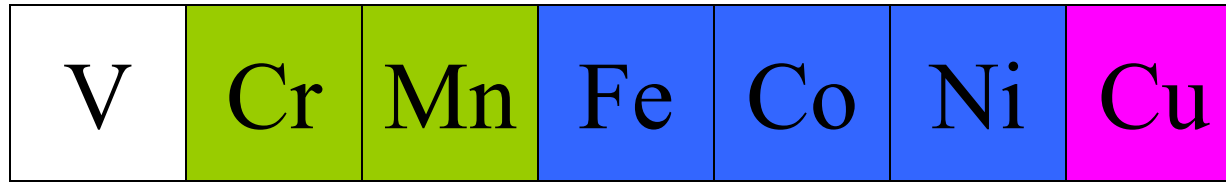
Pearson data-base now has 2,000+ ThCr₂Si₂ entries

*Can be stabilized with different bonding patterns
→ extremely wide variety of properties.*

Examples: BaZn₂P₂, BaFe₂As₂, BiN₂Th₂, CaAl₂Ga₂,
SrCd₂Ga₂ ...



ThCr₂Si₂ Structure *DT*₂As₂



Strong spin dependent *T*-As hybridization, G-type AF with high T_N .
BaCr₂As₂ is itinerant metal. BaMn₂As₂ is a semiconductor.

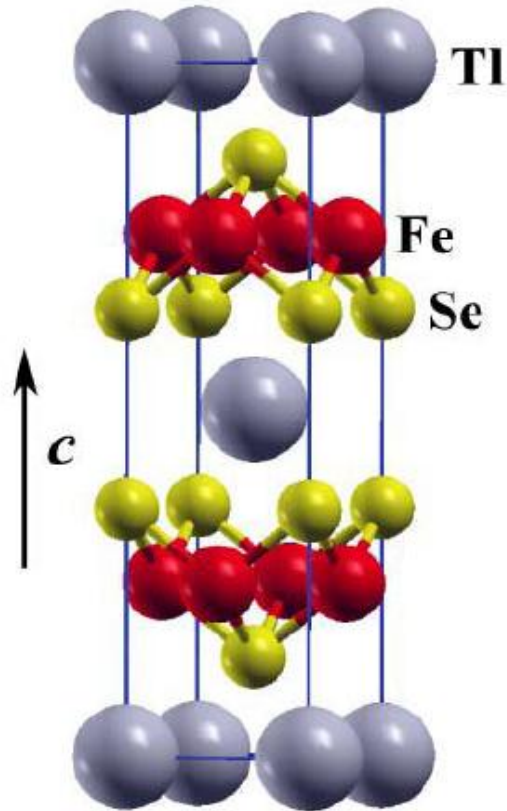
Metallic M^{2+} sheets. As is anionic. *M* can be alloyed.
Fe: SDW and superconductivity.
Co: Near FM
Ni: electron-phonon superconductor.

BaCu₂As₂ has Cu d^{10} with As-As and Cu-As sp bonding.

Chemistry of chalcogenides may be expected to differ.

Properties of the Over-Doped Side: TlFe_2Se_2

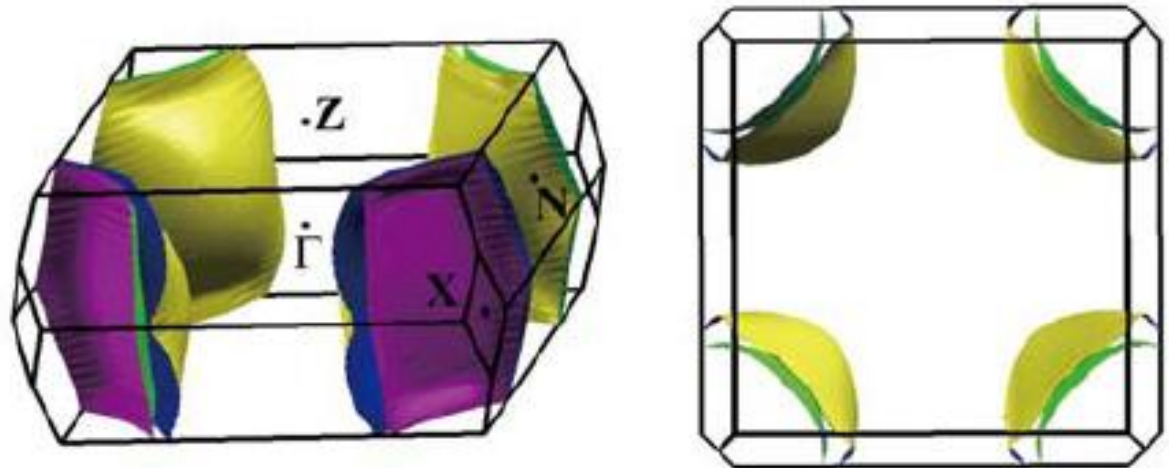
Haggstrom, 1986



Antiferromagnetic
with $T_N \sim 450$ K.
Unknown order.

First Principles Results (GGA):

- Electronic structure is very similar to FeSC, but with higher electron count (0.5 e/Fe).
- Strong instability against nearest neighbor AFM (78 meV/Fe) and weaker instability against FM (44 meV/Fe). No instability for SDW type chain order \rightarrow itinerant n.n. AFM

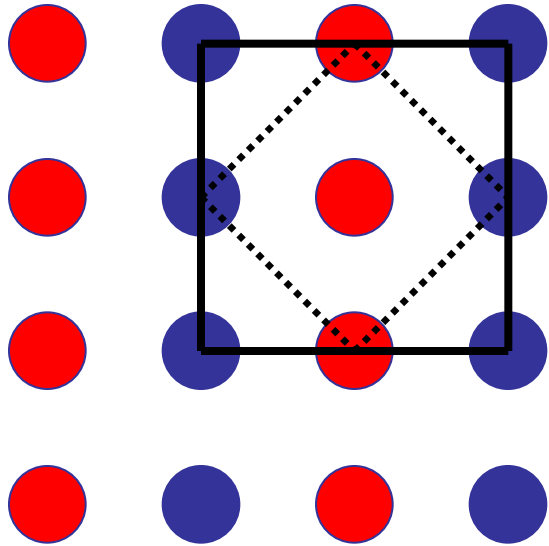


Non spin polarized Fermi surface

Competing Magnetic States

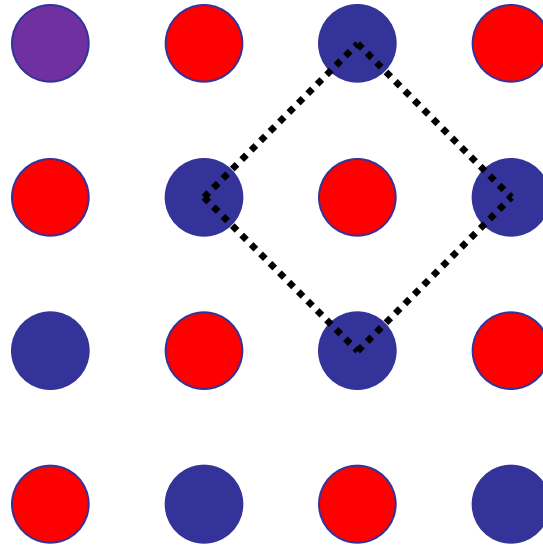
Competition between different magnetic states provides phase space for fluctuations and works against ordering.

SDW - $c(2 \times 2)$



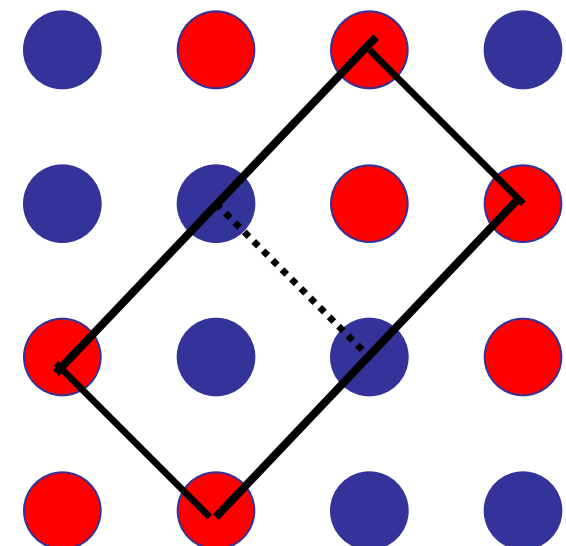
LaFeAsO

N.N (1x1)



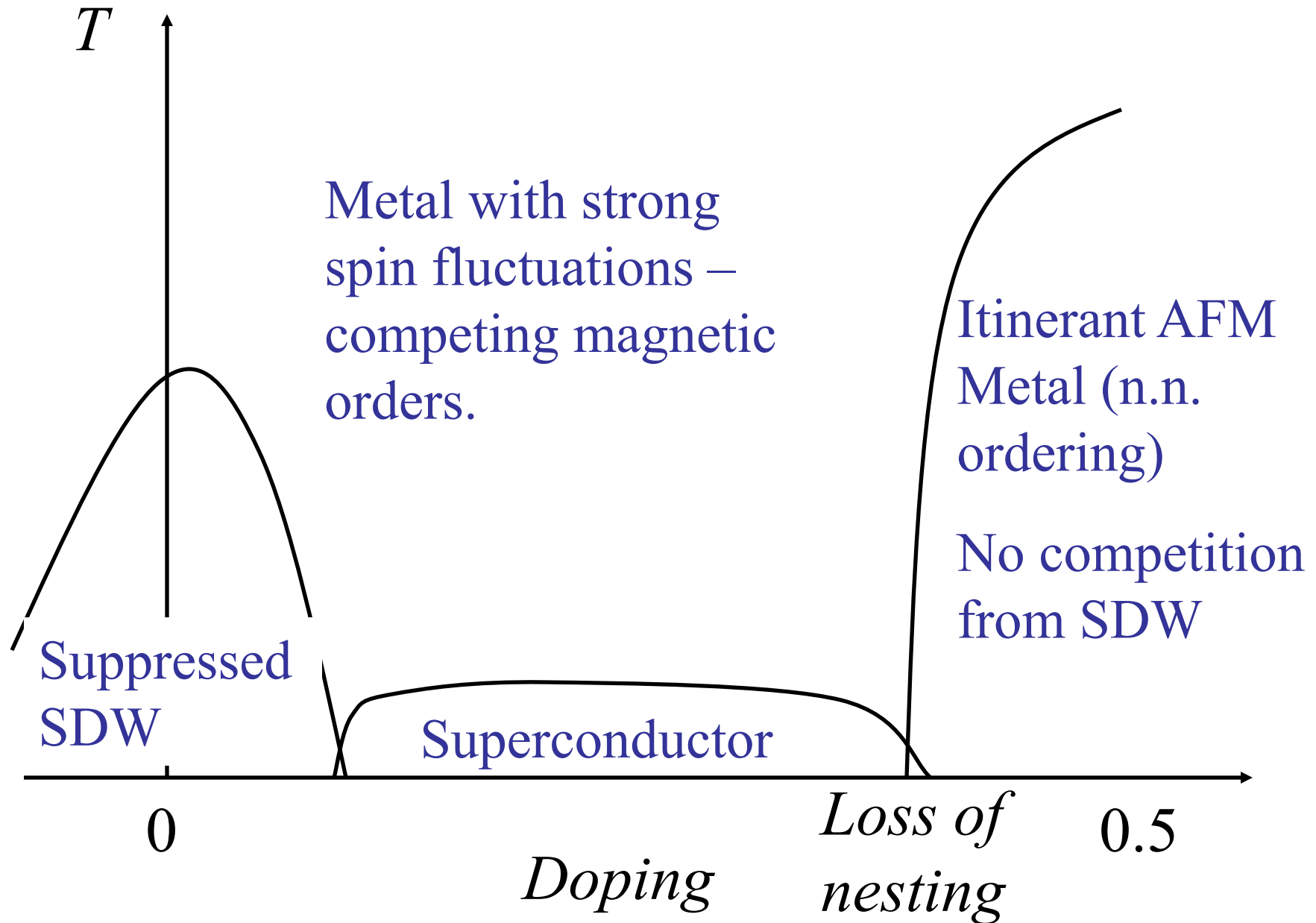
TlFe₂Se₂

(2x1)



Fe_{1+x}Te

Possible Electron Doped Phase Diagram

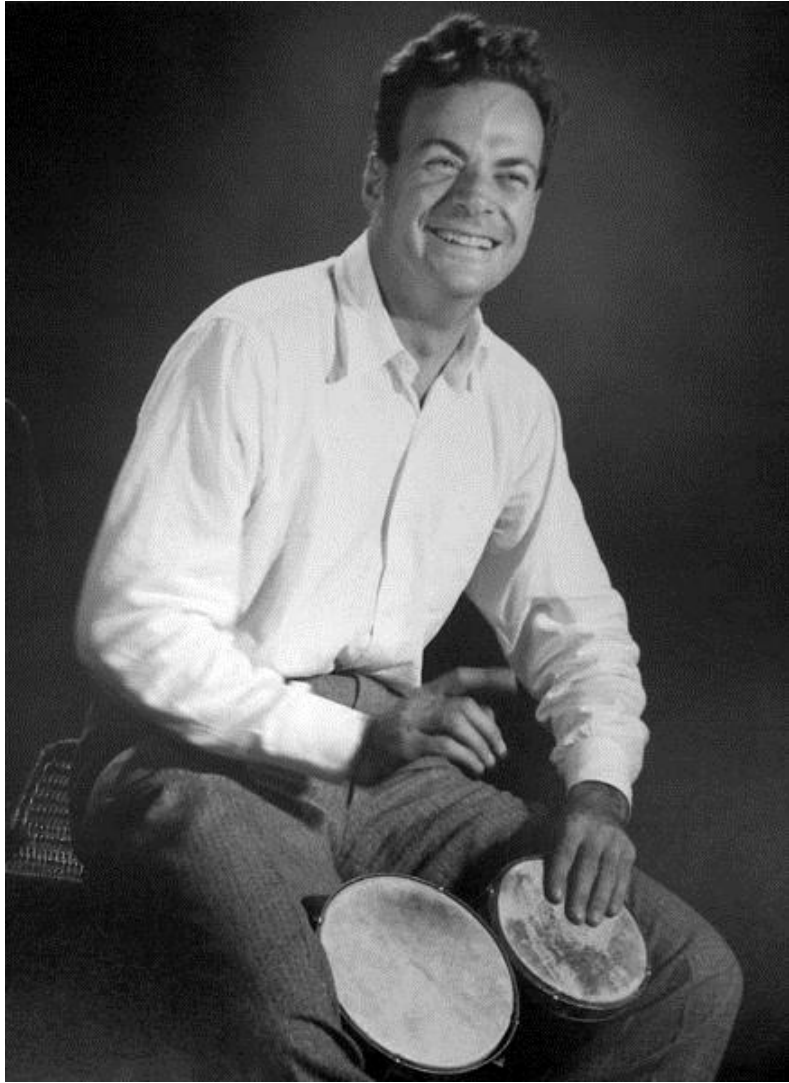


Conclusions

- Iron superconductors behave very differently from cuprates – perhaps a rather different mechanism or perhaps we need to look deeper for the connections.
- Strong renormalization of magnetic properties due to strong spin fluctuations – almost certainly necessary for understanding of the normal state and the superconductivity.
- Extended s-wave (+/-) state.
- Interesting interplay between magnetism and structure.
- *Competition between different magnetic states helps set up superconductivity as opposed to order magnetism in Fe-based superconductors and Ruthenates.*

Questions

- Can we identify materials with “strong” spin fluctuations and quantify “strong”?
- Can we identify competing magnetic states, even those with relatively weak q -dependence?
- Could we connect inelastic scattering with magnetic renormalization (fluctuation-dissipation)?
- Can we connect with transport experiments?
- Can we identify trends in magnetic behavior that would allow us to predict new superconductors, or ways to vary composition to improve superconductivity?
- ...



Hands On Science

SOME NUMBERS

Binding energy of Fe:	2541.025 Ry	
bcc-fcc energy difference in Fe:	0.013 Ry	(austenite-ferrite in steels)
Binding of PZT (Piezoelectrics):	46730.476 Ry	
Ferroelectric instability in PZT:	0.006 Ry	
Binding of Mn-ferrite (oxide mag.):	15987.192 Ry	
Magnetic coupling of Mn-ferrite:	0.070 Ry	

Small differences between very large energies are the keys to materials properties

→ We rely on careful choice of numerical methods and error cancellation in the differences.

The Linearized Augmented Planewave (LAPW) Method

$$E_T[\rho] = T_s[\rho] + E_{ei}[\rho] + E_H[\rho] + E_{xc}[\rho] + E_{ii}$$

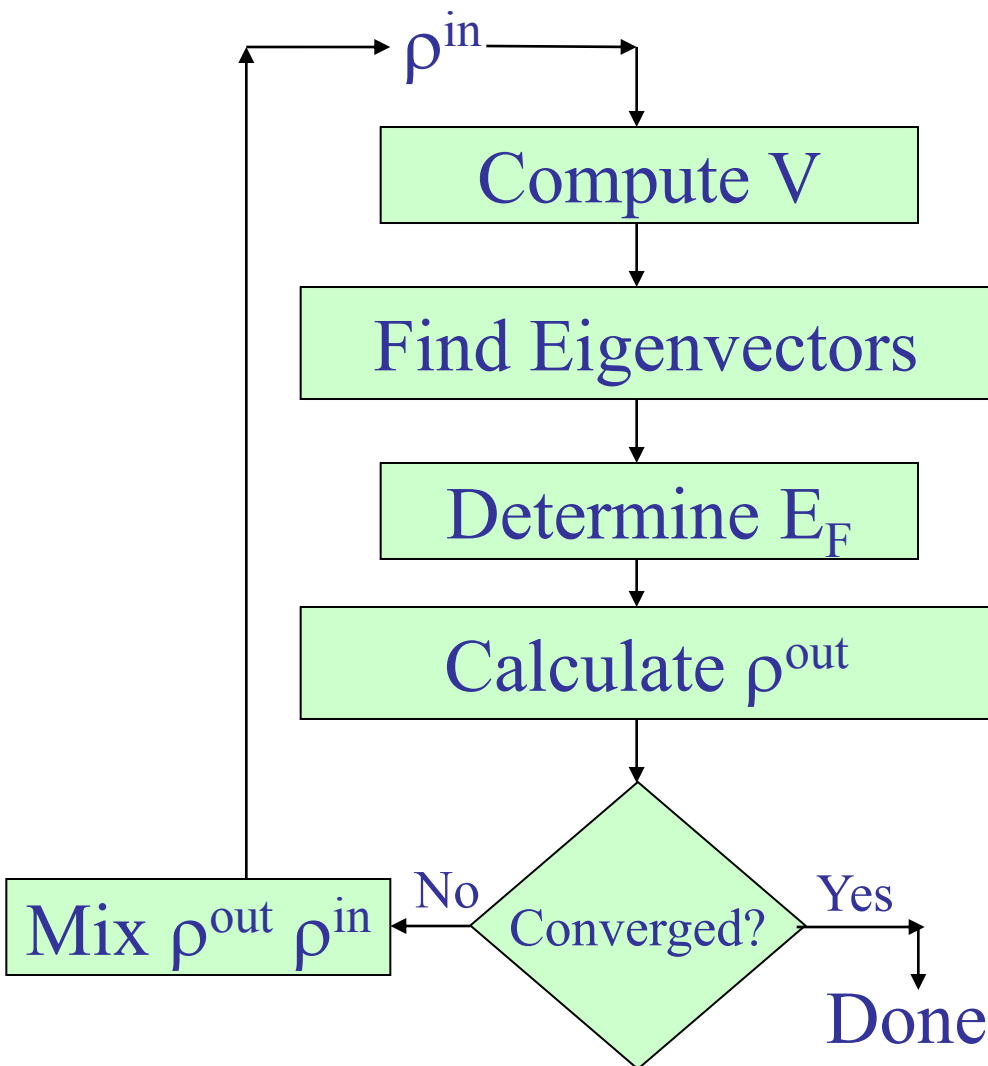
$$\{T_s + V_{ks}[\rho, \mathbf{r}]\} \varphi_I(\mathbf{r}) = \varepsilon_i \varphi_i(\mathbf{r})$$

Need tools that are reliable and predictive.

DFT ALGORITHMS

- Find φ_I and ρ to solve:

$$\{ T_s + V_{KS}[\rho, r] \} \varphi_I(r) = \varepsilon_i \varphi_i(r)$$



Standard Solution:

- Expand φ_i in a basis $\{\phi_j\}$.
- Many methods, PW, FE, LAPW, LMTO, LCAO ...
- For fixed V_{KS} get a linear algebra problem. (eigenvalue).

$$\langle \phi | H | \phi \rangle x_i = \varepsilon_i \langle \phi | \phi \rangle x_i$$

- Iterate to find self-consistent ρ .

Some Numbers:

- # $\varphi_i \sim 10$ / atom.
- # $\phi_j \sim 10$'s - 1000's / atom.
- # atoms (State of the Art): 100 – 1000's.

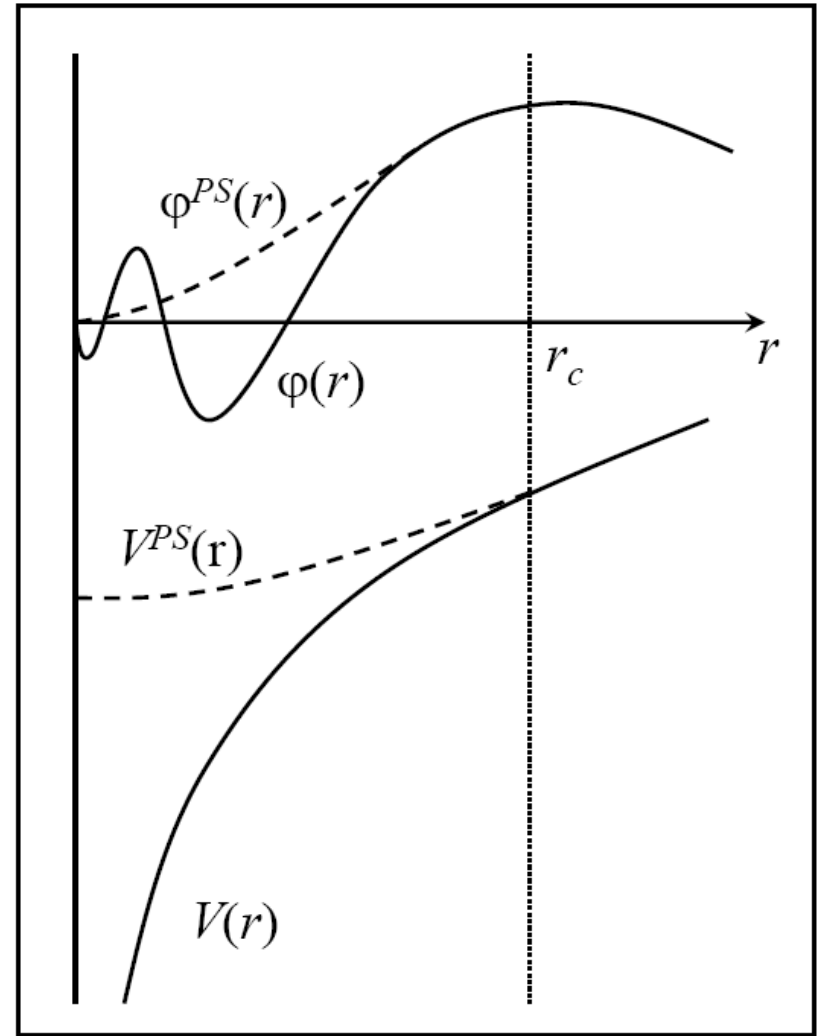
Motivation for Augmentation

Schrödinger Equation:

$$(T+V-\varepsilon)\varphi = 0$$

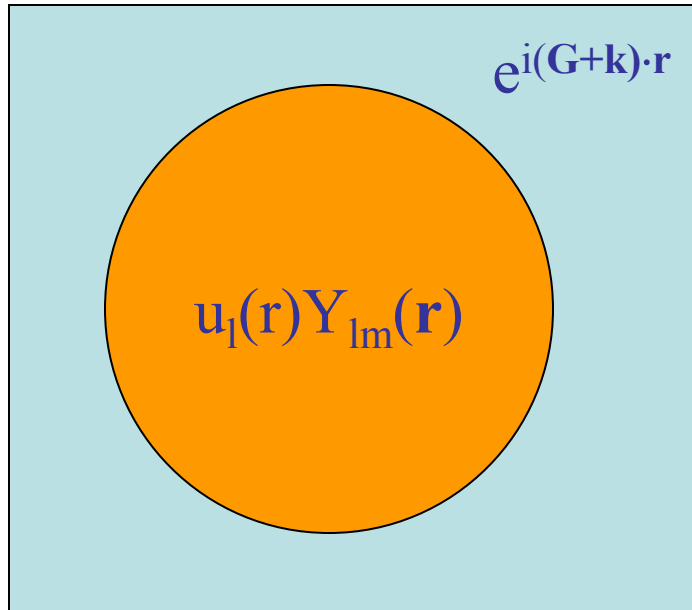
For valence states: ε is small \rightarrow

$T\varphi$ is also small except where V is strong, i.e. near the nucleus.



Augmented Planewave (APW) Method

• J.C. Slater, *Phys. Rev.* **51**, 846 (1937); *Phys. Rev.* **81**, 385 (1951).



Divide Space Into 2 Regions:

- Atom Centered Spheres
- Interstitial

“Basis” Consists of Planewaves in the Interstitial and Radial Functions in the Spheres.

$$\varphi(\mathbf{r}) = \begin{cases} \Omega^{-1/2} \sum_{\mathbf{G}} c_{\mathbf{G}} e^{i(\mathbf{G}+\mathbf{k})\cdot\mathbf{r}} & \mathbf{r} \in \text{Interstitial (I)} \\ \sum_{lm} A_{lm} u_l(r) Y_{lm}(\mathbf{r}) & \mathbf{r} \in \text{Sphere (S)} \end{cases}$$

- $u_l(r)$ are the radial solutions of Schrodinger's equation at the energy of interest (i.e. the band energy).

Augmented Planewave (APW) Method

$$\varphi(\mathbf{r}) = \begin{cases} \Omega^{-1/2} \sum_{\mathbf{G}} c_{\mathbf{G}} e^{i(\mathbf{G}+\mathbf{k})\cdot\mathbf{r}} & \mathbf{r} \in \text{Interstitial (I)} \\ \sum_{lm} A_{lm} u_l(r) Y_{lm}(\mathbf{r}) & \mathbf{r} \in \text{Sphere (S)} \end{cases}$$

Key points:

1. The A_{lm} are not variational parameters. They are determined by a matching condition. That is the value of the basis functions, $\phi_{\mathbf{k}+\mathbf{G}}$ is fixed to be continuous at the sphere boundary.
2. The full crystal potential can be used because one may show that the u_l are orthogonal to “core” states.

$$[-d^2/dr^2 + l(l+1)/r^2 + V(r) - E_l] ru_l(r) = 0$$

So:

$$(E_2 - E_1) r u_1 u_2 = u_2 (d^2 ru_1/dr^2) - u_1 (d^2 ru_2/dr^2)$$

Integrate by parts to get overlap of u_1 and u_2 . They are orthogonal if one of them is 0 on the sphere boundary.

Problems with the APW Method

- 1) Must solve secular equation for each energy band: prohibitive for many bands. No clear way to make full-potential.
- 2) Asymptote problem: cannot match at energies where $u(r)$ is zero on the sphere boundary. This will in general happen at some energy – particular problem for d and f band materials.

The Linearized Augmented Planewave (LAPW) Method

O.K. Andersen, Phys. Rev. B **12**, 3060 (1975).

Key Ideas:

- The problem with the APW method is the energy dependence of the secular equation which is a result of the energy dependence of the augmenting function.
- Solution: Add variational freedom: particularly $\dot{u}(r) = \partial u(r)/\partial E$.

$$\varphi(\mathbf{r}) = \begin{cases} \Omega^{-1/2} \sum_{\mathbf{G}} c_{\mathbf{G}} e^{i(\mathbf{G}+\mathbf{k})\cdot\mathbf{r}} & \mathbf{r} \in \text{I} \\ \sum_{lm} (A_{lm} u_l(r) + B_{lm} \dot{u}_l(r)) Y_{lm}(\mathbf{r}) & \mathbf{r} \in \text{S} \end{cases}$$

- Where A_{lm} *and* B_{lm} are determined by matching the value and derivative of the basis functions at the sphere boundary.

THE LAPW METHOD

Results of adding \hat{u}_l to the basis:

1. Basis is flexible enough to use a single diagonalization (energy errors are now $O(\delta^4)$).
2. Must have additional matching conditions to connect both u and \hat{u} to the planewaves. This means that for a given level of convergence, more planewaves are needed.
3. The transferability also extends to variations in the potential: this enables full-potential methods.

The full potential, all electron, nature combined with the flexible basis (fully flexible in the interstitial) made the (F)LAPW method the state of the art for calculating electronic structures, especially for transition elements and their compounds – Many groups developed codes 1980 – present.

References

1. D.J. Singh and L. Nordstrom, *Planewaves, Pseudopotentials and the LAPW Method* (Springer, 2005). **Details about the LAPW method, connection with pseudopotentials and inner workings of codes.**
2. O.K. Andersen, Phys. Rev. B **12**, 3060 (1975). **Formalism for the LAPW method.**
3. D. Singh, Phys. Rev. B **43**, 6388 (1991). **Local orbitals.**
4. E. Sjöstedt, L. Nordstrom and D.J. Singh, Solid State Commun. **114**, 15 (2000). **APW+LO method.**
5. J.C. Slater, Phys. Rev. **51**, 846 (1937). **APW method.**
6. T.L. Loukes, *The Augmented Planewave Method* (Benjamin, 1967). **Details about APW implementation.**

The Elk FP-LAPW Code

An all-electron full-potential linearised augmented-plane wave (FP-LAPW) code with many advanced features. Written originally at [Karl-Franzens-Universität Graz](#) as a milestone of the EXCITING EU Research and Training Network, the code is designed to be as simple as possible so that new developments in the field of density functional theory (DFT) can be added quickly and reliably. The code is freely available under the [GNU General Public License](#).

Latest version: 1.3.31

[News](#) | [Features](#) | [Download](#) | [Documentation](#) | [FAQ](#) | [Forums](#) | [Mailing list](#) | [Contributions](#) | [Wiki](#) | [CECAM tutorial](#) | [Links](#)

<http://elk.sourceforge.net/>



Contents lists available at ScienceDirect

Solid State Sciences

journal homepage: www.elsevier.com/locate/ssscie



Superconducting-like behaviour of the layered Chalcogenides CuS and CuSe below 40 K

B. Raveau*, Tapati Sarkar

Laboratoire CRISMAT, UMR 6509 CNRS ENSICAEN, 6 bd Maréchal Juin, 14050 CAEN, France

ARTICLE INFO

Article history:

Received 21 July 2011

Accepted 26 July 2011

Available online 3 August 2011

Keywords:

Superconductivity

Layered chalcogenides

ABSTRACT

The investigation of strongly sintered “quasi molten” CuS and CuSe chalcogenides shows that they exhibit a sharp diamagnetic transition and a resistivity drop around 40 K. The reminiscence of such high temperature superconductivity features, never observed to date for these phases, is strongly supported by two chemical characteristics: bidimensionality of the structure and mixed valency of copper. The absence of zero resistance suggests that the internal chemical pressure in the samples has a key role in the existence of superconductivity: the S–S or Se–Se interlayer distances are very sensitive to the pressure, so that the critical distance for the percolation can be reached in the core of the samples, but not at the vicinity of the surface, where relaxation may appear.

© 2011 Elsevier Masson SAS. All rights reserved.

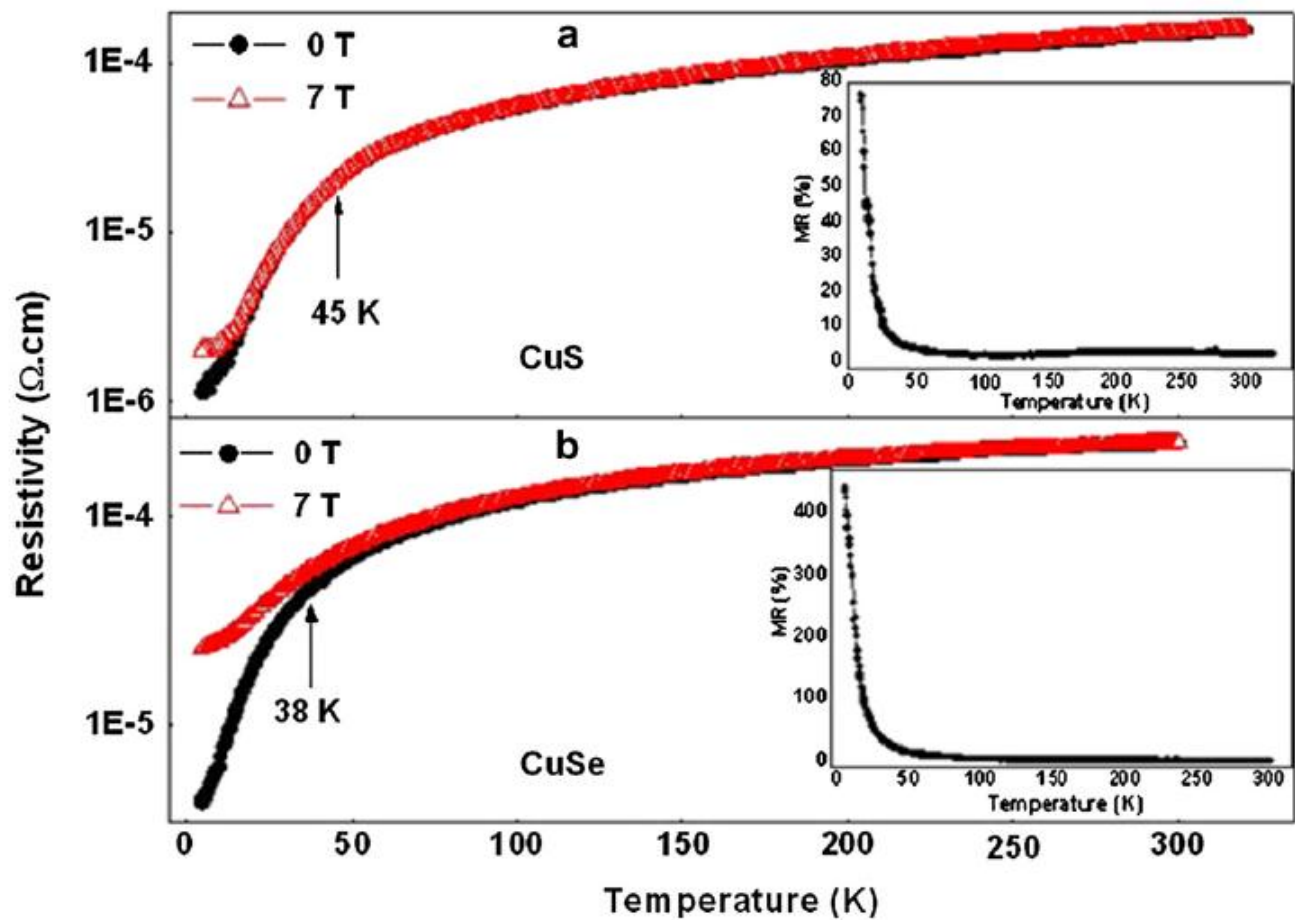


Fig. 3. Temperature dependence of resistivity of (a) CuS (sample 1) and (b) CuSe (sample 2) in the presence and absence of external magnetic field. The insets show the variation of the % MR as a function of temperature for the two samples.

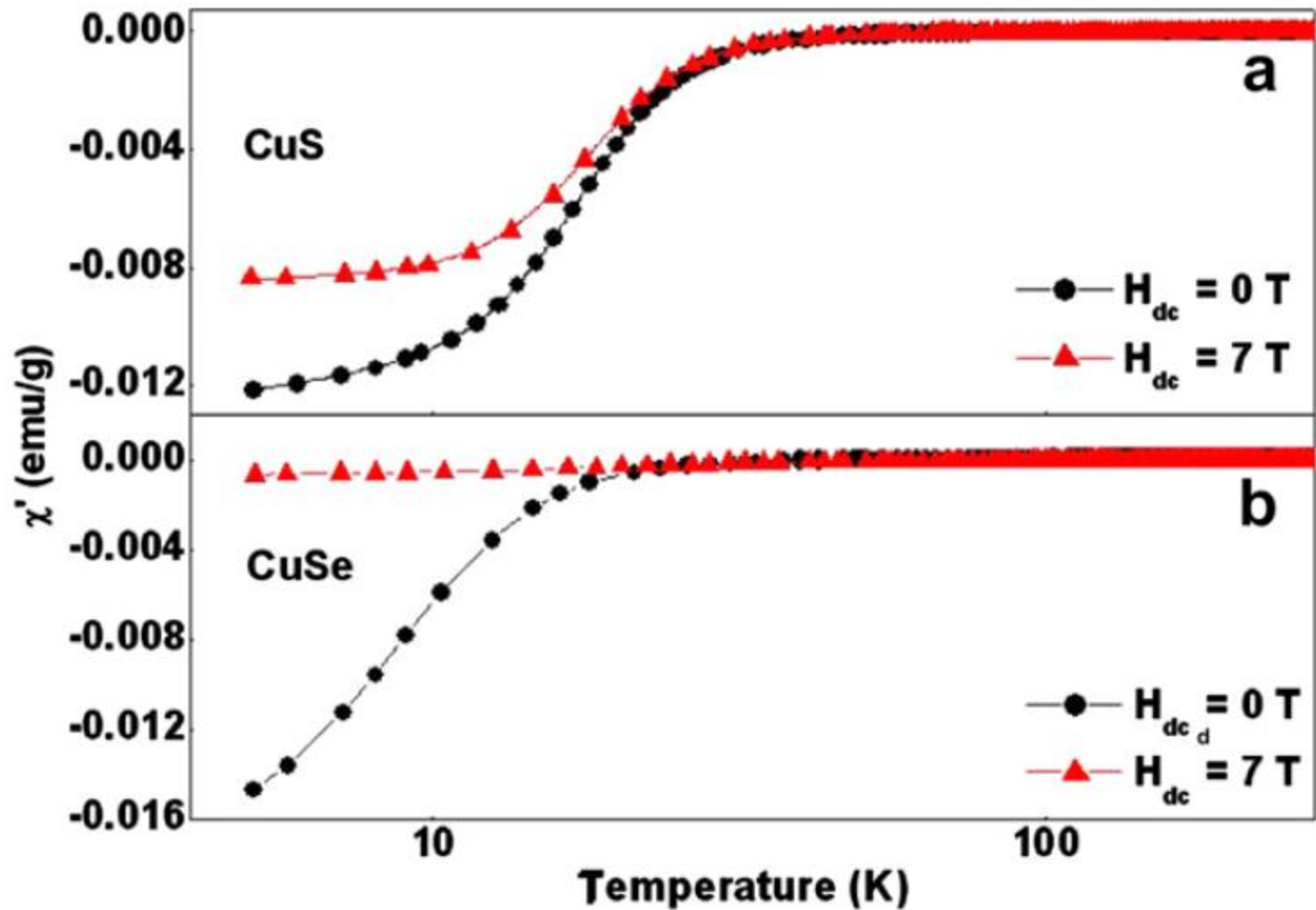
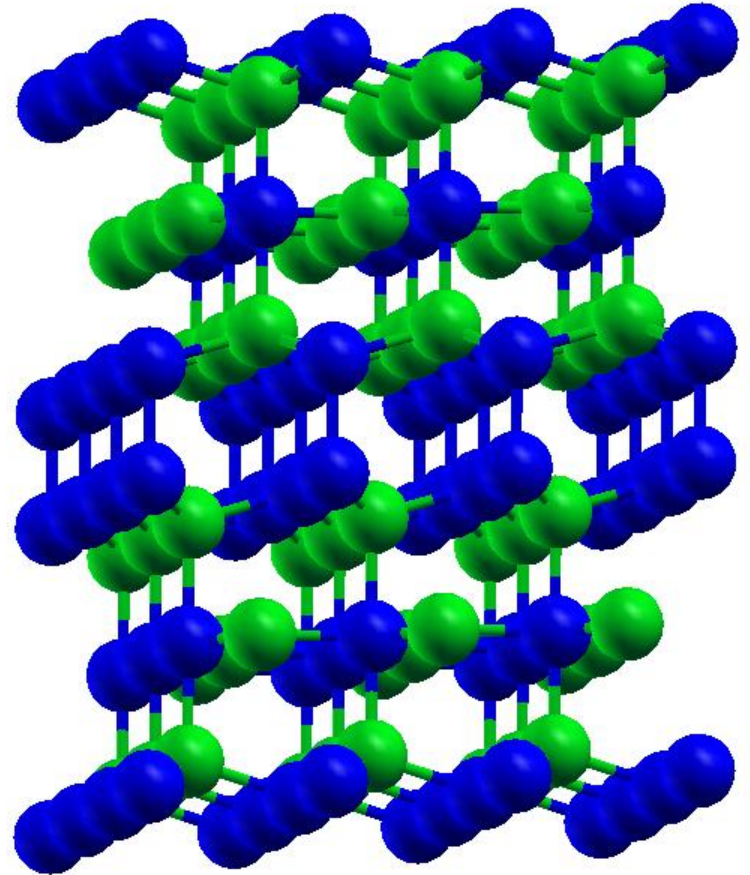
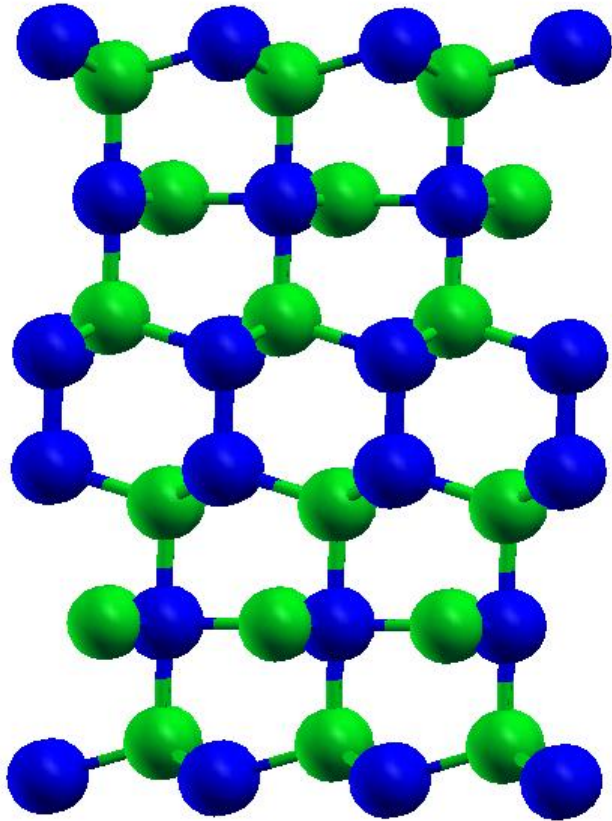


Fig. 2. Temperature dependence of a.c. magnetic susceptibility of (a) CuS (sample 1) and (b) CuSe (sample 2) measured in the presence of two different d.c. magnetic fields.

Structure of CuS



Experimental and theoretical investigation of the crystal structure of CuS

H J Gotsis†, A C Barnes‡§ and P Stranget

† Physics Department, Keele University, Keele, Staffs ST5 5BG, UK

‡ Neutron Division, Rutherford–Appleton Laboratory, Chilton, Didcot, Oxon OX11 0QX, UK

Received 24 August 1992, in final form 14 October 1992

Abstract. The crystal structure of CuS has been confirmed experimentally using the powder diffraction method on the high-resolution powder diffractometer at the Rutherford–Appleton Laboratory. The observed crystal structure is $P6_3/mmc$. Standard density functional calculations on CuS on a variety of crystal structures are also reported. The calculations also predict $P6_3/mmc$ as the stable crystal structure. On the basis of the agreement between theory and experiment we are able to discuss the details of the bonding in this material.

Klockmannite, CuSe: structure, properties and phase stability from *ab initio* modeling

Victor Milman

Accelrys, The Quorum, Barnwell Road,
Cambridge CB5 8RE, England

Correspondence e-mail: vmilman@accelrys.com

The details of the electronic and crystal structure, the nature of the interatomic bonding and the phase stability of three modifications of klockmannite, CuSe, are analysed using first principles modeling. The hexagonal modification of CuSe is predicted to be less stable than the orthorhombic phase under pressure. The stabilizing force for the orthorhombic phase is identified as the Cu–Cu bond formation between the Cu atoms in the flat hexagonal CuSe layer and in the buckled Cu₂Se₂ layer. Furthermore, klockmannite is shown to be unstable under compression with respect to the decomposition into umangite, Cu₃Se₂, and krutaite, CuSe₂ II.

Received 29 September 2001

Accepted 18 February 2002